Florida Institute of Technology
High Tech with a Human Touch™

Ground Tire Rubber as a Stabilizer for Subgrade Soils
Final Report

FDOT Contract Number: BDK81 977-03
Date Prepared: May 7, 2014

Florida Institute of Technology
Department of Civil Engineering
150 West University Boulevard
Melbourne, Florida 32901
www.fit.edu • (321) 674-8048

Submitted by:

Paul Cosentino, Ph.D., P.E.
Florida Institute of Technology
Department of Civil Engineering
150 West University Boulevard
Melbourne, FL 32901-6975
(321) 674-7555
Email: cosentin@fit.edu

Submitted to:

The Florida Department of Transportation
Research Center
605 Suwannee St., MS 30
Tallahassee, FL 32399
c/o David Horhota Ph.D., P.E.

EN-364-514

Disclaimer

Metric Conversion Table

Symbol		Multiply By	To Find	Symbol
LENGTH				
in	inches	25.4	millimeters	mm
ft	feet	0.305	meters	m
AREA				
in^2	square inches	645.2	square millimeters	mm^2
ft^2	square feet	0.093	square meters	m^2
yd^2	square yards	0.836	square meters	m^2
VOLUME				
ft^3	cubic feet	0.028	cubic meters	m^3
MASS				
oz	ounces	28.35	grams	g
lb	pounds	0.454	kilograms	kg
T	short tons (2,000lb)	0.907	megagrams ("metric ton")	Mg (or "t")
UNIT WEIGHT				
pcf	lbf/ft^3	16.02	kilograms/ cubic meter	kg/m^3
TEMPERATURE (exact degrees)				
°F	Fahrenheit	5 (F-32)/9 or (F-32)/1.8	Celsius	°C
FORCE and PRESSURE or STRESS				
lbf	pound force	4.45	newtons	N
kip	1,000 lbf	4.45	kilonewtons	kN
ton	2,000 lbf	8.90	kilonewtons	kN
lbf/in^2	pound force/ square inch	6.89	kilopascals	kPa
ksi	kips / square inch	6.89	megapascals	MPa
tsf	tons/square foot	95.76	Kilopascals	KPa

Technical Report Documentation Page

1. Report No.	2. Government Accession No.	3. Recipient's Catalog No.
4. Title and Subtitle Ground Tire Rubber as a Stabilizer for Subgrade Soils DRAFT Final Report		5. Report Date May 5 2014 6. Performing Organization Code Index 201
7. Author(s) P. J. Cosentino, A. M. Bleakley, A. T. Armstrong, A.M. Sajjadi, T. J. Misilo		8. Performing Organization Report No.
9. Performing Organization Name and Address Florida Institute of Technology Civil Engineering Department 150 West University Blvd. Melbourne, FL 32901-6975 (321) 674-7555		10. Work Unit No. (TRAIS) 11. Contract or Grant No. Contract Number BDK81 977-03
12. Sponsoring Agency Name and Address Florida Department of Transportation 605 Suwannee Street Tallahassee, Florida 32399-0450		13. Type of Report and Period Covered June 2012 – May 2014 14. Sponsoring Agency Code
15. Supplementary Notes		

16. Abstract

Over 250 million scrap tires are generated annually in the U.S. Historically, a significant portion of these tires have been processed into finely ground tire rubber (GTR), or crumb rubber, for use as an additive in hot mix asphalt (HMA) pavements to improve pavement performance. Recently, improved synthetic polymer additives have been developed that more economically provide the same performance improvements as GTR. This development has decreased the demand for GTR in HMA, potentially freeing supplies of GTR for other applications.

Over the past two decades, the Florida Department of Transportation (FDOT) has conducted a significant amount of research on ways to re-use waste materials such as energy generation ash, tires, glass, reclaimed asphalt pavement, and reclaimed concrete in roadway construction. FDOT initiated this study to investigate whether blending GTR with subgrade soils would be a beneficial practice.

The objective of this research was to determine the effect of GTR on subgrade soil engineering properties. Three representative sizes of GTR, 1 inch (25.4 mm), 3/8 inch (9.51 mm), and #40 (0.422 mm) were blended in varying percentages with three subgrade soils. Subgrade soils were selected with low, medium, and high limerock bearing ratio (LBR) strength. Blends were evaluated with 4, 8, 16, 24, and 32% GTR by volume. Blends were evaluated for grain size, moisture-density, LBR, permeability, consolidation, resilient modulus (M_r), and creep.

Ground tire rubber does not make a good stabilizing agent for subgrade soils. Blending GTR with subgrade soils reduced both LBR and M_r significantly. Blending has minimal impact on consolidation or permeability. Blending increases creep in the tested soils, however the creep remained within acceptable limits.

Blending GTR with soil did reduce the density of the blend. Additional research should be conducted to evaluate whether soil/GTR blends would be suitable for low-density fill applications where the benefits from reduction in vertical and horizontal soil pressures would offset the reduction in strength.

17. Key Word	18. Distribution Statement
Ground Tire Rubber, Subgrade Blends	Document is available to the U.S. public through the National Technical Information Service, Springfield, Virginia 22161

19. Security Classif. (of this report)	20. Security Classif. (of this page)	21. No. of Pages	22. Price
Unclassified	Unclassified	158	

Form DOT F 1700.7 (8-72) Reproduction of completed page authorized

Acknowledgements

This work was completed under FDOT contract number BDK81-977-03. The authors would like to acknowledge the following people for their invaluable guidance and help in the completion of this study.

The support of Dr. David Horhota, P.E., Mr. Jose Hernando, P.E., Mr. John Shoucair, P.E., and James Musselman, P.E., of the Florida Department of Transportation State Materials Office throughout the project was critical to its successful completion. The hard work and assistance of Bruce Swidarski, Todd Britton, Kyle Shepard, Kevin Haddix, and Glenn Johnson at the FDOT State Materials Office is most appreciated.

The authors also wish to acknowledge the valuable assistance from Mr. Mark Bailey and the entire staff at Global Tire Recycling in Wildwood, Florida, for graciously providing the research team with ground tire rubber samples and allowing us to tour their facilities.

The following Florida Institute of Technology undergraduate students helped with performing numerous laboratory tests: Patrick Hammond, Julius Reid, Christopher Welcome, Raymond Quincy Sy, Alvaro Urcuyo, Mara Bancroft, and Alandre Melton.

Executive Summary

by

Paul J. Cosentino, Ph.D., P.E.

Albert M. Bleakley, PhD., P.E.

Alexander T. Armstrong

Thaddeus J. Misilo

Amir M. Sajjadi

Over 250 million scrap tires are generated annually in the U.S. Historically, a significant portion of these tires have been processed into finely ground tire rubber (GTR), or crumb rubber, for use as an additive in hot mix asphalt (HMA) pavements to improve pavement performance. Recently, improved synthetic polymer additives have been developed that more economically provide the same performance improvements as GTR. This development has decreased the demand for GTR in HMA, potentially freeing supplies of GTR for other applications.

Over the past two decades, the Florida Department of Transportation (FDOT) has conducted a significant amount of research on ways to re-use waste materials such as energy generation ash, tires, glass, reclaimed asphalt pavement, and reclaimed concrete in roadway construction. FDOT initiated this study to investigate whether blending GTR with subgrade soils would be a beneficial practice.

The objective of this research was to determine the effect of GTR on subgrade soil engineering properties. Three representative sizes of GTR, 1 inch (25.4 mm), 3/8 inch (9.51 mm), and #40 (0.422 mm) were blended in varying percentages with three subgrade soils. Subgrade soils were selected with low, medium, and high limerock bearing ratio (LBR) strength. Blends were evaluated with 4, 8, 16, 24, and 32% GTR by volume. Blends were evaluated for grain size, moisture-density, LBR, permeability, consolidation, resilient modulus (M_r), and creep.

Ground tire rubber does not make a good stabilizing agent for subgrade soils. Blending GTR with subgrade soils reduced both LBR and M_r significantly. Blending has minimal impact on consolidation or permeability. Blending increases creep in the tested soils, however the creep remained within acceptable limits.

Blending GTR with soil did reduce the density of the blend. Additional research should be conducted to evaluate whether soil/GTR blends would be suitable for low-density fill applications where the benefits from reduction in vertical and horizontal soil pressures would offset the reduction in strength.

Table of Contents

List of Figures

List of Tables

List of Abbreviations

AASHTO – American Association of State Highway and Transportation Officials

ARL – Applied Research Laboratory on FIT's Campus

ASTM – American Standard for Testing and Materials

FDOT – Florida Department of Transportation

FIT – Florida Institute of Technology

FM – Florida Method

GTR – Ground Tire Rubber

High – High LBR Subgrade Material

LBR – Limerock Bearing Ratio

Low – Low LBR Subgrade Material

Medium – Medium LBR Subgrade Material

M_r- Resilient Modulus

SMO – State Materials Office

1. Introduction

Over 250 million scrap tires are generated annually in the U.S. Currently, many of these scrap tires are stockpiled or placed in a land fill. A portion of the tires are re-used in a variety of ways, including export, power generation, and manufacture of rubber products. Historically, a significant portion of these tires have been processed into finely ground tire rubber (GTR), or crumb rubber, for use as an additive in hot mix asphalt (HMA) pavements to improve pavement performance. Recently, improved synthetic polymer additives have been developed that more economically provide the same performance improvements as GTR. This development has decreased the demand for GTR in HMA, potentially freeing supplies of GTR for other applications.

Over the past two decades, the Florida Department of Transportation (FDOT) has conducted a significant amount of research on ways to re-use waste materials such as energy generation ash, tires, glass, reclaimed asphalt pavement and reclaimed concrete in roadway construction (Cosentino et al., 2012, 2008, and 2003). FDOT initiated this study to investigate whether blending GTR with subgrade soils would be a beneficial practice.

1.1. Objective

The objectives of this research were to determine the key pavement engineering properties of GTR-stabilized Florida subgrade soil blends and to provide conclusions detailing which blends are acceptable for roadway applications.

1.2. Approach

The proposed objective was completed over 24 months by performing the following tasks,

1.2.1. Task 1: Literature Search

The literature concerning the use of GTR in highway applications was investigated.

1.2.2. Task 2: Determine GTR Sources

Several Florida GTR producers were identified and contacted. Meetings were conducted with the key suppliers and the goals of our research were conveyed. Based on these discussions, the team selected a GTR supplier and range of nominal sizes to test.

1.2.3. Task 3: Determine Subgrade Sources

LBR was the basic engineering property used to select sources for the subgrade materials. FDOT's State Materials Office (SMO) aided in obtaining these materials. A range of subgrade soils were selected including:

1) Poor bearing materials with an LBR in the 20 to 30 range (typically an A-3 fine sand));
2) Good bearing materials with an LBR in the 50 to 60 range (typically an A-2-4 silty or clayey sand) and
3) Marginal bearing materials with an LBR of approximately 40 (typically borderline A-3/A-2-4 soils).

1.2.4. Task 4: Test Program Development

A testing program was developed to evaluate engineering properties of the GTR/subgrade soil blends. The research team determined that in addition to grain size, strength-deformation and drainage characteristics were critical to understanding the behavior of GTR/Subgrade blends.

1.2.5. Task 5: Database Development

A database was developed to store, retrieve, and analyze specified results. This task produced improvements in data manipulation and retrieval. Appendix H contains an outline of the database system and portions of the software to give the reader an overview.

1.2.6. Task 6: Testing Program Sampling

Samples of sufficient size were obtained from approved FDOT GTR subgrade soil sources. Proper sampling protocol was followed to obtain all samples. Samples were transported from the source location to the Florida Institute of Technology Highway Engineering Research Laboratory.

1.2.7. Task 7: Testing

The following tests were conducted:

1. Grain Size (FM 1-T 027 Sieve Analysis for Coarse and Fine Aggregates)
2. Atterberg Limits (ASTM T-89 and T-90)
3. Permeability (FM 1-T215 Constant Head Testing)
4. Moisture-Density (FM 1-T 180 Modified Proctor Testing)
5. Soaked LBR (FM 5-515)
6. Resilient Modulus (AASHTO T 307 Resilient Modulus) with testing performed by FDOT SMO.
7. Consolidation testing on selected soils and associated GTR blends
8. Creep testing on selected soils and associated GTR blends (one-dimensional oedometer test developed at FIT).

1.2.8. Task 8 Data Reduction:

The data obtained during the testing program was reduced to useful engineering tabular and graphical formats. The database system was used to categorize the data for use in the analysis.

1.2.9. Task 9 Data Analysis:

The reduced data was analyzed to determine useful correlations related to the overall project objective. These findings are presented in this report.

1.2.10. Task 10 Technology Transfer:

Quarterly Progress reports were prepared throughout the research, presentations were made to FDOT personnel throughout Florida at annual Geotechnical Research in Progress (GRIP) meetings, and a comprehensive final report was prepared for the technology transfer.

2. Literature Review

The team conducted a literature search to identify previous research on blends of ground tire rubber and base or subbase soils.

2.1. Strength-Deformation Characteristics of GTR Blends

2.1.1. Shear Strength of Waste Tires-Sand Blends

Cabalar (2011) blended GTR with sands from two geologic formations, Leighton Buzzard Sand (LBS) and Ceyhan Sand (CS). These sands were selected for their differences in structure and engineering properties. LBS is coarse with sub angular particles, and CS is fine with angular particles. The rubber particle size was not listed but the particles were described as "flaky." Rubber was blended with each type of sand at 5, 10, 20, and 50% by weight. The rubber's specific gravity was between 1.02 and 1.36.

Each blend was subjected to direct shear tests (ASTM D-3080) using normal stresses of 4.06, 6.09, and 9.86 psi (28, 42, and 68 kPa). Tests were conducted to strains of approximately 18%. The shear stress and internal friction angle of the two mixtures decreased at about 10% rubber concentration and then leveled off. The following equations were presented to estimate the shear strength of the two sands:

$$\tau_{CS} = 11 + 0.404\sigma\varepsilon^{1/2} - 0.357(RC)^{1/2}\sigma^{1/2} - 0.0067\varepsilon\sigma^{1/2}$$
$$\tau_{LBS} = 16 + 0.14\sigma\varepsilon^{1/2} - 1.45(RC)^{1/2}(1/\varepsilon^{1/2})$$

τ_{CS} = CS Shear Stress (kPa)

τ_{LBS} = LBS Shear Stress (kPa)

σ = Normal Stress (kPa)

ε = Horizontal Strain (%)

RC = Rubber Content (%)

The author concluded that the blends were useful as lightweight embankment fill on weak foundation soils and retaining wall backfill material since the sand rubber mixtures were significantly lighter than 100% sand mixtures.

Ghazavi (2004) investigated the suitability of recycled granular rubber as a lightweight backfill material. The author included a survey of waste tire research (Table 2-1).

Table 2-1 Literature Survey (after Ghazavi, 2004)

Rubber application	**Studies**
Road construction	Bosscher et al. (1997) Heimdahl and Druscher (1999) Nightingale and Green (1997)
Erosion control	Poh and Broms (1995)
Slope stabilization	Poh and Broms (1995) Garga and O'Shaughnessy (2000a)
Retaining structure lightweight backfill	Bosscher et al. (1997) Lee et al. (1999) Basheer and Najjar (1996) Sumanarathna et al. (1997) Garga and O'Shaughnessy (2000a) Garga and O'Shaughnessy (2000b)
Landfill leach beds	Foose et al. (1996)
Asphalt concrete additive	Tuncan et al. (1998) Foose et al. (1996) Heimdahl and Druscher (1999)
Sound barriers	Hall (1991)
Limiting freezing depth	Humphrey et al. (1997)
source for creating heat	Lee et al. (1999)
Coal-fired boiler fuel supplement	Ahmed and Lovell (1993)
Vibration isolation	Eldin and Senouci (1994)
Cushioning foams	Bader, 1992 Ahmed and Lovell (1993)
Ductile low strength concrete	Eldin and Senouci (1993)).

Ghazavi tested rubber blended with uniform sand with specific gravity of 2.63 and density ranges from 89.04 lb/ft^3 (14.0 kN/m^3) to 107.48 lb/ft^3 (16.9 kN/m^3). Blends included 10, 15, 20, 50, and 70% rubber particles by weight. The rubber had a nominal size of 0.95 inch (24 mm) with diameters between 0.079 inch (2 mm) to 1.5 inch (38 mm), and specific gravity ranging from 1.08 to 1.18.

Loose compaction was achieved by pouring the sand-rubber mixture into a shear box from a low height, while slightly compacted specimens were placed in a similar box, and compacted with the use of a 4.4 lb (2 kg) hammer dropped from a height of 3.94 inch (100 mm) onto a circular wooden plate covering the specimen. At concentrations of 30% and higher, segregation occurred between the sand and rubber particles, particularly with longer strips of rubber. A summary of the densities achieved with the two-compaction techniques is presented in Table 2-2.

Table 2-2 Density of Rubber/Soil Blends (Ghazavi, 2004)

Rubber Content (%)	Mixture Unit Weight			
	Loose		Slightly Compacted	
	lb/ft^3	kN/m^3	lb/ft^3	kN/m^3
0	89.0	14.0	92.2	14.5
10	82.0	12.9	85.9	13.5
15	78.2	12.3	82.7	13.0
20	69.3	10.9	78.9	12.4
50	49.0	7.7	50.9	8.0
70	40.7	6.4	42.6	6.7
100	29.9	4.7	32.4	5.1

The specimens were subjected to direct shear tests using three normal stresses of 3.4, 7.9, and 14.8 psi (23.3, 54.8, and 102 kN/m^2). Figure 2-1 shows the variation in friction angle for the various GTR blends. The peak friction angles are at zero percent rubber for the dense blends or at the lower percentages for the loose blends. The loose compaction process may produce larger variations in friction angle than the dense blends because any small change in density would change the friction. Therefore, the trend of an increasing friction angle at the low blend percentages may simply be the results of the error typically associated with the loose compaction process. Overall, there is a decrease in the friction angle with increasing percentages of rubber.

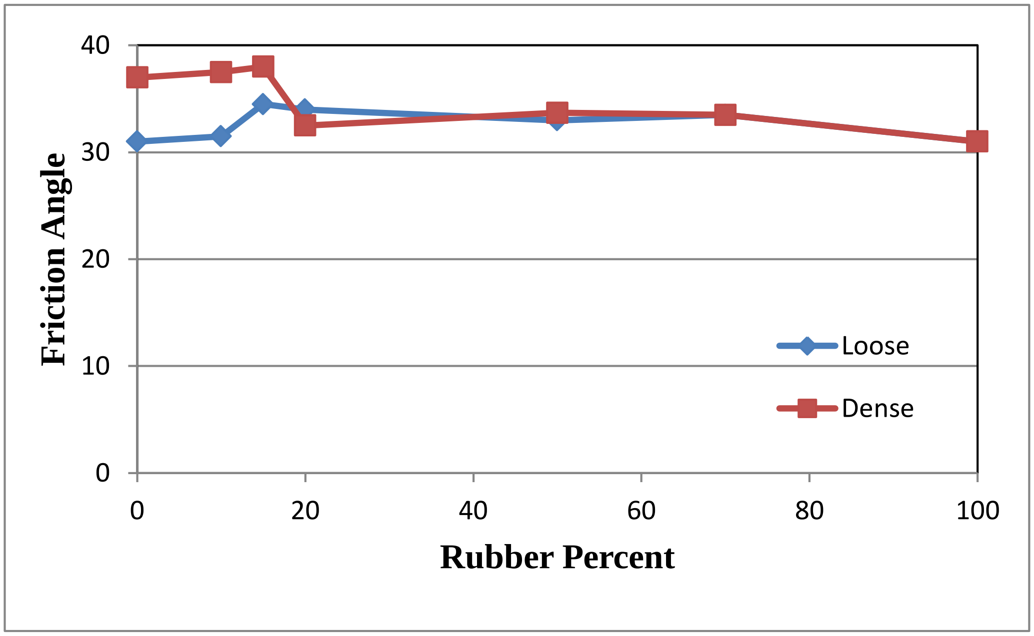

Figure 2-1 Variation of Initial Friction Angle versus Rubber Content for Loose and Compacted Blends (Ghazavi, 2004)

Figure 2-2 shows the variation in unit weight for the sand-rubber blends. The unit weight of the soil was reduced from approximately 14 kN to approximately 8 kN original for the 70% rubber blend. Ghazavi concluded that:

- The addition of rubber to the sand did not improve the shearing resistance of the blends.
- An apparent cohesion of approximately 1.5 psi (10 kPa) was obtained from blends containing rubber grains.
- The initial friction angle of the mixtures decreased with increasing percentages of rubber.
- The unit weight of the blends decreased with the addition of rubber.

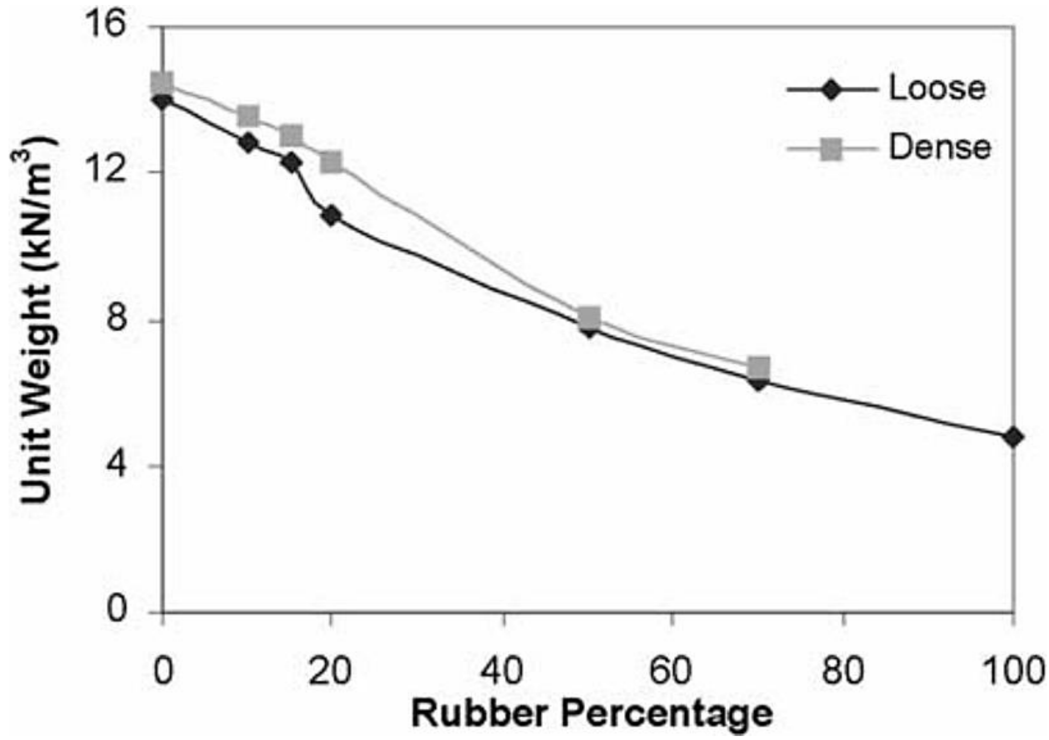

Figure 2-2 Variation in Unit Weight for Sand-Rubber Blends (Ghazavi, 2004)

2.1.2. Compressibility and Strength Behavior of Sand-Tire Chip Mixtures

Ventatappa and Dutta (2006) performed a study with the objective of determining the compressibility and strength characteristics of sand and tire (termed "tyre") chip mixtures. The researchers in this study assessed the suitability of sand-tire chip mixtures for embankments or other road development.

Three sizes of waste tire pieces were used: 0.39 inch x 0.39 inch (10 mm x 10 mm), 0.39 inch x 0.78 inch (10 mm x 20 mm), and 0.78 inch x 0.78 inch (20 mm x 20 mm). The specific gravity of the rubber ranged from 1.02 to 1.26, with an average value used of 1.15. Rubber content had more influence on density than compaction energy, and vibratory compaction was ineffective. The rubber chips experienced most of their compression during initial loading stages and had little elastic rebound, implying that preloading could be useful in reducing consolidation.

The experimental program consisted of confined compressibility, cyclic loading, and triaxial tests. The concentrations of rubber ranged from 0-100% for compressibility, and 0-20% for all other tests. Higher rubber concentrations deformed vertically and horizontally at stresses of over 29 psi (200 kPa).

Table 2-3 shows a summary of the vertical strains recorded at 11.6 and 29 psi (80 and 200 kPa). Vertical strains increased dramatically at rubber contents over 80 percent (Figure 2-3). The authors concluded that compressibility of sand-tire mixtures with 20% or less rubber was 1% or less for a 10m embankment and, hence, was within tolerable limits.

Table 2-3 Confined Vertical Compressive Strain for Sand-Tire Chip Admixtures (after Venkatappa Rao and Dutta, 2006)

	Vertical strain (%) for sand tire chip admixture at a vertical stress of					
	Type I chips		Type II chips		Type III chips	
Tyre chip content (%)	11.1 psi (80 kPa)	29.0 psi (200 kPa)	11.1 psi (80 kPa)	29.0 psi (200 kPa)	11.1 psi (80 kPa)	29.0 psi (200 kPa)
0	0.13	0.33	0.13	0.33	0.13	0.33
5	0.13	0.42	0.22	0.56	0.28	0.56
10	0.19	0.51	0.26	0.66	0.37	0.74
15	0.28	0.67	0.40	0.75	0.50	0.93
20	0.33	0.84	0.49	0.94	0.59	1.10
80	2.06	4.00	3.39	5.09	3.96	5.84
100	8.53	14.91	10.66	18.86	10.84	19.06

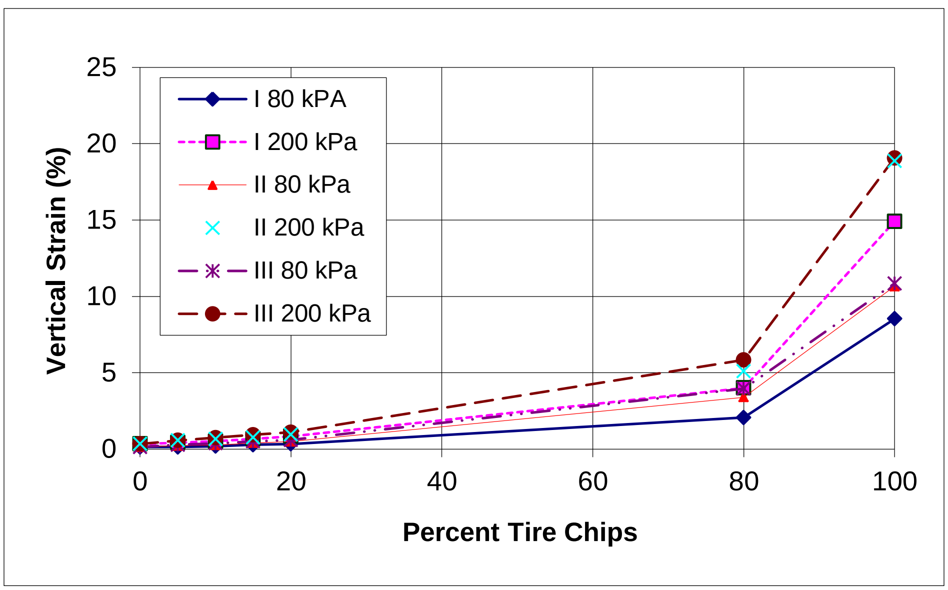

Figure 2-3 Percent Tire Chips versus Vertical Confined Compressive Strain (adapted from Venkatappa Rao and Dutta, 2006)

During the cyclic loading 32.6 psi (225 kPa) was exerted on a specimen for 10,000 cycles. The blends exhibited a fairly linear log-strain rate up to about 2% strain. The three different types of waste tire rubber produced no measureable differences in cyclic compressibility.

As shown in Figure 2-4 and Figure 2-5 the addition of the rubber improved apparent cohesion (c') and internal friction angle (φ'). The GTR produced an apparent cohesion of between 1 and 2.5 psi (7 and 17.5 kPa) and an increase in internal friction from 38 to 40 degrees.

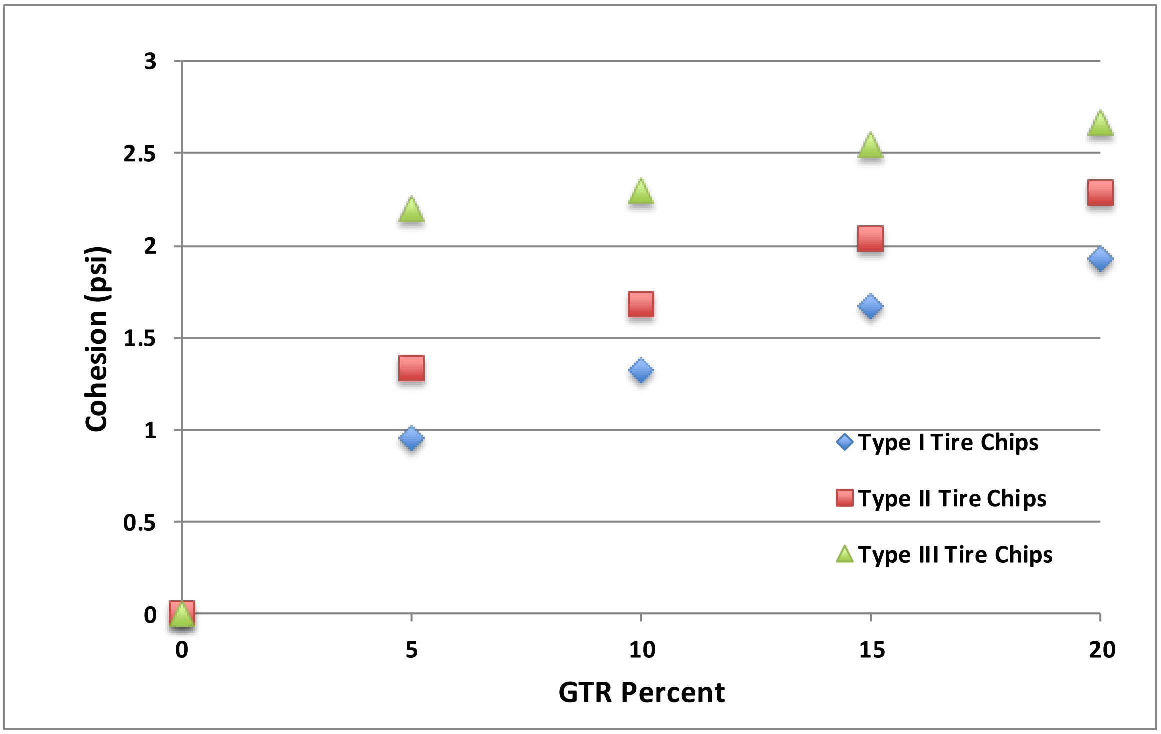

Figure 2-4 Variation in Cohesion for Sand with Tire Chips Type I, II, III for Percentages up to 20% (after Ventakappa Rao and Dutta, 2006)

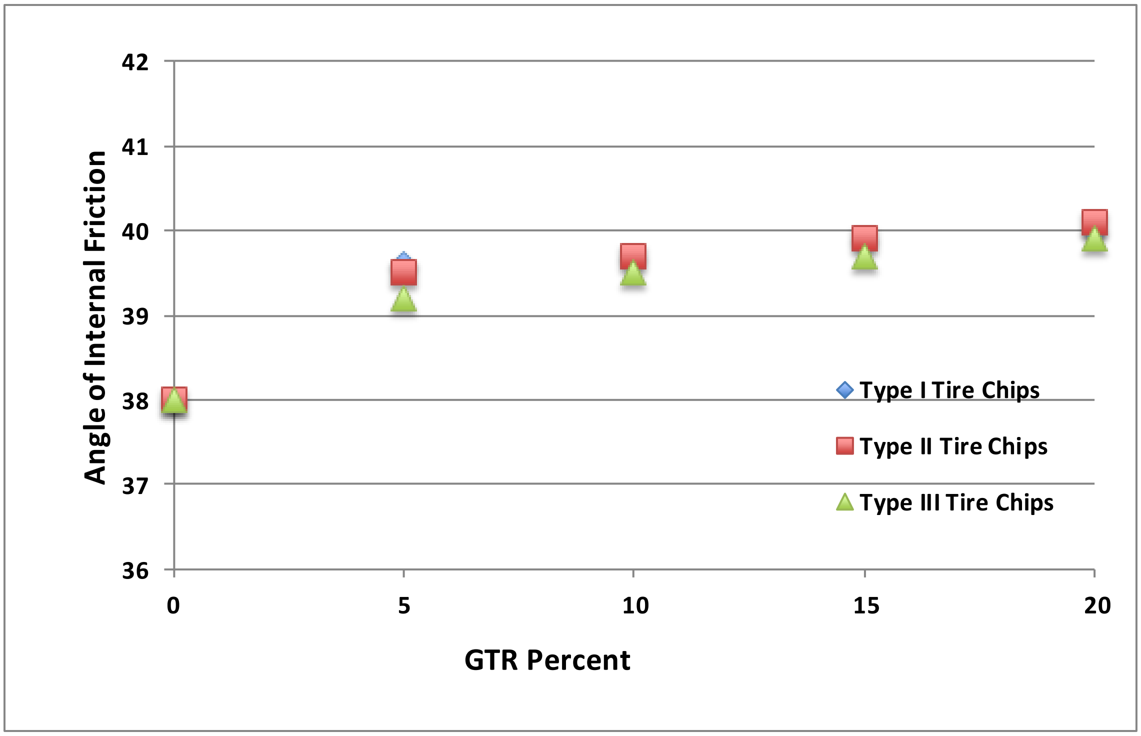

Figure 2-5 Variation in Friction Angle for Sand with Tire Chips Type I, II, III for Percentages up to 20% (adapted from Ventakappa Rao and Dutta, 2006)

The triaxial tests indicated that the resilient modulus increased with confining pressure and decreased with an increase in rubber chip content. The stress-strain behavior of the sand-rubber mixture was similar to that of 100% sand up to a concentration of 20%. These conclusions indicate that the mixes would be acceptable for smaller embankments as well as a substitute or addition to conventional fill material.

2.1.3. Determination of Elastic and Plastic Subgrade Soil Parameters for Asphalt Cracking and Rutting Prediction

Behzadi and Yandell (1996) conducted repeated load triaxial tests to distinguish the residual and resilient deformation of silty clay subgrade material. The project objective was to quantify these deformations to help understand the resulting rutting that would be expected in an asphalt pavement system. The analysis of permanent deformation indicated good agreement with the model proposed by Sweere (1990) for asphalt rutting (Equation 2-1).

$$\varepsilon_p = IN^S \qquad \text{Equation 2-1}$$

where

ε_p = plastic strain (rutting)

S = the slope of the log (ε) versus log (N) plot

I = the intercept of the log (ε) versus log (N) plot

N = the number of load cycles

The slope, S, was found to be independent of stress and density, but very small increases were observed as moisture content increased. The intercept, I**,** was found to be more sensitive to deviator stress. The test results also indicated that I increased with increasing moisture content and decreased as dry density increased. The analysis produced an exponential relationship between I and deviator stress. This model would be able to predict the plastic strain under any number of loads at any specified stress level. The resilient modulus rapidly decreased initially with increasing deviator stress and then increased slightly or was nearly constant.

2.2. Laboratory Performance of GTR Blends

Papp et al., (1997) conducted research on shredded scrap tires blended with subbase soils under flexible pavements. Resilient modulus (M_r) testing was used to determine the plastic and elastic strains. Tests were conducted on cohesionless soils blended with varying amounts of shredded tire chips. Blend ratios ranged from 0.1 to 0.5 tire chips to soil by dry weight. The performance of the shredded tire blends was compared to that of the naturally occurring virgin soil used in subbase applications in New Jersey.

The authors discussed compaction method, optimum shredded tire to soil ratio, optimum size and gradation of shredded tire chips, and California Bearing Ratio (CBR)strength testing. . They noted that steel protruding from the tire chips caused mixing problems. The authors cited production costs of $0.14 per tire for 1.96 inch (50 mm) chips and $0.26 per tire for 0.98 inch (25 mm) chips. Costs were based on a production rate of 500 tires per hour. The specific gravity of the tire chips ranged from 1.235 to 0.986, with 1.1 used for the blending calculations. The virgin subbase was clean well-graded sand with 2% passing #200 sieve (A-1-a).

Their results as shown in Figure 2-6, indicate that dry density decreased with the addition of tire chips in a manner similar to that reported by Ghazavi (2004). As shown in Figure 2-7, and Figure 2-8 CBR and Resilient Modulus decreased with the addition of tire-chips. The size of the tire chips did not significantly influence the results.

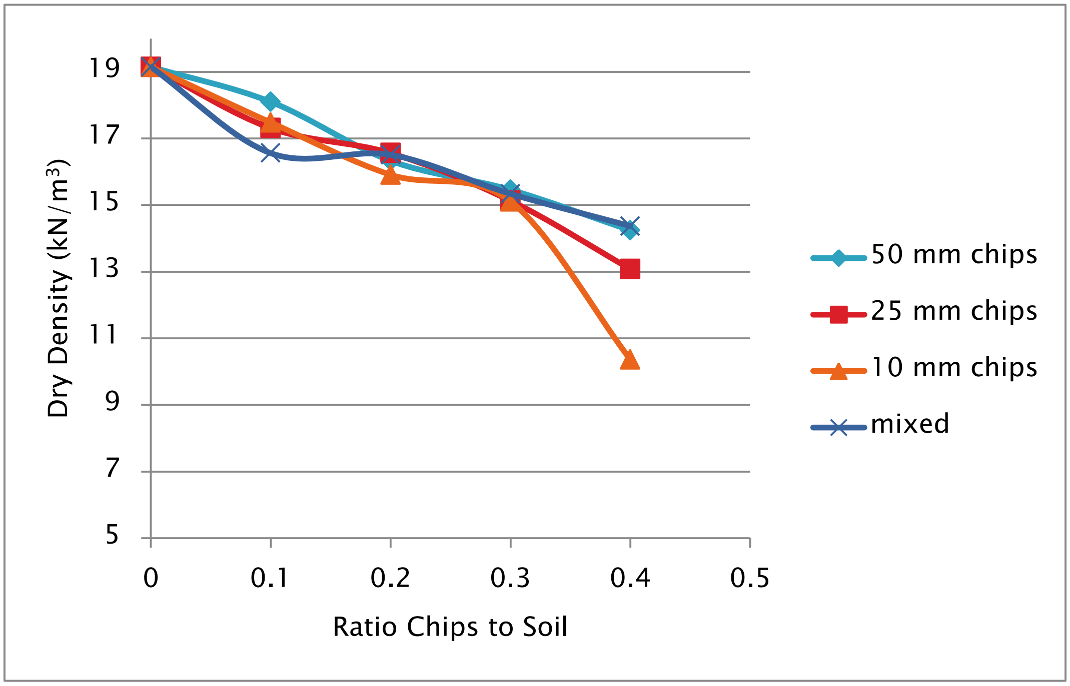

Figure 2-6 Dry Density Results for Tire/Soil Mixture (after Papp et al., 1997)

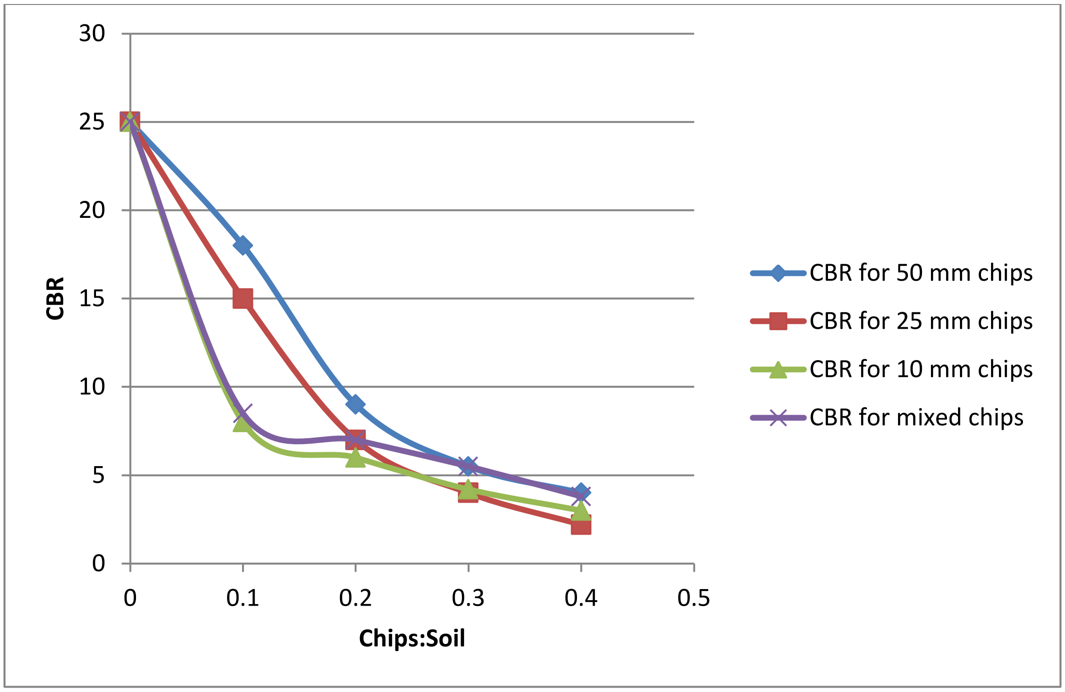

Figure 2-7 CBR Results for Tire/Soil Mixtures (adapted from Papp et al., 1997)

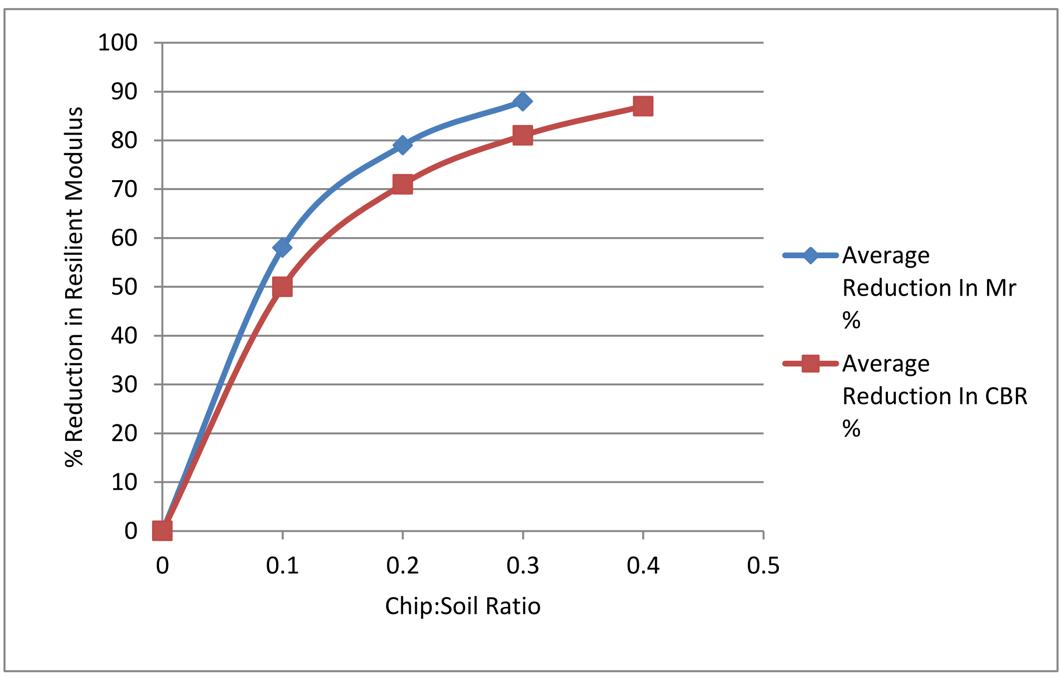

Figure 2-8 Reduction in Resilient Modulus and CBR Values (adapted from Papp et al., 1997)

The authors concluded that physically mixing tire chips with the soil did not present any problems except when excessive steel wires were protruding from the chips. The addition of the tire chips to the soil reduced both density and strength of the soil. The 50-mm (1.96-inch) tire chips were most economical and had the least negative strength impact.

Speir and Witczak (1996) investigated shredded rubber blended with conventional unbound aggregate base and subbase materials for use as structural layers within a pavement system. Two types of aggregate were selected: a graded aggregate base (GAB) and sand subbase material. Blends of 0, 7.5, and 15% rubber by weight were evaluated. The rubber had a nominal dimension of 3/8 inch (9.5 mm) (60 to 70 percent retained on the 3/8-inch (9.5-mm) sieve). This size was selected to meet the ISTEA (Intermodal Surface Transportation Efficiency Act) definition of a less finely ground scrap tire particle (shredded rubber).

The authors reported that the cost of finely ground crumb rubber for HMAC ranges between \$0.10 and \$0.30/lb (\$0.22 and \$0.66/kg), while shredded rubber typically costs between \$0.01 and \$0.03/lb (\$0.02 and \$0.07/kg). The authors estimated that use of shreds rather than crumb rubber in the granular layers could save states between \$0.07 and \$0.29/lb (\$0.15 and \$0.64/kg) of rubber. Speir and Witczak (1996) estimated that nearly 20 times more whole tires will be consumed by blending rubber with the subbase compared with the amount of whole tires consumed by using rubber as an admixture in hot mix asphaltic concrete.

The authors developed the following conclusions:

Shredded rubber in GAB - The addition of shredded rubber causes a decrease in the maximum dry density and a corresponding increase in optimum moisture content for both the modified and standard Proctor compaction. The increased rubber caused significant reductions in CBR values (Figure 2-9). As little as 5% shredded rubber caused moderate reductions in M_r values. On the basis of these observations, it was concluded that use of shredded rubber in a dense-graded aggregate base course is not feasible.

Shredded rubber in sand - Adding shredded rubber to the sand subbase material resulted in a decrease in the optimum density for both modified and standard Proctor compaction. Increasing rubber percentages had little effect on CBR values (Figure 2-9). The coefficient of permeability increased at higher concentrations of rubber, indicating improved drainage. Because the observed properties of the sand in several cases were unaffected by the addition of the rubber, the authors concluded that the use of shredded rubber in sand subbases may be a technically feasible alternative to the use of rubber in pavement systems and that further research is warranted.

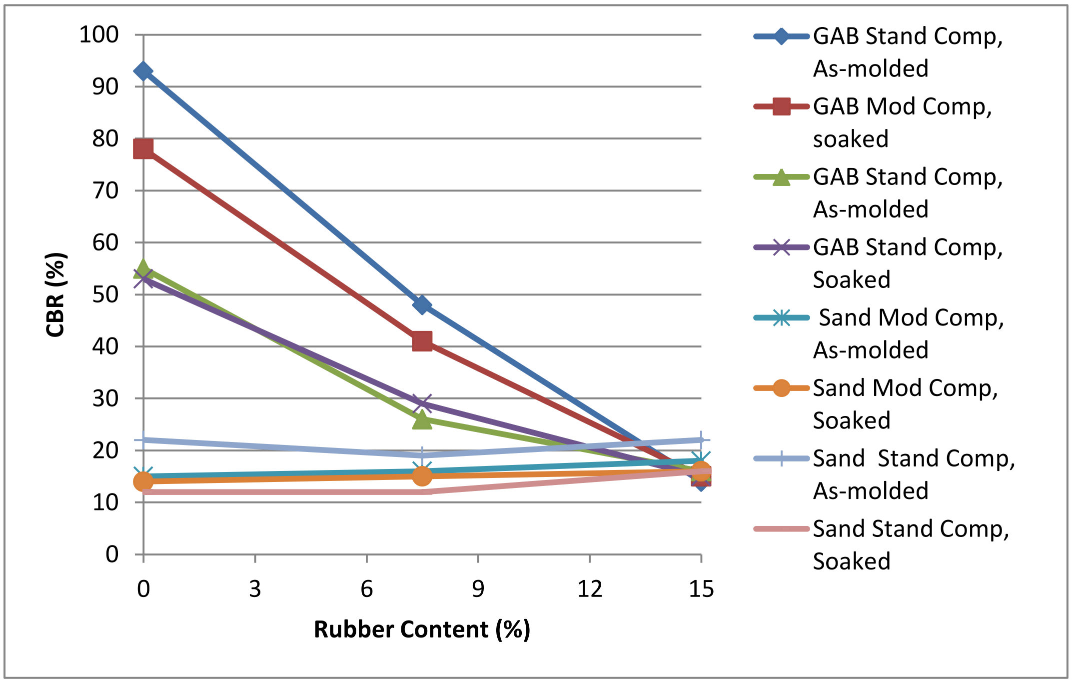

Figure 2-9 CBR Values at Optimum Moisture Contents (after Speir and Witczak (1996))

2.3. Creep Behavior of Subgrade Soils

Singh and Mitchell (1968) developed equations describing the creep relationships between strain and time, and strain rate and time for a variety of soil types. Figure 2-10 shows the general creep behavior of soils subjected to a constant deviator stress (i.e., σ_1-σ_3). The stress level shown was normalized as creep stress divided by the failure stress. At deviator stresses less than 30% of the failure stress the creep deflections were small and ceased over time. Higher stress levels (30 to 90% of failure) resulted in prolonged creep but not rupture. Deviator stresses over 90% of the failure stress resulted in a secondary creep stage with constant creep rate followed by a tertiary stage of accelerating strain rate leading to rupture. The basic Singh and Mitchell (1968) relationship is:

$$\dot{\varepsilon} = Ae^{\propto D}\left(\frac{t_1}{t}\right)^m \qquad \text{(Equation 2-2)}$$

$\dot{\varepsilon}$ =strain rate at any time t
A = the strain rate obtained by plotting log strain rate versus deviator and finding the intercept when *D* = 0
α = slope of the linear portion of the logarithm strain versus deviator-stress plot
D = deviator stress
t = time
t_1 = unit time baseline
m = slope of log (strain) versus log (time) line

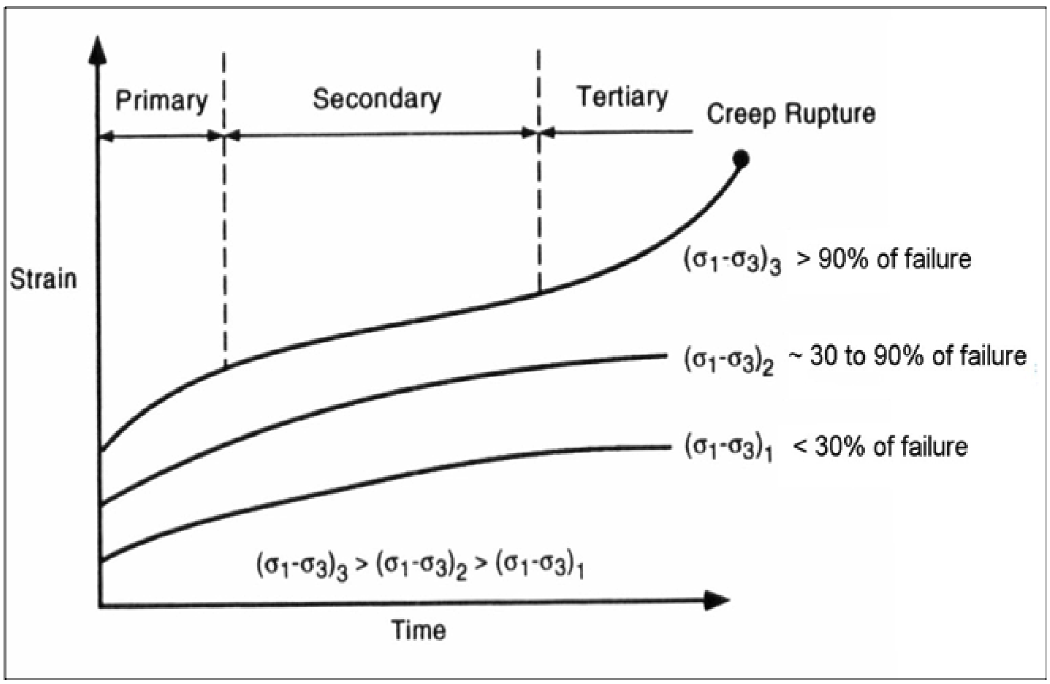

Figure 2-10 Creep under Constant Stress (Singh and Mitchell, 1968)

The stress intensity, *D*, was originally taken as the triaxial creep test deviator stress (σ_1-σ_3) but may be taken as uniaxial stress in an oedometer test (19). The parameters *A*, α and *m*, can be determined by performing two or more creep tests on identical specimens at different stress levels. Plotting the log strain rate versus log time defines *m*. Plotting the log strain rate versus stress for two separate times defines α (slope) and *A* (intercept).

The rate of creep remains constant during the secondary phase of creep settlement. A reasonable approximation of the secondary creep rate can be obtained by performing a logarithmic trend-line fit to experimental creep test data. The primary creep phase is characterized by rapid deformation caused by elastic and plastic soil compression when the load is initially applied. After a brief period the initial compression stabilizes and creep under constant load begins (secondary creep in Figure 2-10). Figure 2-11 shows typical creep test results in both linear and log(time) plots. The critical portion of each of these curves occurs once the slope of the strain versus log(time) plot becomes constant (secondary creep) after approximately 15 minutes. If soil stresses remain in the 30-90% of failure range, this straight-line portion may be used to predict creep displacements over the design life of a pavement. The slope of the secondary creep curve in log time is referred to as the creep strain rate (CSR). As the CSR increases, the creep increases.

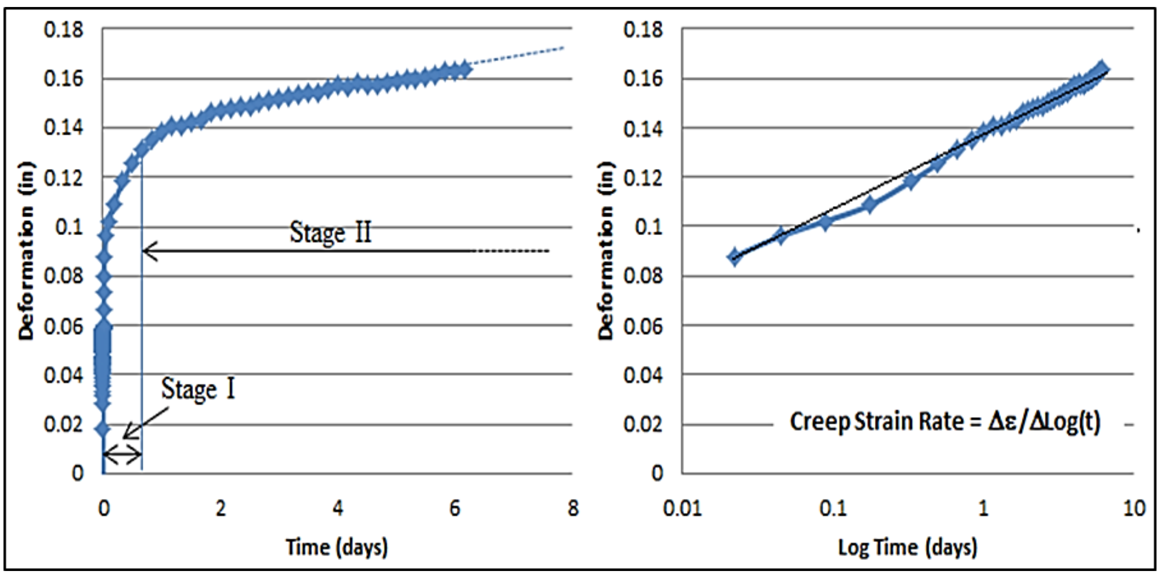

Figure 2-11 Typical Creep Test Results in Linear Time and Log(time)

Figure 2-12 shows the variation in creep strain with time between an AASHTO A-3 sand and subsequent blends of the sand with RAP (Dikova, 2006). The 100% RAP produced excessive amounts of creep and an unacceptable creep strain.

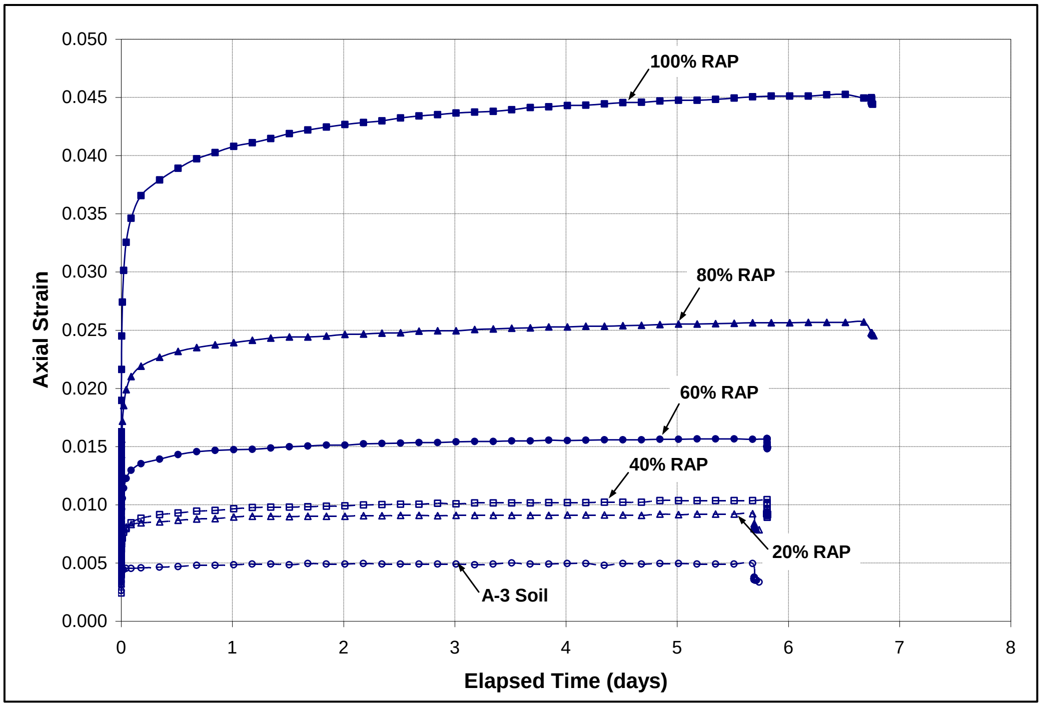

Figure 2-12 Variation in Creep Strain from A-3 Sands to 100 % RAP (Dikova, 2006)

Figure 2-13 shows a summary of the CSR values obtained for common pavement base and subbase materials were tested as part of several FDOT research projects investigating RAP and RAP-soil blends (Cosentino et al., 2003, 2008, and 2012). Conventional base or subbase materials such as limerock, cemented coquina, crushed concrete and A-3 sand show negligible creep. The CSRs for limerock and A-3 sand are approximately one order of magnitude lower than those for 100% RAP specimens. The CSRs for these three materials were used to categorize the CSRs of the GTR/soil blends tested in this research as acceptable or unacceptable.

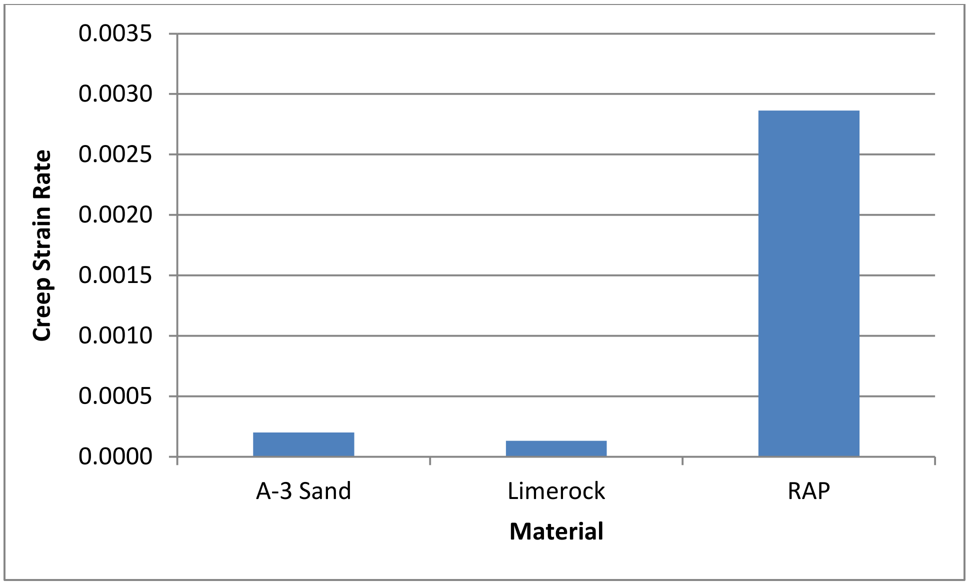

Figure 2-13 Summary of Creep Strain Rates for Various Materials (after Cosentino et al., 2012)

3. Methodology

3.1. Material Selection

The testing program was developed to evaluate engineering properties of GTR/subgrade soil blends. The research team determined that a wide range of GTR sizes and concentrations were critical to understanding the behavior of GTR/subgrade blends. Three soil types were selected through a coordinated effort with FDOT's State Materials Office (SMO). FDOT SMO also provided a list of approved ground tire rubber (GTR) distributors.

3.1.1. Subgrade Soils

As explained in Section 1.2.3, LBR was the basic engineering property used to select sources for the subgrade materials. SMO identified sources and provided assistance in obtaining samples that were delivered to the Florida Institute of Technology laboratory. Sources of and characteristics of the selected subgrade soils are shown in Table 2-1

Table 3-1 Soil Sources Selected for Investigation

Category	**Approximate LBR**	**Source**	**AASHTO classification**
Low LBR Soil	20	Whitehurst Pit	A-3
Medium LBR Soil	40	Orange Heights Pit	A-2-4
High LBR Soil	80	FDOT Maintenance Pit 26105	A-2-4

3.1.2. Ground Tire Rubber (GTR)

After discussion with several suppliers, the research team selected Global Tire Recycling in Wildwood, Florida, as an FDOT-approved crumb rubber source. Global Tire Recycling processes over 2 million tires annually into approximately 16,000 tons of GTR. Global Tire Recycling uses the ambient processing technique of mechanically shredding and pulverizing tires into varying sized particles. The process is physically similar to aggregate production with machines which produce varying size output which is then passed through screens to segregate the material by size. The smaller materials are completely wire, fiber, moisture, and contaminant free. The research team selected the 1-inch (25.4mm), 3/8-inch (9.53-mm), and #40 (0.422-mm) mesh sizes of GTR to include the maximum, median, and minimum sizes of GTR available (large tire strips were ruled out due to complications to be expected in the application process).

3.2. Volumetric Blending

On the construction site, GTR would be blended by placing a lift of loose material on top of a fixed depth lift of soil and then mechanically tilling to blend the materials. To simulate this procedure in the lab, the research team used blending by volume rather than blending by weight. Based on discussions with FDOT personnel the research team selected five representative GTR lift thicknesses blended into 12-inch lifts of loose soil (Table 3-2).

The loose bulk density of each GTR and soil type was determined using the procedure for measuring loose density in vibratory compaction (ASTM 4253). Blends with 4%, 8%, 16%, 24%, and 32% GTR by volume were prepared using the loose densities. The loose densities of the three-subgrade soils averaged 90 pcf and 25 pcf for the GTR sizes.

Table 3-2 Summary of GTR-Subgrade Soils Blend Percentages by Weight and Volume

Soil Type	GTR lift per 12 inches of soil	GTR % by Weight	GTR % by Volume
High LBR	½ inch	1.14	4
	1 inch	2.29	8
	2 inch	4.66	16
	3 inch	7.13	24
	4 inch	9.68	32
Medium LBR	½ inch	1.17	4
	1 inch	2.37	8
	2 inch	4.81	16
	3 inch	7.35	24
	4 inch	9.97	32
Low LBR	½ inch	1.29	4
	1 inch	2.60	8
	2 inch	5.28	16
	3 inch	8.04	24
	4 inch	10.89	32

3.3. Testing Procedures

3.3.1. Sieve Analysis

Grain size analyses were performed by dry sieving (FM 1-T 027) The high and medium LBR materials had a significant fine content so wet sieve analyses were performed (FM 1-T011). Analyses were performed using the U.S. standard sieves shown in Table 3-3:

Table 3-3 Sieve Sizes

1.5 inch (38.1 mm)	#10 (2.00 mm)
1 inch (25.4 mm)	#40 (0.422 mm)
3/4 inch (19.0 mm)	#60 (0.251 mm)
3/8 inch (9.51 mm)	#200 (0.075 mm)
#4 (4.75 mm)	

A motorized sieve shaker was used (see Figure 3-1). Individual batches weighed approximately 1.0 pound (2.20 kg) to limit the quantity of material on a given sieve. Three specimens were tested to generate an average gradation for each source material tested. The results of these tests were used to classify the materials according to the Unified Soil Classification System (USCS) and the AASHTO system. Evaluation included the overall material gradation and calculated properties such as fineness modulus and coefficients of curvature, C_c and uniformity, C_u.

Figure 3-1 Sieve Shaker with Sieves (Diouf, 2011)

3.3.2. Atterberg Limits

ASTM T-89 and T-90 were conducted to determine the liquid and plastic limits of the three soil types.

3.3.3. Optimum Moisture Content

Optimum moisture content for high, medium, and low LBR soils were determined based on modified Proctor compaction (FM 5-515). When trimming specimens blended with 3/8 inch (9.53 mm) and #40 (0.0422 mm) GTR surficial holes were patched with a soil-GTR blend. When trimming specimens blended with 1 inch (25.5 mm) GTR surficial holes in the specimens were patched with smaller diameter soil.

3.3.4. Limerock Bearing Ratio (LBR) Test

Florida DOT specifications use LBR, a variation of the California Bearing Ratio (CBR) test, for evaluating base or subgrade soils. The test determines the bearing value of the soil/GTR blends at their optimum moisture content as determined in the previous set of laboratory tests. The primary difference between the CBR and LBR is that the CBR uses a bearing strength of 1,000 psi (6.89 MPa) as an index basis while the LBR uses 800 psi (5.52 MPa).

3.3.4.1. LBR Procedure

Three specimens of each GTR/Soil blend were compacted by the modified Proctor method (FM 5-515) at optimum moisture content in six-inch LBR molds.

a b

Figure 3-2 a) Modified Proctor Compaction, b) Soaking Specimens

These GTR/soil batches were blended at optimum moisture content and left to sit for 24 hours to ensure proper moisture distribution throughout the batch. Following compaction the specimens were inverted and the spacer plate removed. The specimens were transferred to soaking bath and swell plates were placed on top of the specimens. The specimens were left to soak for 48 hours.

After soaking, the samples were removed from the bath and drained for 15 minutes before being placed in the LBR/CBR testing machine. This machine pushed a three square inch piston into the specimens at a constant rate of 0.05 in/min (1.27 mm). Three 5-pound (2.27 kg) surcharge plates were placed on top of the specimens since this would be a subgrade material. The tests were conducted until a penetration depth of 0.5 inches (12.7 mm) was reached (Figure 3-3). Throughout the testing, a LabView® program was simultaneously recording the resistance load in pounds and penetration in inches. The program also plotted these data points throughout the test where the penetration in inches was placed on the horizontal (x) axis, and the load in pounds on the vertical (y) axis. Once testing was complete, the data points were then saved into a comma separated variable (csv) format which could be opened in Microsoft Excel.

a b

Figure 3-3 a) LBR Surcharge Plates, b) LBR Test with Surcharge Plates

3.3.4.2. LBR Data Reduction

Once the testing data was saved into Excel, deflection versus load plots were created for each test specimen. These curves usually have an initial concave upward shape due to surface irregularities. A tangent slope was then drawn through the region of greatest slope. The point at which this line crossed the horizontal (x) axis was changed to the new origin. From the new origin, the load reading corresponding to the new 0.1-inch (2.54-mm) deflection was recorded for each test. This value was divided by 3 in^2 (1,935 mm^2) to convert the load into a pressure of pounds per square inch (lb/in^2). That value was then divided by 800 and multiplied by 100 as per LBR procedure. LBR values were recorded for each virgin soil and GTR/soil blend. These values were then plotted on several figures to determine any trends within the type of soil or size of GTR.

3.3.5. Resilient Modulus Test

Blends were prepared at FIT using the percentages of GTR by volume previously shown in Table 3-2 for all three subgrade types (high, medium, low). These specimens were then delivered to the FDOT SMO for resilient modulus testing (AASHTO T 307). The complete test data are shown in Appendix C.

Figure 3-4 shows a photo of the SMO resilient modulus loading-frame and triaxial cell, with the linear variable differential transducers (LVDT's) mounted outside the chamber. During testing, the confining stresses varied from 2 to 6 psi (14 to 42 kPa) and deviator stresses varied from 2 to 10 psi (14 to 70 kPa).

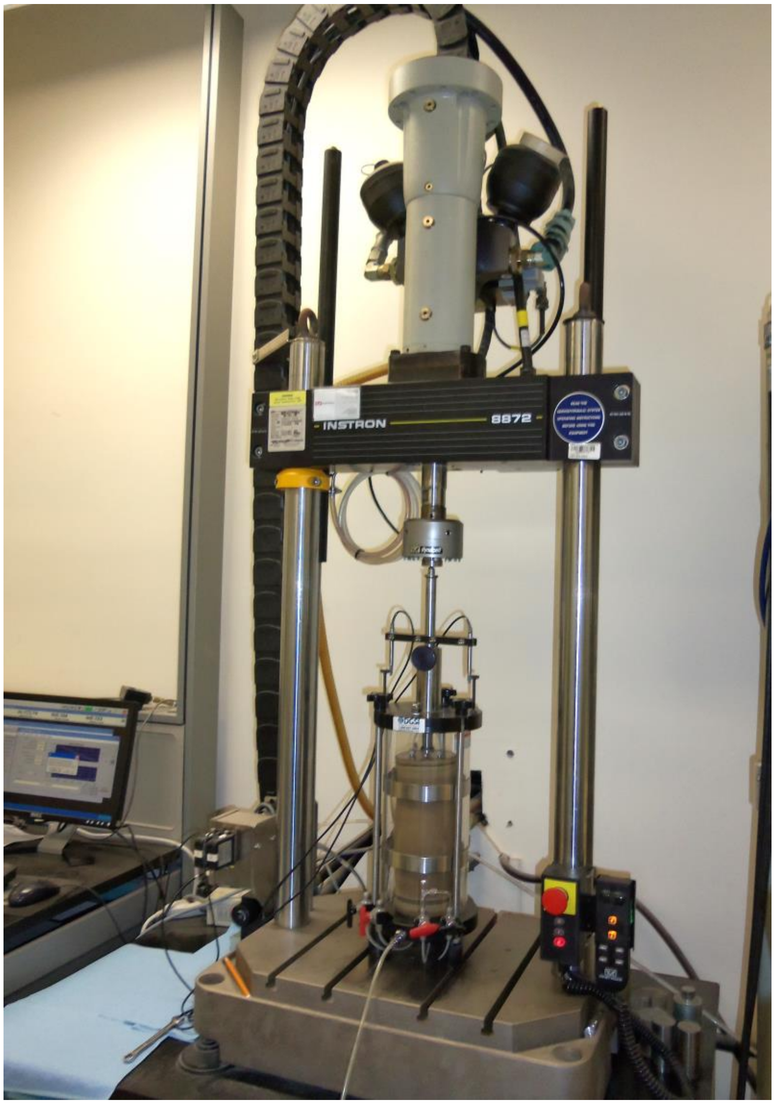

Figure 3-4 FDOT SMO Resilient Modulus Testing Equipment

3.3.6. Consolidation Test

The consolidation test was used for determining the rate and magnitude of consolidation of soil when it is restrained laterally and loaded and drained axially (FM 1-T 216). This test is usually reserved for cohesive soils, but was used in this case to determine the drainage and settlement characteristics of GTR/soil blends. The standard test on cohesive soils requires a 2-inch (50.8 mm) diameter test ring. The diameter of the testing ring must be at least 4 times the largest particle diameter. The standard ring met this criterion for the 3/8-inch (9.53 mm) and #40 (0.422 mm). A modified consolidation test was implemented to accommodate the large 1-inch

GTR pieces. The research team had a set of 4-inch (101.6 mm) diameter testing specimen rings fabricated along with grooved drainage plates to ensure double drainage (Figure 3-5).

a b

Figure 3-5 a) 4-inch (101.2-mm) Consolidation Apparatus, b) Consolidation Testing

3.3.6.1. Consolidation Procedure

The specimens were blended using the same method as the LBR test. After water was added to achieve the target moisture contents, the specimens were stored in closed containers for 24 hours to ensure even moisture distribution. The specimens were then compacted by the Modified Proctor method (FM 5-515). Following compaction, the specimens were separated from the compaction plates and placed on the consolidation apparatus. A 4-inch (101.2 mm) porous stone was placed on each end. The apparatus was then placed in a soaking basin within the testing apparatus. The specimens remained soaked throughout the entire test and were progressively loaded in seven increments: 0.25, 0.50, 1.00, 2.00, 4.00, 8.00, and 16.00 tsf (23.9, 47.9, 95.8, 191, 383, 766, and 1,244 kPa).

The same loading apparatus was used for consolidation and creep testing. The loading apparatus consisted of a frame and 4-inch piston actuated by pressurized nitrogen. The loading increments were controlled using the valve on the tanks and recorded on the dial reader connected to the piping system. A LabView® program developed by the research team was used to record the deflection increments for each set of consolidation pressures. The program recorded data every second for the first 30 seconds, then every two seconds until 5 minutes after which it record deflections every minute.

The values from the Labview® program were saved as a .csv file which was then converted to an Excel spreadsheet. After the 16-tsf (1,244 kPa) increment was completed, the file was saved with a unique identification and then two unloading pressures (4 and 1 tsf) (383 and 95.8 kPa) were conducted manually in order to obtain rebound data

3.3.6.2. Consolidation Data Reduction

Plots of deflection versus the square root of time and deflection versus log(time) were prepared in order to estimate values for t_{50} and t_{90} (times to reach 50% and 90% of consolidation respectively). Due to the nearly instantaneous nature of granular soil consolidation, the values for t_{50} were too inconclusive to be included in the test findings. The values for t_{90} were extrapolated from the deflection versus square root time plot and used to determine the Coefficient of Consolidation (c_v) for each specimen. These values were plotted versus consolidation pressure on a semi-log plot.

In addition to the c_v versus consolidation pressure plots, the test data was used to create plots of void ratio versus consolidation pressure on semi-log plots (e versus log(p) plots). Compression Index (C_c) and Recompression Index (C_r) values were determined from these plots. The values of C_c were taken from all tests and plotted on multiple graphs to determine trends among the multiple soil types or GTR sizes.

3.3.7. Constant Head Permeability Test

The Constant Head Permeability of Granular Soils test (FM 1-T 215) is used to determine the coefficient of permeability for the laminar flow of water through granular soils. This test was conducted on the GTR/soil blends to determine the drainage characteristics of the different soil blends and determine their suitability as a subgrade material.

3.3.7.1. Constant Head Permeability Procedure

The GTR/soil specimens were blended and compacted by the modified Proctor method (FM 5-515). The compaction process is similar to LBR testing procedure, but the mold does not require the 1.5-inch solid metal spacer.

Once the sample was compacted, it was removed from the compaction plate and transferred to the rest of the permeameter apparatus which included a bottom plate with a porous stone that drained through a valve, a top collar that housed the top porous stone and springs (to keep the porous stone in contact with the sample), and the top plate with another valve (Figure 3-6).

Figure 3-6 Permeability Test Apparatus

The specimens were then attached to the constant head water system built for this test. This system included a reservoir tank that maintained a constant water level with the use of an overflow tube, a series of six barbed connectors with shutoff valve combinations that allowed up to six specimens to be tested simultaneously. These barbed connections were connected to the bottom valve on the permeameter via rubber tubing. The flow of water entered the bottom of the specimen in order to expel any air bubbles from the specimen, thus creating a state of 100% saturation in the permeameter. The specimens were tested at three pressure head levels based on the step setup.

The water was initially allowed to flow into the permeameters to fully saturate the specimens. This initial saturation took from 20 minutes for the low LBR blends, up to 5 days for the high LBR blends. Once the specimens were fully saturated and water started flowing out of the top of the permeameters, a bucket was placed under each specimen to collect the water for the duration of the test. The duration of each test varied in order to collect a sufficient amount of water to be measured. Test results were collected and analyzed in an Excel spreadsheet.

3.3.7.2. Constant Head Permeability Data Reduction

Test data were used in Equation 3-1 to determine the coefficient of permeability (k) for each trial. The values for each trial were averaged to determine each blend’s k value. These values were then plotted against percentage of GTR to evaluate trends.

$$k = \frac{QL}{Ath} \qquad \text{Equation 3-1}$$

Q = volume of water discharged
T = time of flow
H = head difference
L = length of specimen
A = cross-sectional area of the specimen

3.3.8. Creep Test

Creep is the tendency of a solid material to slowly move or deform under constant stress. One-dimensional creep tests were conducted to assess the long-term deformation response of different GTR/subgrade blends subjected to a constant pressure over a seven-day period. Tests were performed using the three GTR sizes blended with the low, medium, and high LBR subgrade soils using 0%, 16%, and 32% GTR concentrations. These percentages were selected to enable the creep from the virgin material to be compared to the creep from the middle and maximum GTR percentages. FIT researchers fabricated and instrumented 12 one-dimensional creep testing devices. Six of these 12 devices and the data acquisition (DAQ) computer are shown in Figure 3-7.

Each loading apparatus consisted of two aluminum beams joined by two threaded rods. A pneumatic piston, mounted to the top beam was pressurized using compressed nitrogen to apply pressure to the top of the specimen. This pressure was transferred through a 1.0-inch (25.4 mm) diameter ball bearing to a 0.5-inch (12 mm) thick aluminum plate resting on the surface of the specimen. This ball bearing plate assembly allowed for the uniform transfer of the load to the specimen. Digital output signals from potentiometers mounted to the molds were used to record the deflection.

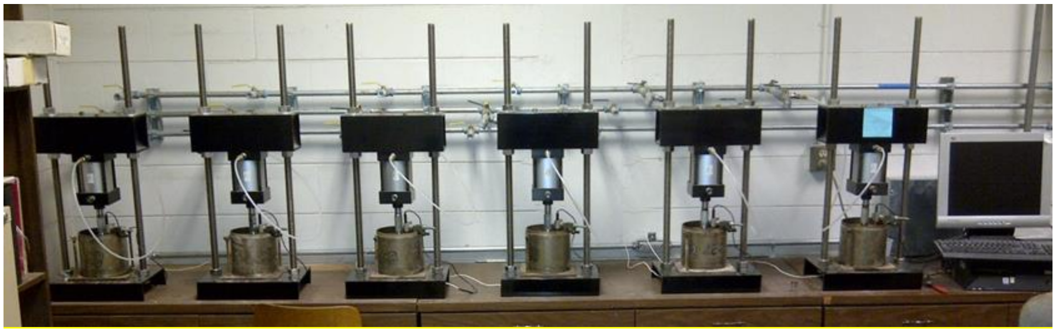

Figure 3-7 Six Creep Test Devices and Data Acquisition Computer (Diouf, 2011)

The DAQ equipment monitored the deflection of the specimen with respect to time under a constant applied pressure. Deflections from the potentiometers were recorded by a Labview® application (Figure 3-8) every second for the first two minutes of testing. The sampling interval then doubled for each specimen (2 sec, 4 sec, 8 sec, etc.) until the interval reached 4 hours. Readings continued at 4-hour intervals until the completion of the test which was typically 7 days. This sampling pattern was similar to that of the consolidation test.

The program stored the readings in a (.csv) extension file which can be used in various software packages. Data from up to 12 tests was recorded simultaneously, each test being recorded as the user chooses a different tab located on top of the Lab View® interface (Figure 3-8).

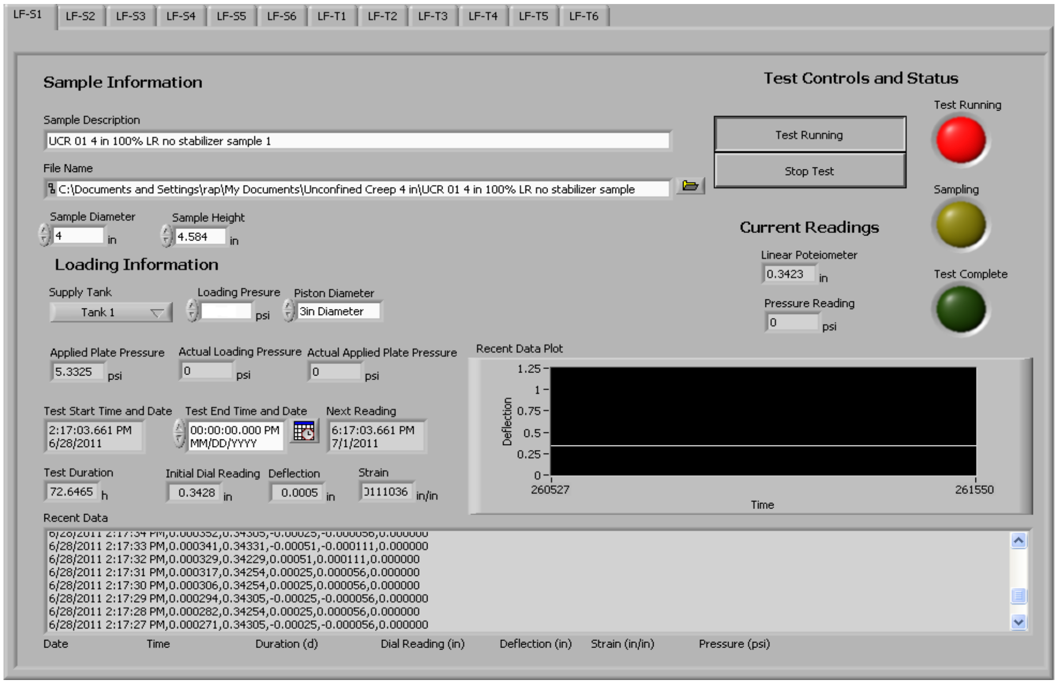

Figure 3-8 Creep Data Acquisition Program Screen (Cosentino et al., 2012)

4. Findings

4.1. Sieve Analysis Test Results

The grain size distribution results for the three-subgrade soils are shown in Table 4-1. The FIT research team and FDOT SMO performed independent testing resulting in two sets of data in each applicable property. The grain size plots are contained in Appendix A. All three soils classified as USCS sands. The percent fines ranges from a low of about 4 to a high of about 21%, with the medium LBR material having the highest fines content.

Table 4-1 Summary of Grain Size Data for Three Subgrade Sources

Property	Testing Lab	Low LBR	Medium LBR	High LBR
D_{10} (mm)	FDOT	0.08	0.08	0.08
	FIT	0.09	0.08	0.08
D_{30} (mm)	FDOT	0.12	0.85	0.18
	FIT	0.14	0.90	0.20
D_{60} (mm)	FDOT	0.17	0.15	0.32
	FIT	0.21	0.17	0.35
Uniformity Coefficient	FDOT	2.13	2.00	4.27
	FIT	2.33	2.27	4.67
Curvature Coefficient	FDOT	1.06	64.22	1.35
	FIT	1.04	63.53	1.52
Passing #200	FDOT	6.30%	21.10%	11.40%
	FIT	3.60%	18.50%	13.30%
USCS Group Symbols	FIT	SP	SM	SM

4.2. Atterberg Limits Test Results

Based on Atterberg limit tests, all three soils had non-plastic fines.

4.3. Optimum Moisture Content Test Results

Table 4-2 shows the results from the modified Proctor tests conducted to determine optimum density and moisture content (FM 5-515). The medium LBR material produced the highest dry density. The moisture-density plots are contained in Appendix B.

Table 4-2 Summary of Modified Proctor Tests on Subgrade Sources

Source	Maximum Dry Density (pcf)	Optimum Moisture Content (%)
Low LBR	107.0	12.5
Medium LBR	115.3	10.0
High LBR	122.1	7.5

4.4. Limerock Bearing Ratio Test Results

Preliminary soaked LBR tests were conducted on the virgin subgrade soils with no GTR added for baseline results. The results of those tests are shown in Table 4-3. The three soils had LBR values below, near to, and above the required value for subgrade soils (LBR = 40).

Table 4-3 LBR for Virgin Subgrade Soils

Soil	**Soaked LBR**
High	88
Med	38
Low	20

Figure 4-1, Figure 4-2, and Figure 4-3 show the variation in LBR with GTR percentage for the high, medium, and low LBR blends. The LBR plots are contained in Appendix C. The LBR values for both the 1-inch and 3/8-inch GTR decreased approximately linearly from the virgin soil value, whereas the LBR values from the #40 GTR decreased significantly initially and then decreased slightly in a linear fashion. Only the high LBR GTR blends with up to eight percent GTR would meet FDOT subgrade requirements for LBR values greater than 40 for either the 3/8-inch or 1-inch GTR blends. One set of tests was performed on a blend of high LBR material with 1.5% GTR to investigate the effect of a very low GTR concentration. Although this blend retained almost all of the virgin soil's LBR strength, it would not be practical to blend this small a concentration in the field. For the remaining tests, 4% GTR by volume was used as the lowest concentration since this modeled a 0.5-inch (12.7-mm) lift of GTR in a 12-inch (30.4-cm) lift of soil.

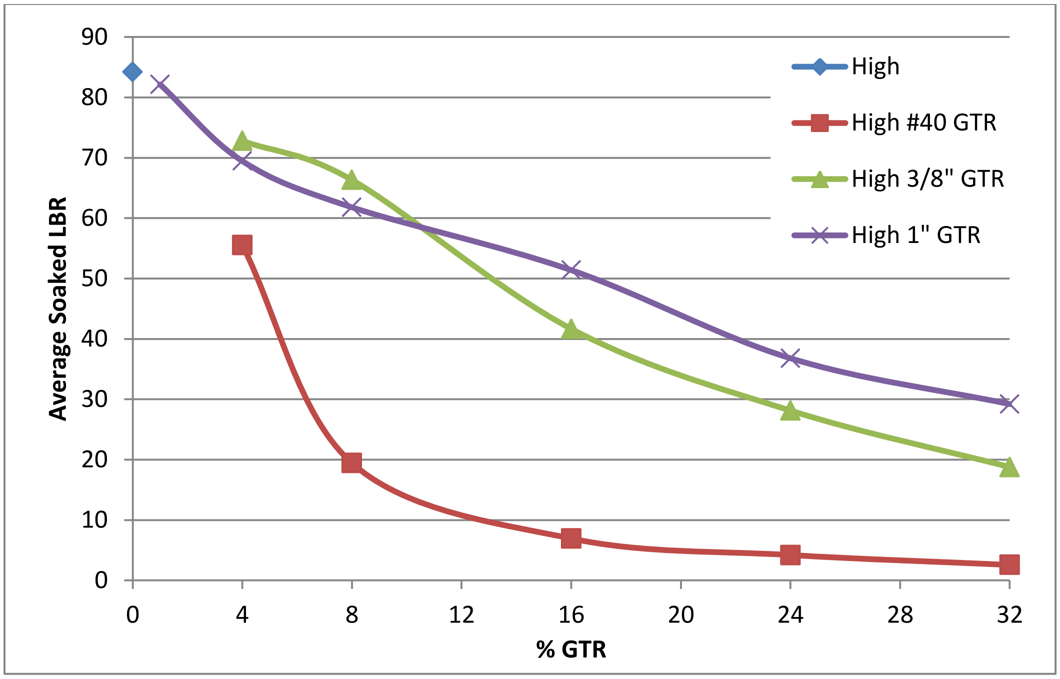

Figure 4-1 Average Soaked LBR vs GTR% for High LBR/GTR Blends

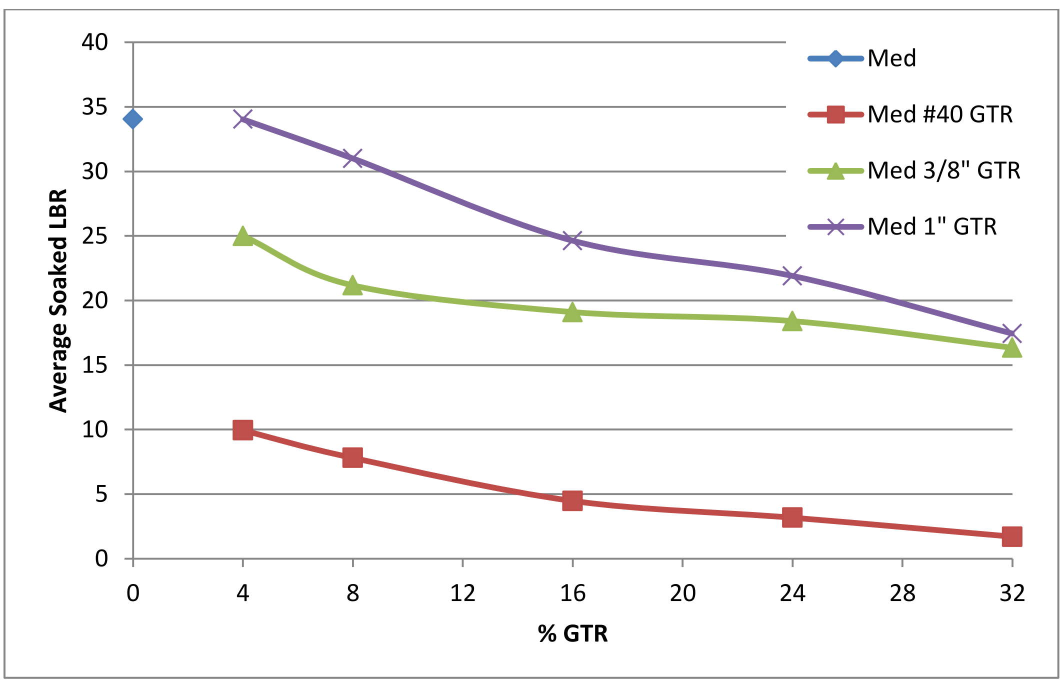

Figure 4-2 Average Soaked LBR versus GTR% for Medium LBR/GTR Blends

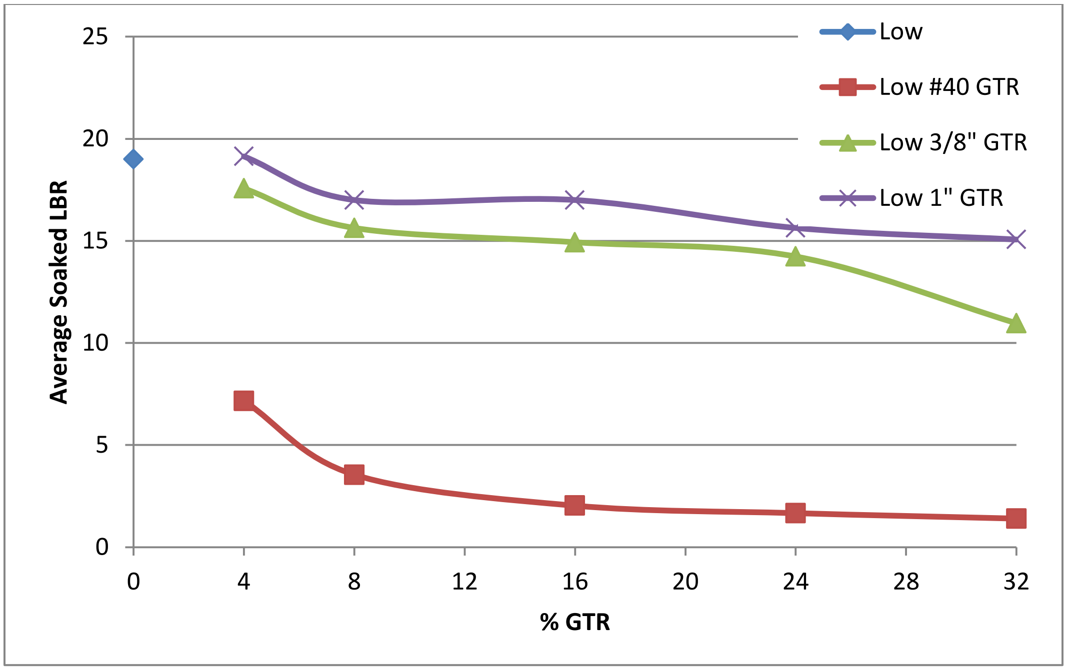

Figure 4-3 Average Soaked LBR versus GTR% for Low LBR/GTR Blends

The largest percent decreases occurred with the High LBR materials. The LBR values decreased from 65 to 95% for all GTR sizes. The #40 mesh GTR blends produced more severe LBR reductions than either the 1 inch or 3/8inch GTR blends for all three-soil types, resulting in LBR reductions of over 90% in each soil. The overall percent decrease in LBR for each soil type is summarized in Figure 4-4, Figure 4-5 and Figure 4-6.

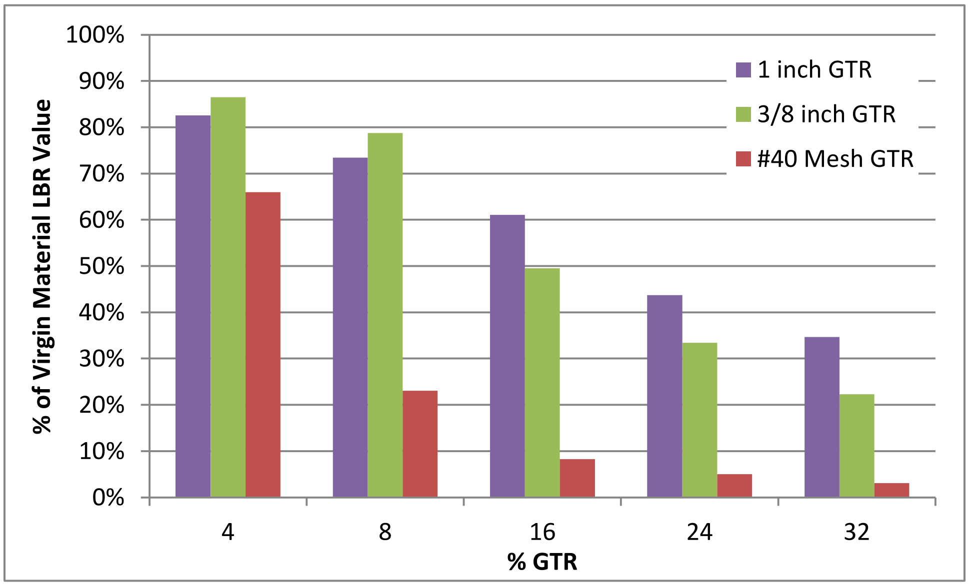

Figure 4-4 High LBR Soil Decrease in LBR Value

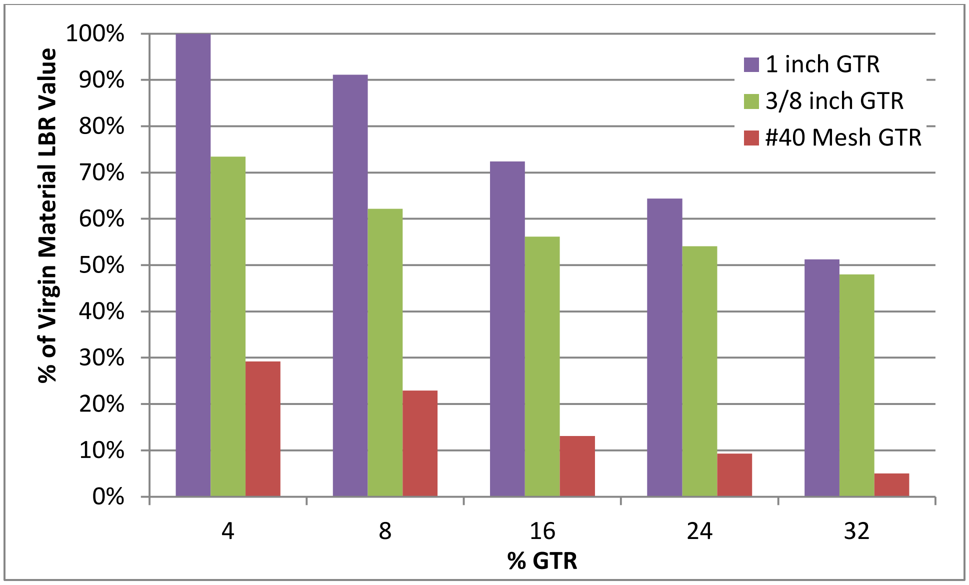

Figure 4-5 Medium LBR Soil Decrease in LBR Value

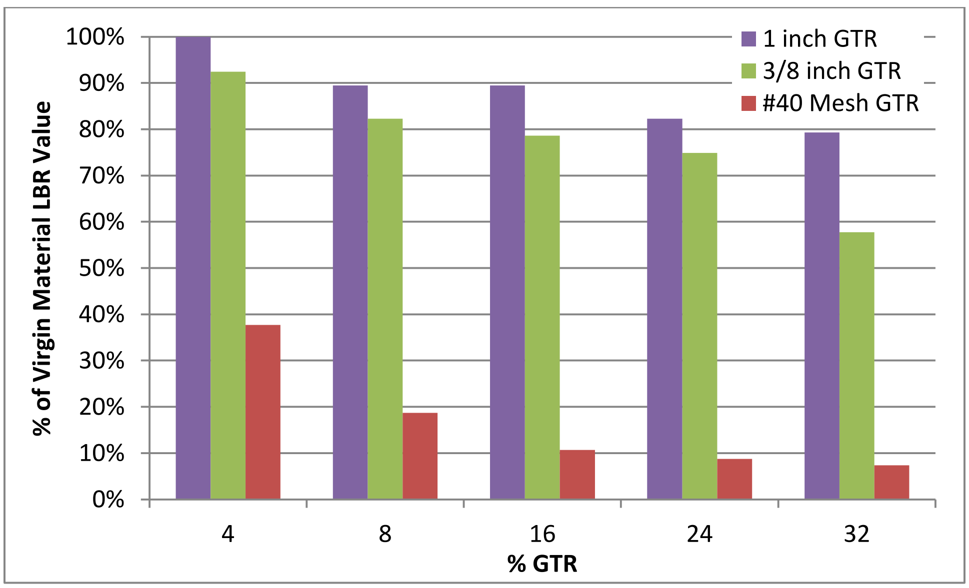

Figure 4-6 Low LBR Soil Decrease in LBR Value

GTR% versus dry density plots shown in Figure 4-7, Figure 4-8 and Figure 4-9,were developed to determine the effect the GTR addition had on the density. Because the densities of the different GTR sizes were similar to each other yet lower than that of the soil types, the changes in densities are fairly similar throughout the different GTR/soil blends.

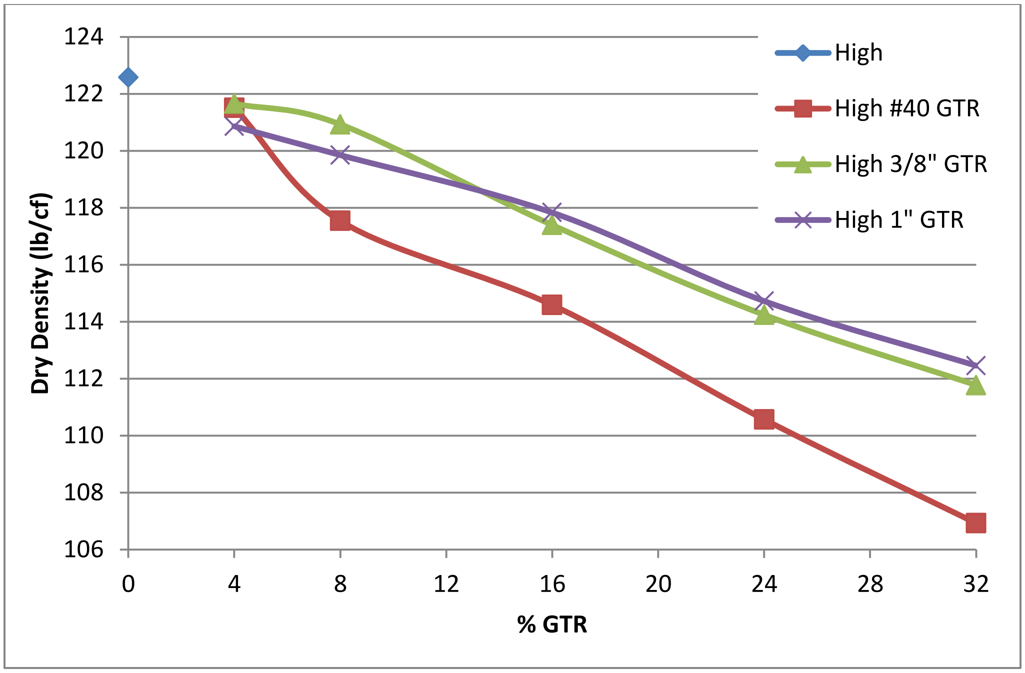

Figure 4-7 Dry Density versus GTR% for High LBR/GTR Blends

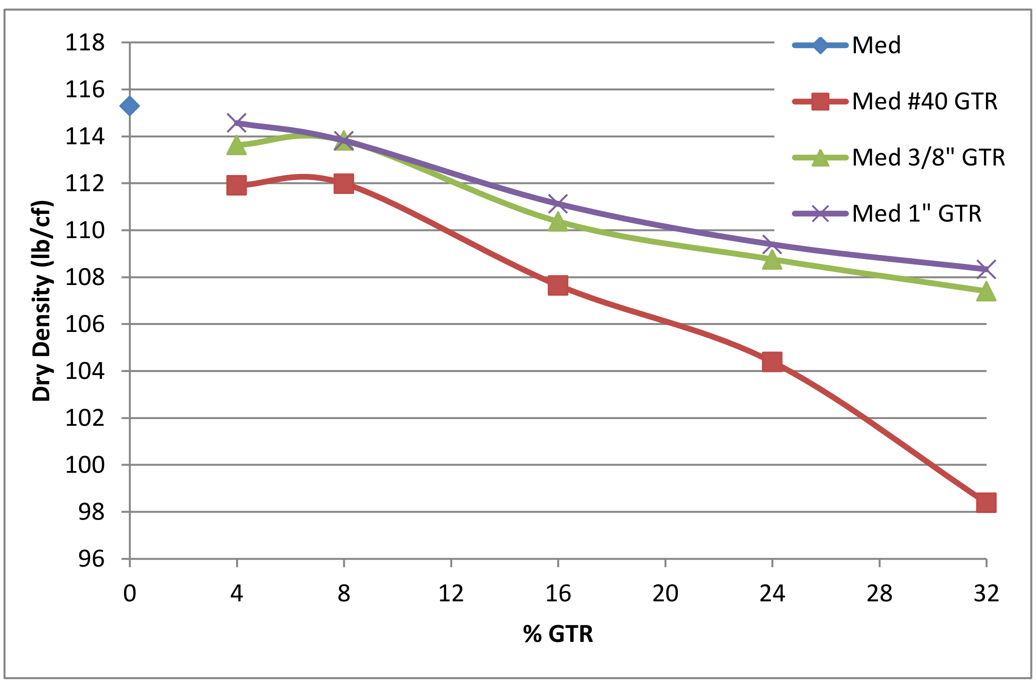

Figure 4-8 Dry Density versus GTR% for Medium LBR/GTR Blends

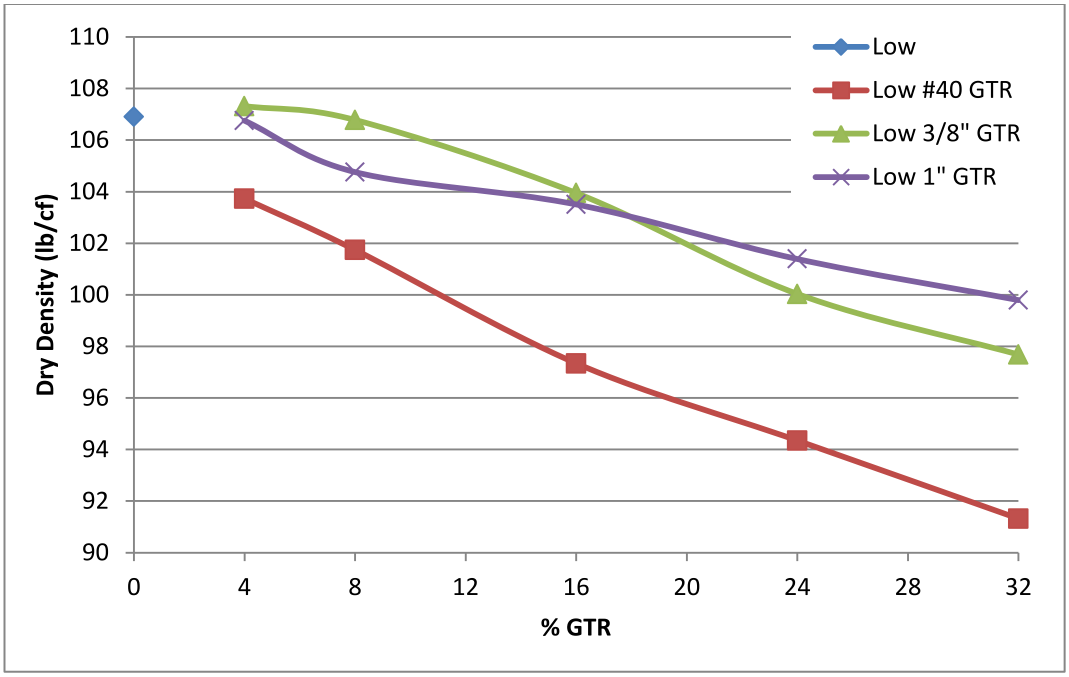

Figure 4-9 Dry Density versus GTR% for Low LBR/GTR Blends

4.5. Resilient Modulus Test Results

Resilient modulus testing (AASHTO T 307) for the 4, 8, 16, and 32% GTR/subgrade blends from all three subgrades was completed by the SMO. To produce M_r values, the applied stress was divided by the strain determined from the average deflections from two LVDT's on top of the triaxial cell. The results from the testing (Appendix D) were provided to the research team in both raw and reduced formats. The raw data included the loads and deflections for each confining and deviator stresses. The reduced data included the data and associated log-log plot of M_r versus bulk stress (θ). To produce one M_r value from each series of tests, θ of 15 psi was used as the input into Equation 4-1.

$$M_r = K_1 \theta^{K2} \qquad \text{Equation 4-1}$$

Mr = Resilient modulus
K_1 = constant associated with M_r of 1
K_2 = the slope from the plot.
θ = bulk stress ($\sigma_1 + \sigma_2 + \sigma_3$)

The variations in dry density and M_r were evaluated to determine any trends with respect to GTR content. Figure 4-11, Figure 4-12 and Figure 4-14 summarize the results from the M_r

tests for the high, medium and low LBR material. Similar to the LBR results shown earlier, M_r decreased as the percentage of GTR increased for all GTR/soil blends and GTR sizes tested. The percent decrease for each GTR blend is shown in Figure 4-11, Figure 4-13 and Figure 4-15. The largest percent decrease occurred for the High LBR soils, with similar percent decreases for the Medium and Low LBR soils.

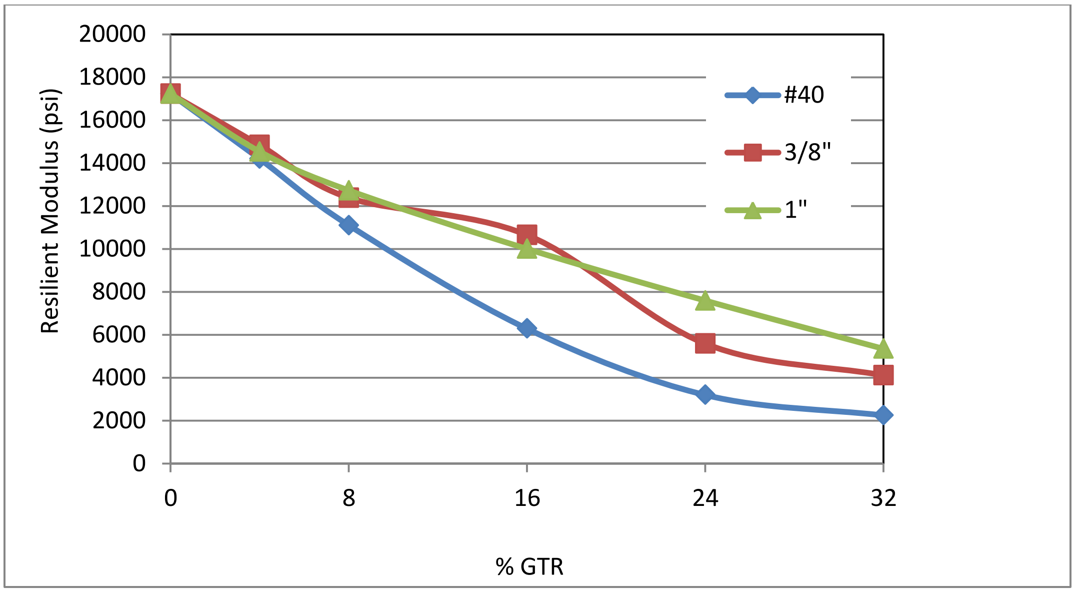

Figure 4-10 Variation in Resilient Modulus versus High LBR Soil GTR Blends

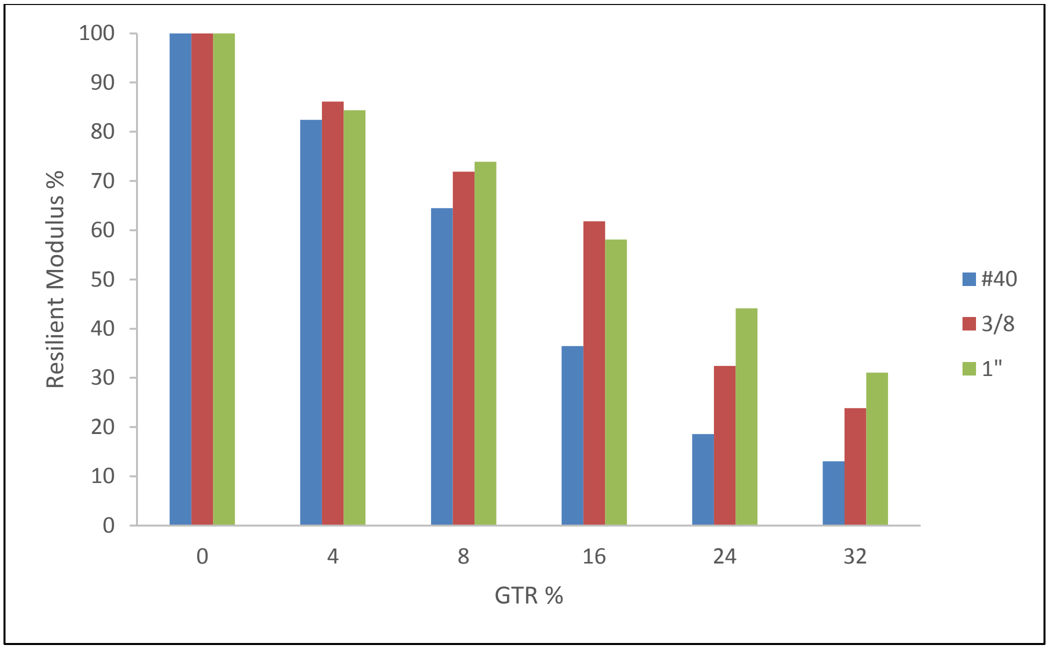

Figure 4-11 Percent GTR versus Percent Resilient Modulus for High LBR Soil GTR Blends

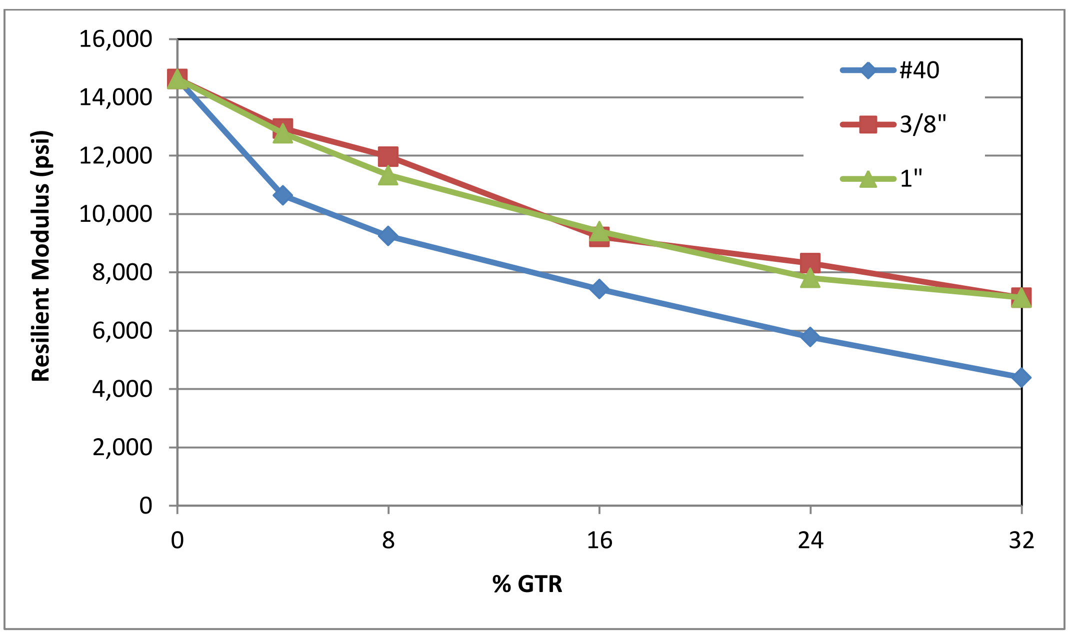

Figure 4-12 Variation in Resilient Modulus versus Medium LBR Soil GTR Blends

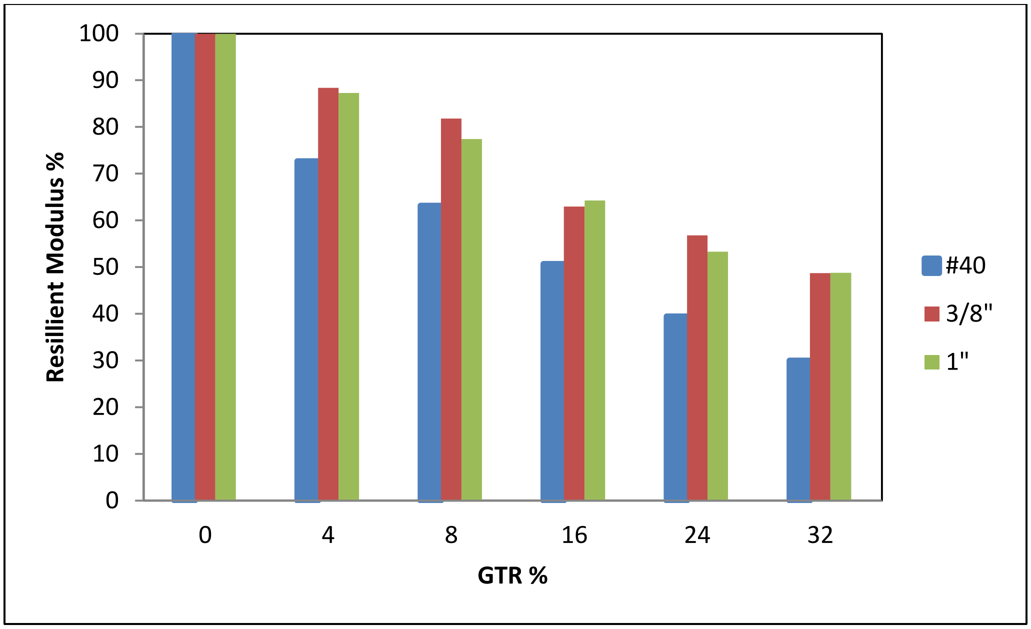

Figure 4-13 Percent GTR versus Resilient Modulus for Medium LBR Soil GTR Blends

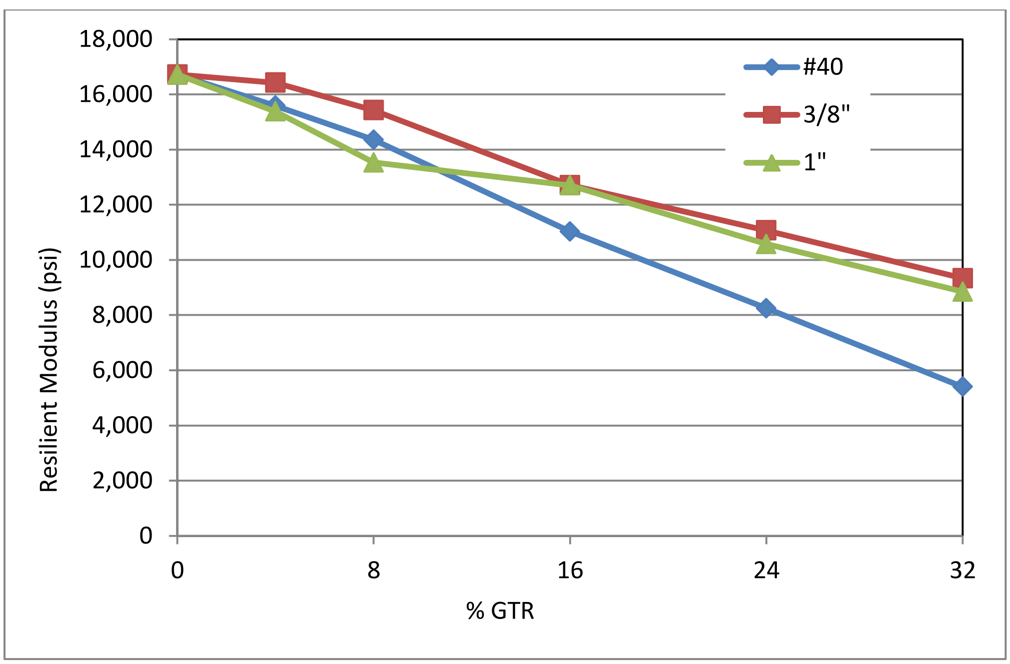

Figure 4-14 Variation in Resilient Modulus versus Low LBR Soil GTR Blends

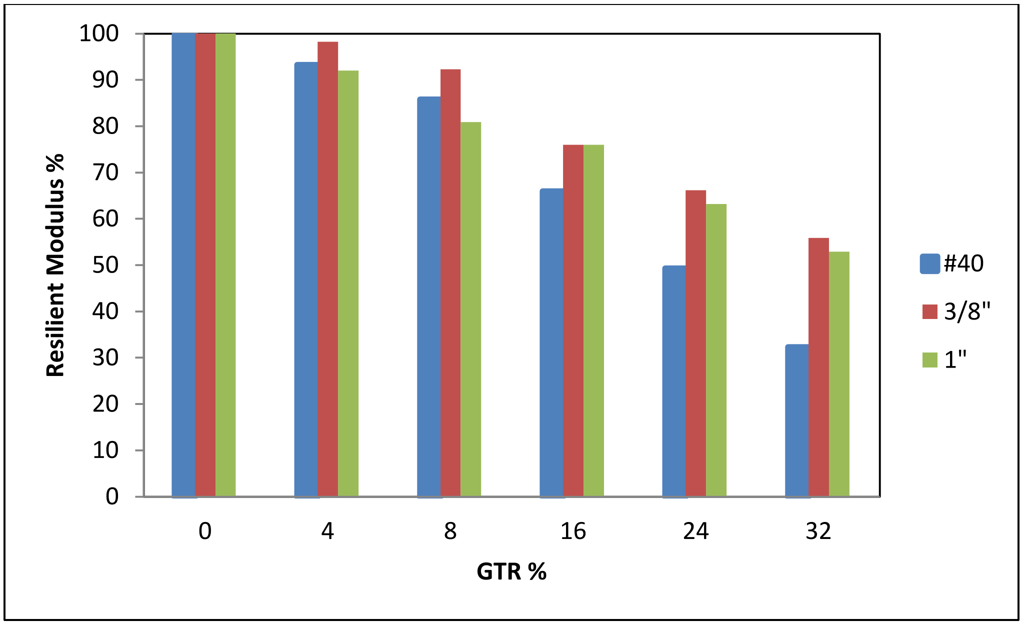

Figure 4-15 Percent GTR versus Percent Resilient Modulus for Low LBR Soil GTR Blends

4.6. Consolidation Test Results

For the three A-3 or A-2-4 granular specimens with non-plastic fines tested, most of the consolidation happened within the first 4 to 6 seconds. There was little to no movement after 5 minutes of testing at any pressure. Complete results are shown in the deflection versus square root of time plots in Appendix E.

Due to this near-instantaneous consolidation, the values for t_{90} fitting time (the time required to reach 90% of the total observed consolidation) and compression index (C_c) (rate of consolidation settlement in log(time)) are dissimilar to typically observed values for cohesive soils. The values for C_c of the virgin soil materials are presented in Table 4-4.

Table 4-4 Compression Index for Virgin Soils

Soil	Compression Index, C_c
High	0.010
Med	0.007
Low	0.008

After determining the C_c values for each of the three virgin soils, tests were conducted with 16 and 32% GTR/soil blends. The C_c results for the high, medium and low LBR blends are summarized in Figure 4-16, Figure 4-17 and Figure 4-18. Overall, the values of C_c increased more with the low LBR blends than with the high LBR blends. Within each soil, the 1 inch and 3/8 inch GTR C_c values increased slightly over the testing range, but the #40 GTR increased by magnitudes of three, four, and five for the high, medium, and low LBR/GTR blends, respectively.

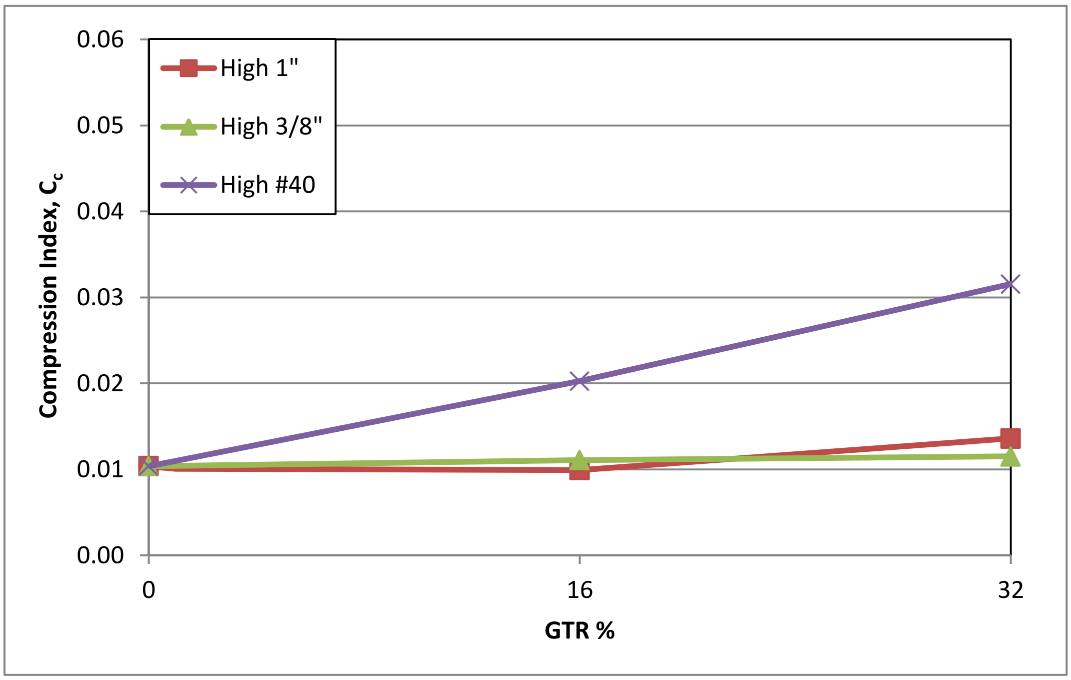

Figure 4-16 C_c versus GTR% for High LBR/GTR Blends

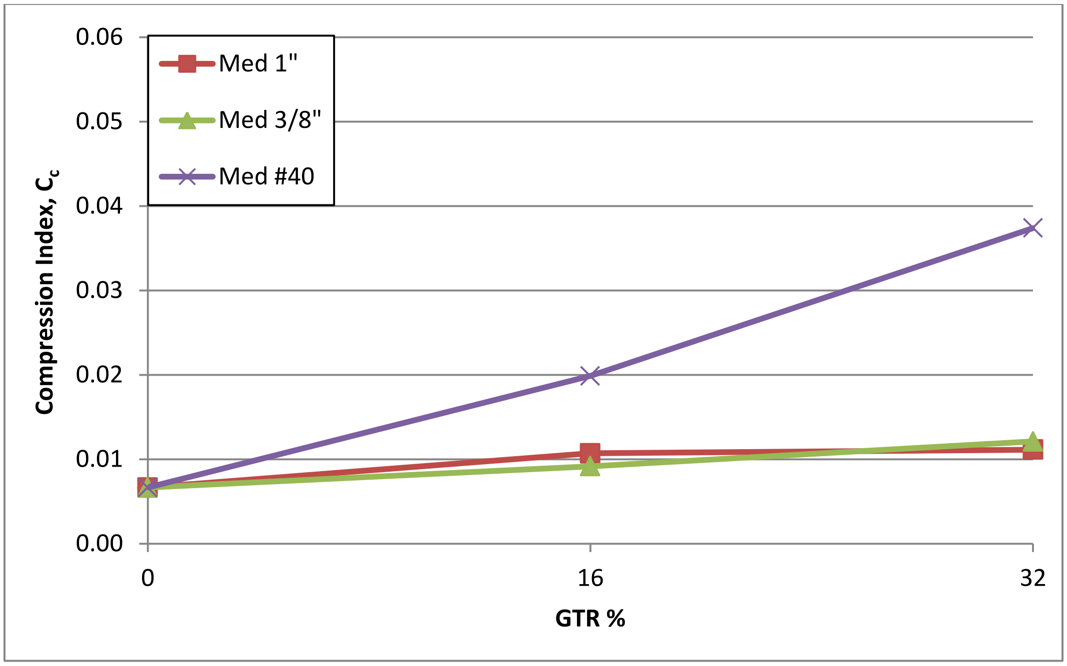

Figure 4-17 C_c versus GTR% for Medium LBR/GTR Blends

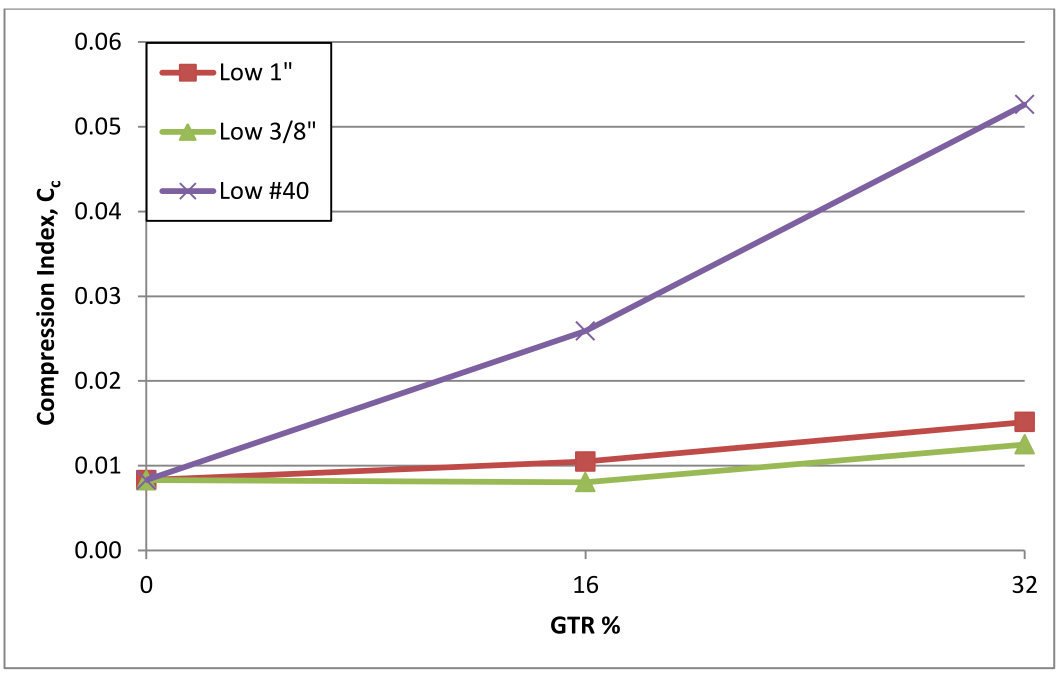

Figure 4-18 C_c versus GTR% for Low LBR/GTR Blends

Values for the coefficient of consolidation (C_v) were difficult to obtain due to the immediate nature of the granular consolidation. Plots of C_v versus consolidation pressure for each soil type are shown in Figure 4-19, Figure 4-20, and Figure 4-21.

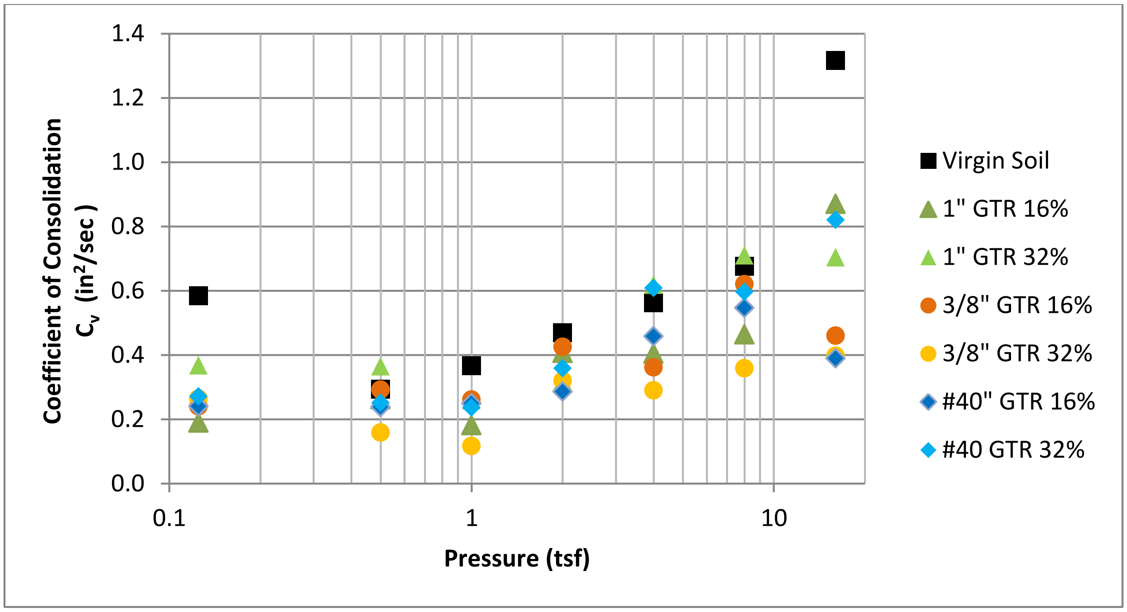

Figure 4-19 C_v versus log-P for High LBR/GTR Blends

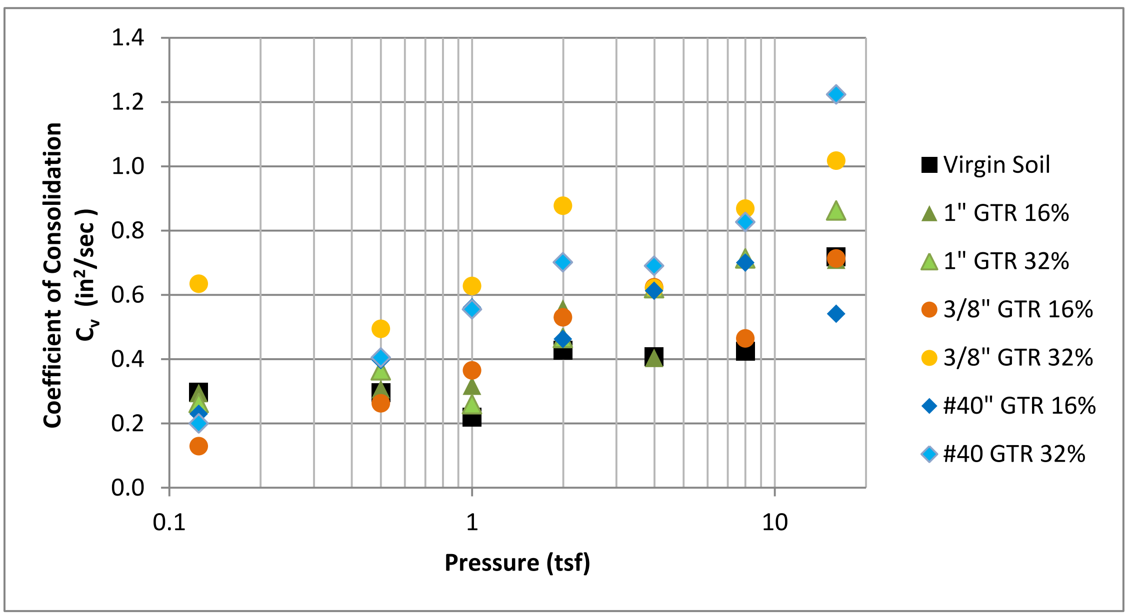

Figure 4-20 C_v versus log-P for Med LBR/GTR Blends

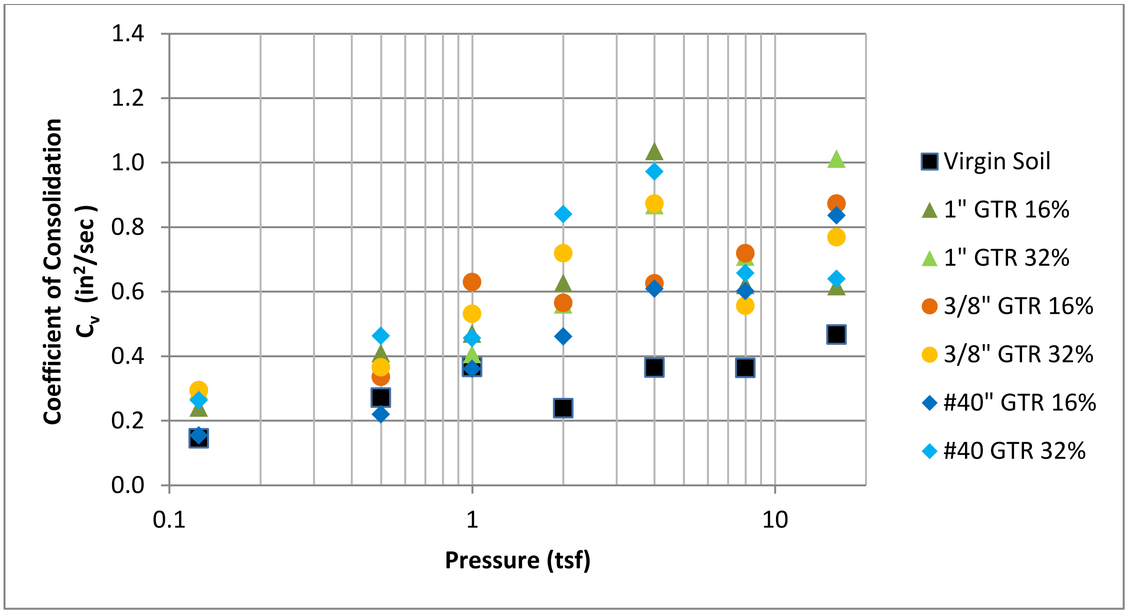

Figure 4-21 C_v versus log-P for Low LBR/GTR Blends

4.7. Constant Head Permeability Test Results

Permeability testing was conducted on all soil/GTR blends to determine the drainage characteristics of the blends and how the drainage was affected by the addition of the different GTR sizes. The permeability testing data are contained in Appendix F. The test was first conducted on the virgin soils with no GTR to determine the initial values of each soil type. These results are summarized in Table 4-5.

Table 4-5 Hydraulic Conductivity Values for Virgin Soils

Soil	Hydraulic Conductivity, k (cm/sec)	Percent Passing #200 Sieve	Void Ratio, e
High LBR	$1.2x10^{-5}$	12%	0.393
Medium LBR	$2.8x10^{-6}$	20%	0.389
Low LBR	$3.7x10^{-4}$	5%	0.533

The medium LBR soil had the lowest permeability of the three soils due to the highest percent fines and lowest void ratio among the virgin soils; likewise, the low LBR soil has the highest permeability because of the absence of fines and high void ratio.

For each blend, two specimens were compacted and tested at three different head pressure trials. The samples were tested at three pressure heads to determine any changes in permeability as the water discharged from the sample transitioned from laminar to turbulent flow. The averages were then plotted in k versus GTR% graphs to evaluate trends (Figure 4-22, Figure 4-23 and Figure 4-24).

The high LBR/GTR blends showed the most change in permeability with increasing GTR. The permeability blends with all three GTR sizes increased from 1 x10^{-5} to about 5 x 10^{-5} cm/sec with increase in GTR percentage. The results for the medium and low LBR/GTR blends were similar, both showing an insignificant change in permeability over the range of GTR percentages. The three semi-log plots are shown with the same vertical axis to show the change of magnitude for each soil/GTR blend. Overall, the addition of GTR did not significantly affect permeability. The permeability of the high LBR blends improved slightly within the same order of magnitude 10^{-5} cm/sec range. The permeability for the medium and low LBR blends was not affected by the addition of GTR.

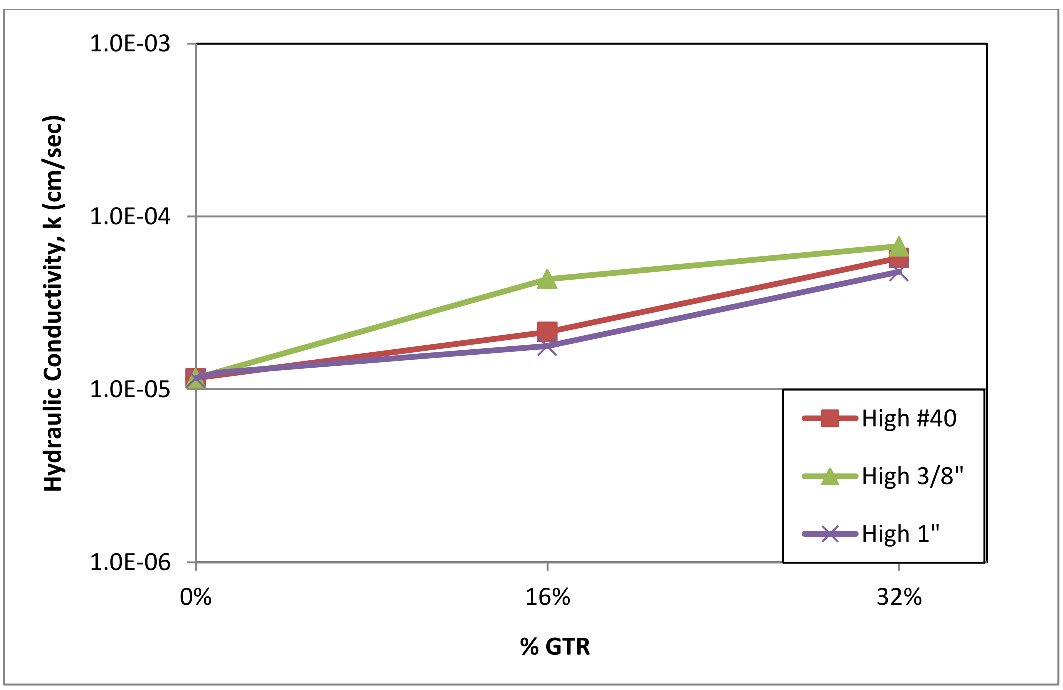

Figure 4-22 Hydraulic Conductivity versus GTR% for High LBR/GTR Blends

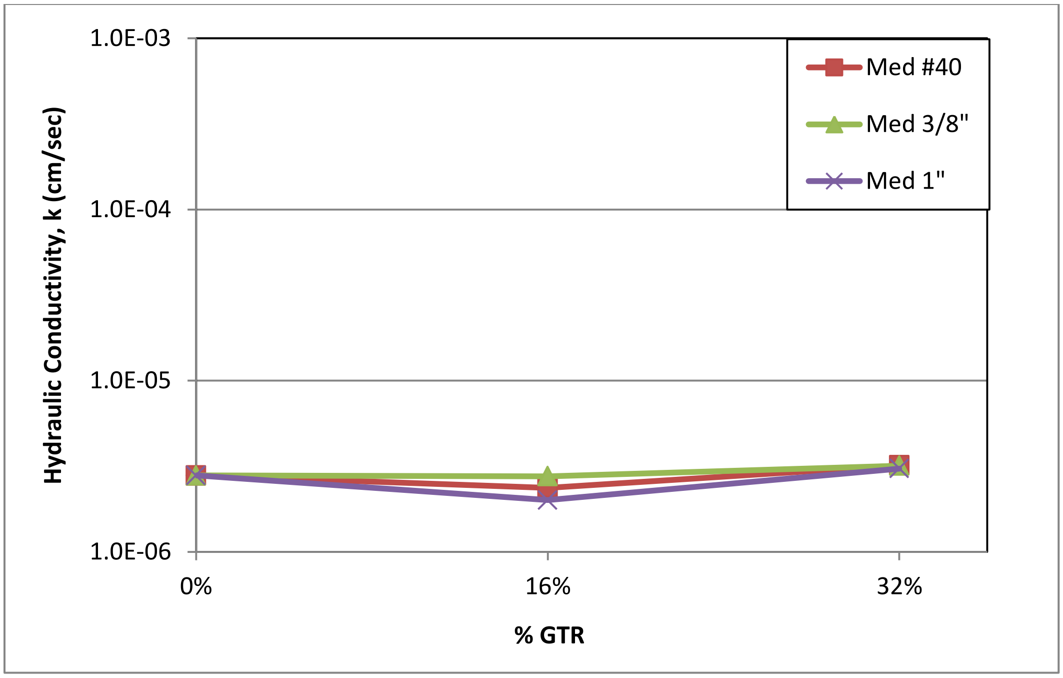

Figure 4-23 Hydraulic Conductivity versus GTR% for Medium LBR/GTR Blends

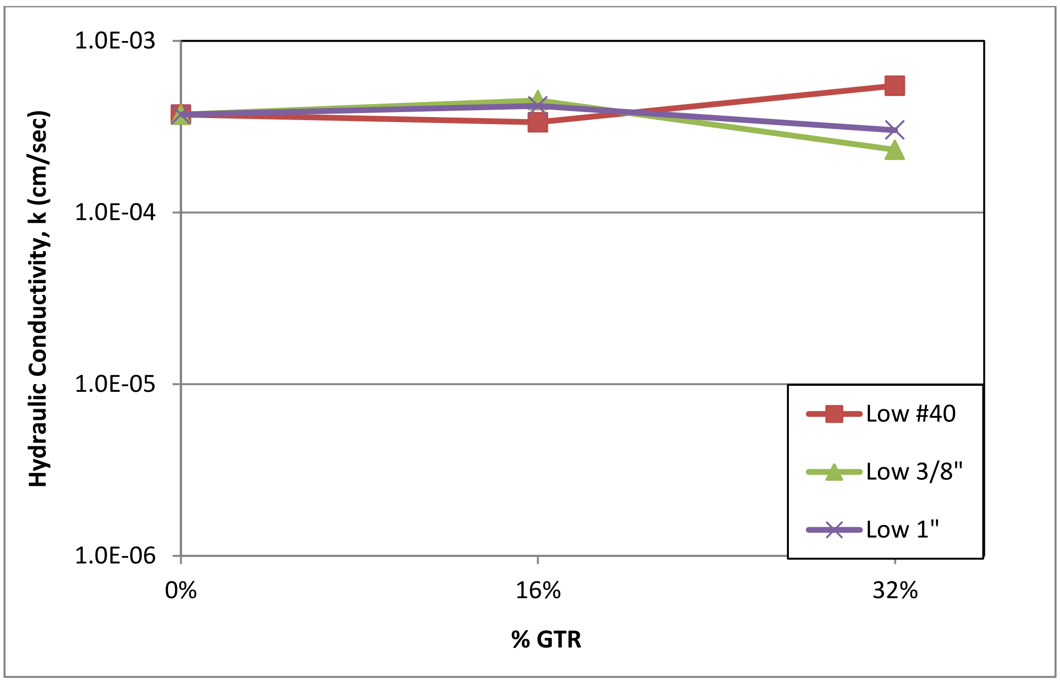

Figure 4-24 Hydraulic Conductivity versus GTR% for Low LBR/GTR Blends

4.8. Creep Test Results

Creep test results were conducted as explained in Section 3.3.8. The creep testing data are contained in Appendix G. The data was analyzed using Excel. Strains versus log(time) plots were generated and the slopes (CSR) were determined. Creep generally increased with increasing GTR concentrations, however the rate of creep for the blends was still of the same order of magnitude as the virgin material. Figure 4-25, Figure 4-26, and Figure 4-27 show the strain versus time plots for the high, medium, and low LBR materials respectively.

Creep strain rates for each of the GTR/subgrade blend combinations are shown in Figure 4-28, Figure 4-29, and Figure 4-30. The high LBR material only showed a small increase in CSR. The low and medium LBR materials showed the greatest increase. The 1 inch (25.4 mm) GTR had the least effect on creep. The #40 (0.422 mm) GTR had the greatest effect on creep, especially with in the low LBR blends.

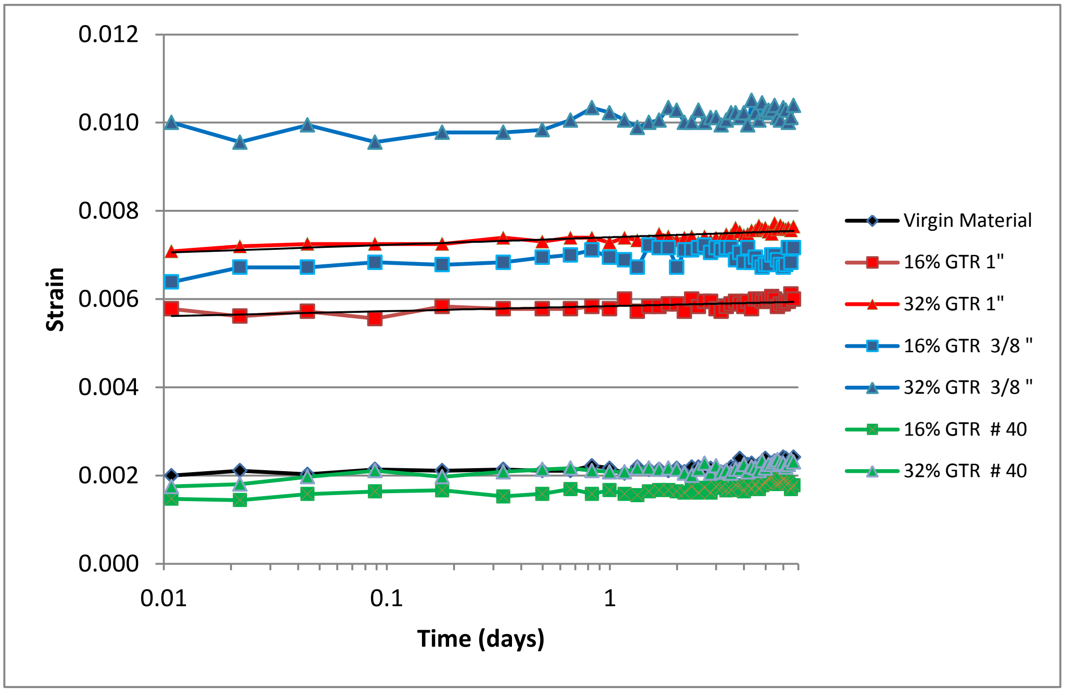

Figure 4-25 Strain versus Time (Days) for High LBR Material

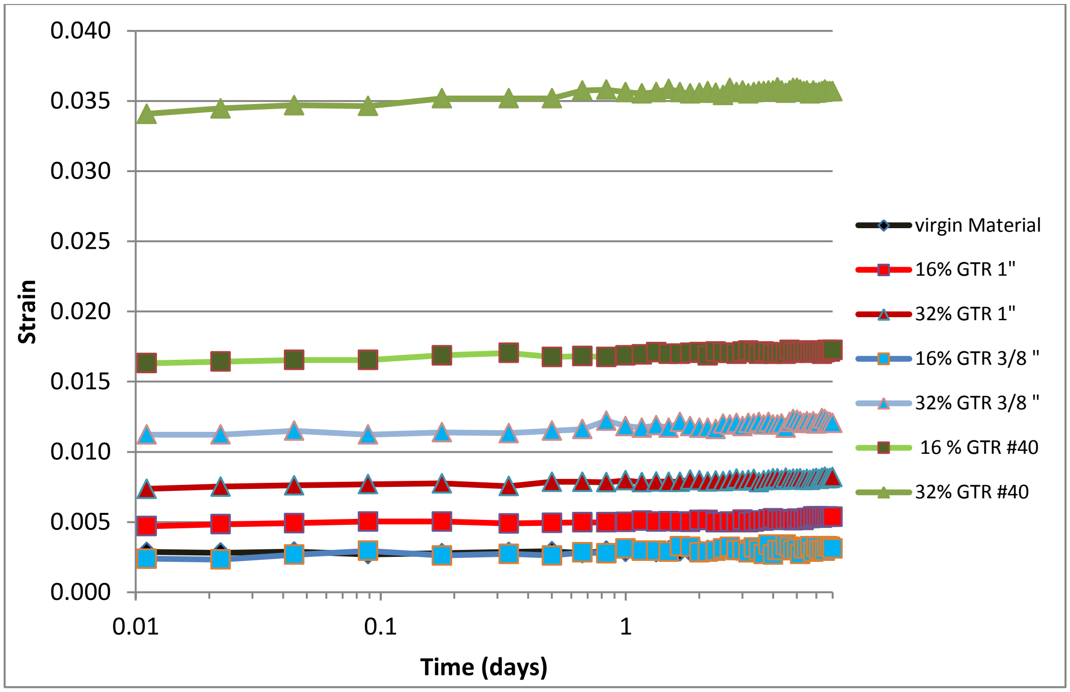

Figure 4-26 Strain versus Time (Days) for Medium LBR Material

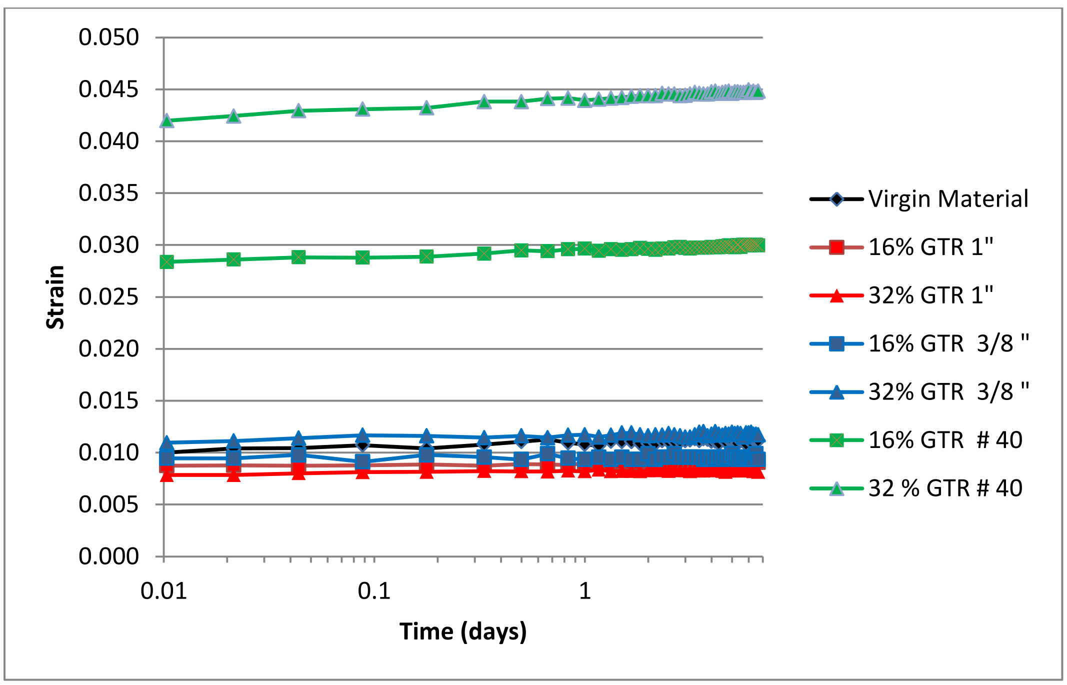

Figure 4-27 Strain versus Time (Days) for Low LBR Material

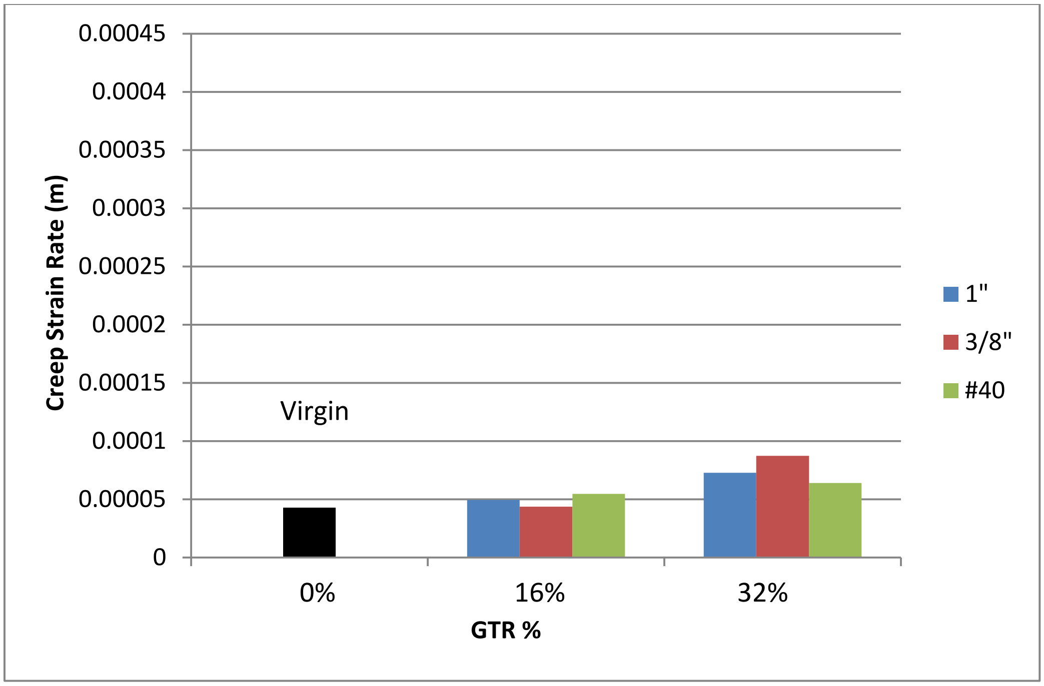

Figure 4-28 Strain Rate versus GTR Percentage for High LBR Subgrade

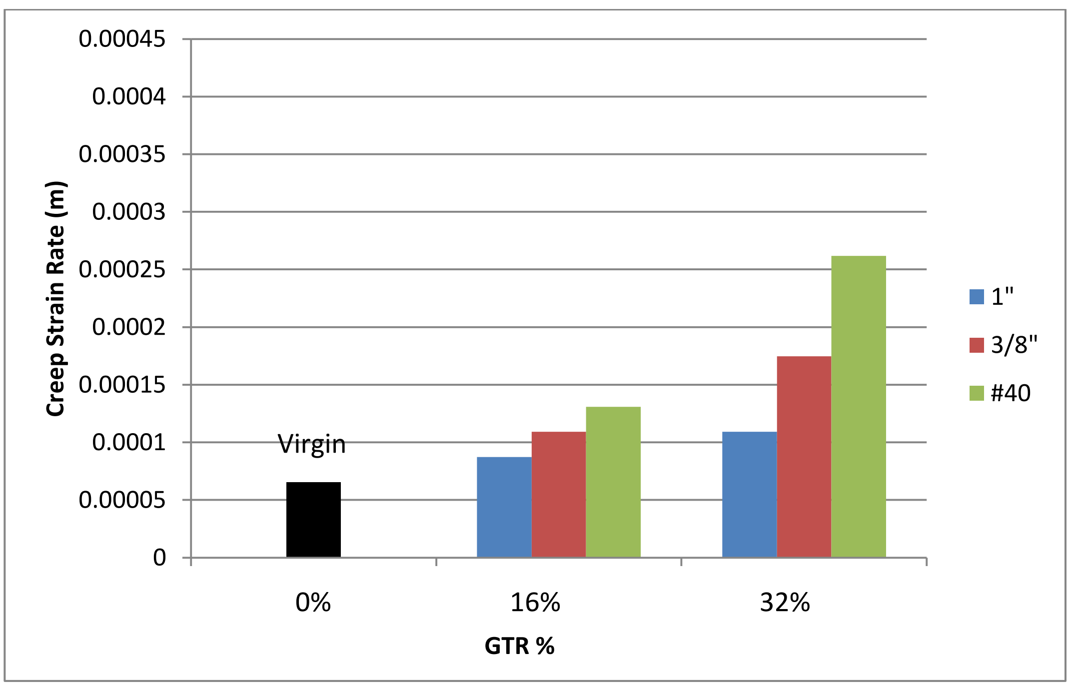

Figure 4-29 Strain Rate versus GTR Percentage for Medium LBR Subgrade

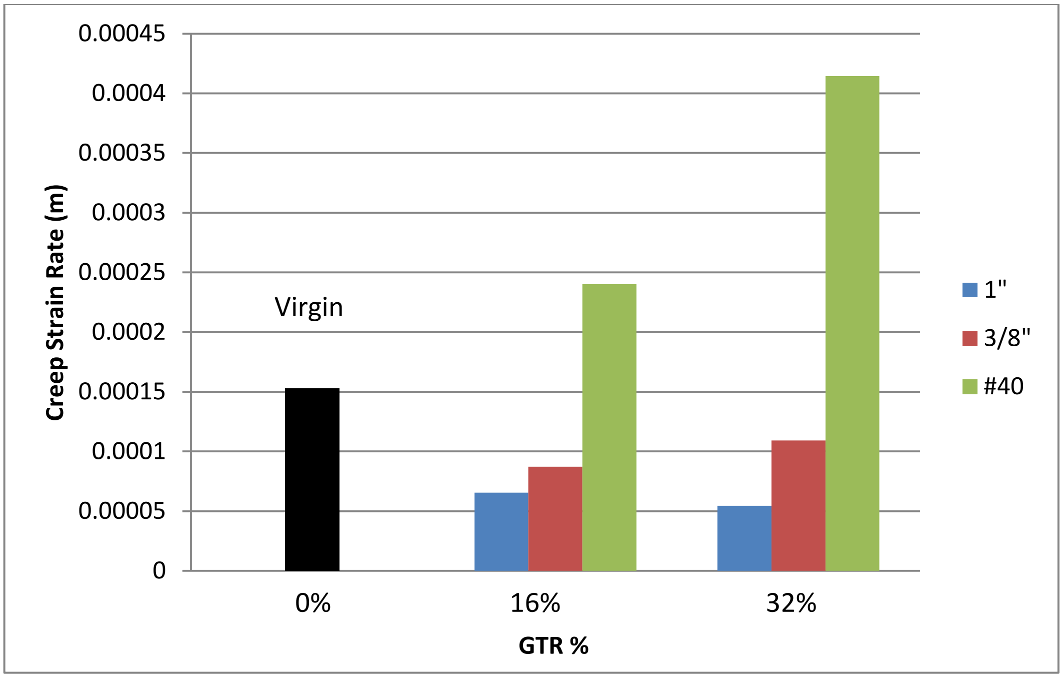

Figure 4-30 Strain Rate versus GTR Percentage for Low LBR Subgrade

For comparison, Figure 4-31 shows the highest creep material, low LBR with 32% #40 GTR, with the CSR of A-3 sand, limerock, and RAP previously shown in Figure 2-13.

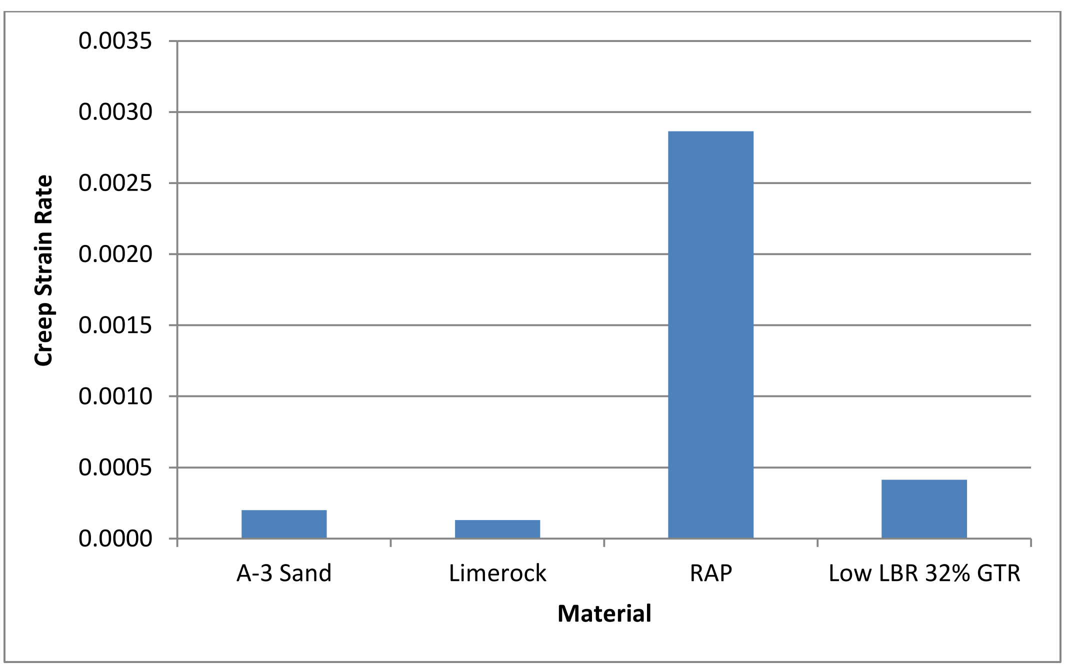

Figure 4-31 Summary of Creep Strain Rates for Various Materials with GTR Blends

4.9. Correlations

A significant amount of research has been performed relating M_r to CBR. Heukelom and Foster (1960) developed a correlation between M_r and CBR values below 10 is

$$M_r = 1{,}500(CBR) \qquad \text{Equation 4-2}$$

Heukelom and Foster noted that the 1,500 coefficient was determined for a typical soil, however the coefficient can vary widely between 300 and 3,000 depending on the soil type and CBR range. They cautioned against using the formula outside the documented range (CBR < 10). Another commonly used correlation was developed by Powel et al. (1984) at the U. K. Transportation Research Laboratories:

$$M_r(psi) = 2{,}555(CBR)^{0.64} \qquad \text{Equation 4-3}$$

These two equations plus a linear equation were evaluated using the data from this research. The data shown in Figure 4-32 was used and these correlations were evaluated.

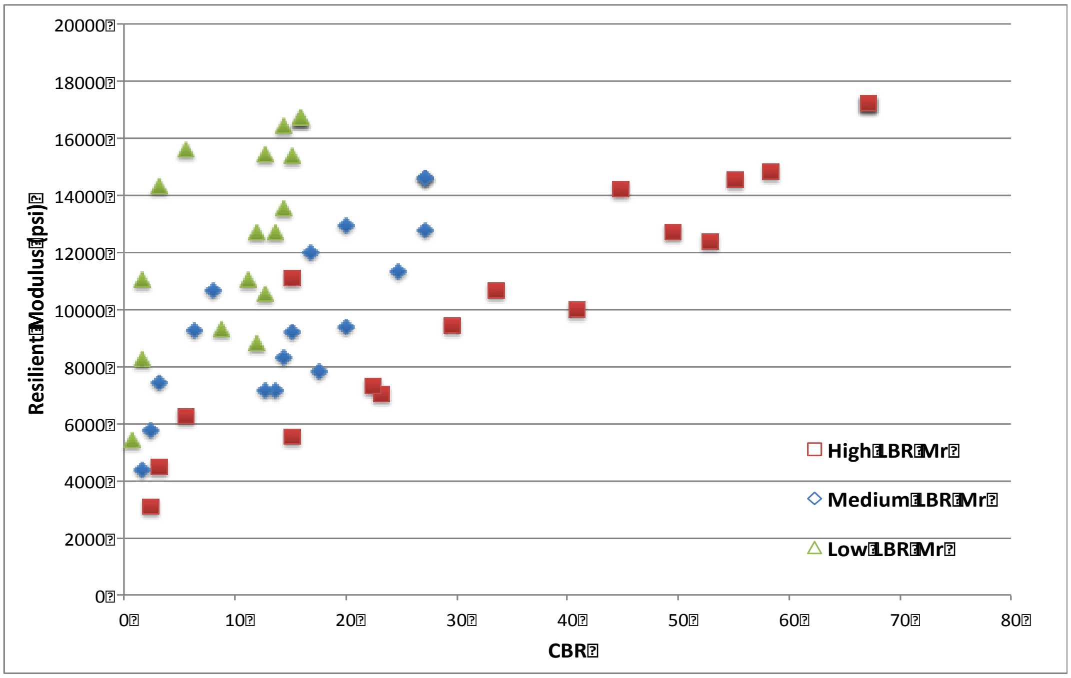

Figure 4-32 Comparisons between M_r and CBR from Low, Medium and High LBR/GTR Blends

The correlation equations evaluated from this data are summarized in Table 4-6. The Heukelom and Foster (1960) equation (Equation 4-2), was not shown because the CBR values are higher than the recommended maximum and it therefore produced poor results. A linear correlation and the Powell et al. (1984) equation (Equation 4-3) were used for the entire range of GTR sizes and blend percentages. The regression coefficients indicate that these correlations are highest for the high LBR blends, second highest for the medium LBR blends and lowest for the low LBR blends. The linear correlations are slightly higher than the power law correlation coefficients for the high and medium LBR/GTR Blends. The quality of the correlations is also visible through inspection of Figure 4-32.

Table 4-6 Summary of M_r versus CBR Correlations from Subgrade/GTR Blends

Equation	Linear	R^2	Mr=B*CBR ^A	R^2
High LBR	189(CBR)+3972	0.90	2304(CBR)^0.45	0.86
Medium LBR	296(CBR)+5268	0.70	4264(CBR)^0.32	0.67
Low LBR	391(CBR)+8733	0.39	7778(CBR)^0.22	0.46

5. Conclusions

5.1. Limerock Bearing Ratio Test

Blending GTR reduced the LBR of all three subgrade soils tested. The low LBR soil failed to meet subgrade LBR requirements before blending and became worse after blending. The medium soil was initially marginal but fell below the subgrade LBR standard with the addition of all sizes and concentrations of GTR. Only the high LBR soil/GTR blends with up to 16% of 3/8th inch or 1-inch nominal GTR met the FDOT subgrade specification of 40 LBR.

The density also decreased with increasing percentages of GTR for all three subgrade blends. The density decrease was largely independent of the size of GTR used.

5.2. Resilient Modulus Test

The M_r decreases as the percentage of GTR increases for all three soils and all three GTR sizes tested indicating that the blends would not be acceptable subgrade materials.

5.3. Consolidation Test

Compressibility of the soil/GTR blends increased slightly with the addition of 1 inch and 3/8 inch GTR and increased three to five times with the #40 GTR/soil blends.

5.4. Constant Head Permeability Test

No significant changes were observed in permeability with the addition of GTR to the subgrade soils.

5.5. Creep Test

Blending GTR moderately increased creep in all three soils tested. The high LBR soil showed the least increase in creep with the addition of GTR. The medium and low LBR materials showed progressively greater creep increase with the addition of GTR. The 1-inch (25.4 mm) GTR had the least effect on creep; the #40 (0.422 mm) GTR had the greatest effect. Even the largest creep observed (low LBR with #40 (0.422 mm) GTR) was acceptable and would not pose an engineering concern.

5.6. CBR- M_r Correlations

Equation 4-3 (Powell et al., 1984) produced strong CBR and M_r correlations for the high and medium LBR/GTR blends. A linear correlation produced similar strong regression coefficients for the high and medium LBR/ GTR blends. The low LBR/ GTR blends produced medium correlations using both approaches.

6. Recommendations

Ground tire rubber is not recommended as a stabilizing agent for subgrade soils.

Blending GTR with soil did reduce the density of the blend; therefore, additional research should be conducted to evaluate whether soil/GTR blends would be suitable for low-density fill applications where the benefits from reduction in vertical and horizontal soil pressures would offset the reduction in strength.

7. References

Ahmed, I. and C. Lovell. Use of Rubber Tires in Highway Construction. In *Utilization of Waste Materials in Civil Engineering Construction,* American Society of Civil Engineers, New York, N.Y., 1993, pp. 166–181.

Bader, C. Where will all the tires go? *Municipal Solid Waste Management,* Volume 2, Issue 7, 1992, pp. 25-34.

Basheer, I.A. and Y.M Najjar. Rubber Tires and Geotextiles. *Journal of Performance of Constructed Facilities,* 10(1), American Society of Civil Engineers, New York, N.Y., 1996, pp.40–44.

Behzadi, G., and W. O. Yandell. Determination of Elastic and Plastic Subgrade Soil Parameters for Asphalt Cracking and Rutting Prediction. In *Transportation Research Record,* 1540, TRB, National Research Council, Washington, D.C., 1996, pp.97-104.

Bosscher, P.J., T. B. Edil, and S. Kuraoke. Design of Highway Embankments using Tire Chips. *Journal of Geotechnical and Geoenviromental Engineering 123(4),* American Society of Civil Engineers, New York, N.Y., 1997, pp. 297–304.

Cabalar, A. F. Direct Shear Tests on Waste Tires-Sand Mixtures. *Geotechnical and Geological Engineering,* Volume 29, Issue 4, 2011, pp. 411-418.

Cosentino, P. J., E. H. Kalajian, C. S.Shieh, W. J .K. Mathurin, F. A. Gomez, , E. D.Cleary, A.Treerattakoon. *Developing Specifications for Using Recycled Asphalt Pavement as Base, Subbase, or General Fill Materials, Phase II. Final Report.* FL/DOT/RMC/06650-7754 BC 819. Florida Departement of Transportation, Tallahassee, 2003.

Cosentino, P. J., E. H. Kalajian, D. Dikova, M. Patel, C. Sandin. *Investigating the Statewide Variability and Long Term Strength Deformation Characteristics of RAP and RAP-Soil Mixtures: Final Report.* FL/DOT/RMC/06650-7754 BCB 809. Florida Departement of Transportation, Tallahassee, 2008.

Cosentino, P.J., E. H. Kalajian, A.M. Bleakley, B.S. Diouf, T.J. Misilo III, A. J. Petersen, R. E. Krajcik, and A. M. Sajjadi. *Improving the Properties of Reclaimed Asphalt Pavement for*

Roadway Base Applications, Final Report. FL/DOT/BDK81 977-02. Florida Departement of Transportation, Tallahassee, 2012.

Dikova, D. *Creep Behavior of RAP-Soil Mixtures in Earthwork Applications*. M.S. Thesis, Florida Institute of Technology, 2006.

Diouf, B. *Gradation Modification Effects on Engineering Performance of Reclaimed Asphalt Pavement for Use as Roadway Base.* M.S. Thesis, Florida Institute of Technology, 2011.

Edil, T.B. and P.J. Bosscher. Engineering Properties of Tire Chips and Soil Mixtures. *Geotechnical Testing Journal*, Volume 17, Issue 4, 1994, pp. 453–464.

Eldin, N.N. and A.B.Senouci. Rubber-Tire Particles as Concrete Aggregate. *Journal of Materials in Civil Engineering*, Volume 5, Issue 4, 1993, pp. 478–496.

Foose, G. J., C. H. Benson, and P. J. Bosscher. Sand Reinforced with Shredded Waste Tires. *Journal of Geotechnical Engineering*, Volume 122, Issue 9, 1996, pp.760–767.

Garga, V.K. and V. O'Shaughnessy. Tire-Reinforced Earthfill. Part 1: Construction of a Test Fill, Performance, and Retaining Wall Design. *Canadian Geotechnical Journal*, Volume 37, 2000, pp. 75–96.

Garga, V.K. and V. O'Shaughnessy. Tire-Reinforced Earthfill. Part 2: Pull-Out Behavior and Reinforced Slope Design. *Canadian Geotechnical Journal*, Volume 37, 2000, pp. 97–116.

Ghazavi, M. Shear Strength Characteristics of Sand-Mixed With Granular Rubber. *Geotechnical and Geological Engineering*, Volume 22, Issue 3, 2004, pp. 401-416.

Hall, T. Reuse of Shredded Tire Material for Leachate Collection System. In: *Proceedings. 14th. Annual Conference, Department of Engineering Professional Development*, University of Wisconsin, Madison, 1991, pp. 367–376.

Heimdahl, T. C. and A. Druscher. Elastic Anisotropy of Tire Shreds. *Journal of Geotechnical and Geoenviromental Engineering*, Volume 125, Issue 5, 1999, pp. 383–389.

Heukelom, W., and C. R. Foster. Dynamic Testing of Pavements. *Journal of Soil Mechanics and Foundations*, Volume 86, Number SM1, 1960, pp. 1-28

Humphrey, D. N., L.E. Katz, and M. Blumenthal. Water Quality Effects of Tire Chip Fill Placed Above the Groundwater Table. In *Testing Soil Mixed with Waste or Recycled Materials*, M.A. Wasemiller and K.B. Hoddinott (eds.), *ASTM STP 1275*, American Society of Testing Materials, 1997.

Lee, J.H., R. Salgado, A. Bernal, and C. W. Lovell, Shredded Tires and Rubber-Sand as Lightweight Backfill. *Journal of Geotechnical and Geoenviromental Engineering,* Volume 125, Issue 2, 1999. pp. 132–141.

Nightingale, D.E.B. and W. P. Green. An Unsolved Riddle: Tire Chips, Two Roadbeds, and Spontaneous Reactions. In *Testing Soil Mixed with Waste or Recycled Materials,* M.A. Wasemiller and K.B. Hoddinott (eds.), *ASTM STP 1275*, American Society of Testing Materials, 1997.

Papp Jr., W.J., M. H. Maher, and R. F. Baker. Use of Shredded Tires in the Subbase Layer of Asphalt Pavements. In *Testing Soil Mixed with Waste or Recycled Materials,* M.A. Wasemiller and K.B. Hoddinott (eds.), *ASTM STP 1275*, American Society of Testing Materials, 1997.

Poh, P.S.H. and B. B. Broms. Slope Stabilization using Old Rubber Tires and Geotextiles. *Journal of Performance of Constructed Facilities*, Volume 9, Issue 1, 1995, pp. 76–80.

Powell, W. D., Potter, J. F., Mayhew, H. C., and Nunn, M. E. (1984). The Structural Design of Bituminous Roads, TRRL report LR.

Singh, A., and Mitchell, J. K., *General Stress-Strain-Time Function for Soils. Journal of the Soil Mechanics and Foundation Division*, Volume 94, Number SM1, 1968, pp. 21-47.

Speir, R. H., and M. W. Witczak. Use of Shredded Rubber in Unbound Granular Flexible Pavement Layers. *Transportation Research Record. Journal of the Transportation Research Board, Number 1547,* Transportation Research Board of the National Academies, Washington, D.C., 1996, pp. 96-106.

Sumanarathna, I.H.D., D.P. Mallawarctchie, and S.A.S. Kulathilaka. Stabilization of Slopes by Anchored Type Retaining Structures, In *Proceedings 14th International Conference of Soil Mechanics and Foundation Engineering*, New Delhi, India, 1997, pp. 1261–1264.

Sweere, G.T.H.. Unbound Granular Base for Roads. Ph.D. dissertation, University of Delft, Netherlands, 1990.

Tuncan, M., A. Cetin, M. Tuncan, and H. Koyuncu. Assessment of Waste Tires and Plastic on Asphalt Concrete Pavement Mixtures, In: *Proceedings of Third International Congress on Environmental Geotechnics*, Lisbon, Portugal, 1998, pp. 667–672.

Venkatappa Rao, G. and R. K**.** Dutta. Compressibility and Strength Behaviour of Sand-Tyre Chip Mixtures. *Geotechnical and Geological Engineering*, Volume 24, 2006, pp.711–724.

Viyanant, C., E.M. Rathje, and A.F. Rauch. Creep of Compacted Recycled Asphalt Pavement. *Canadian Geotechnical Journal*, Volume 44, Number 6, 2007, pp. 687-697.

Appendices

Appendix Contents

Appendix Figures

Appendix Tables

Appendix A – Sieve Analysis

SMO and FIT Grain Size Data for three Subgrade Materials

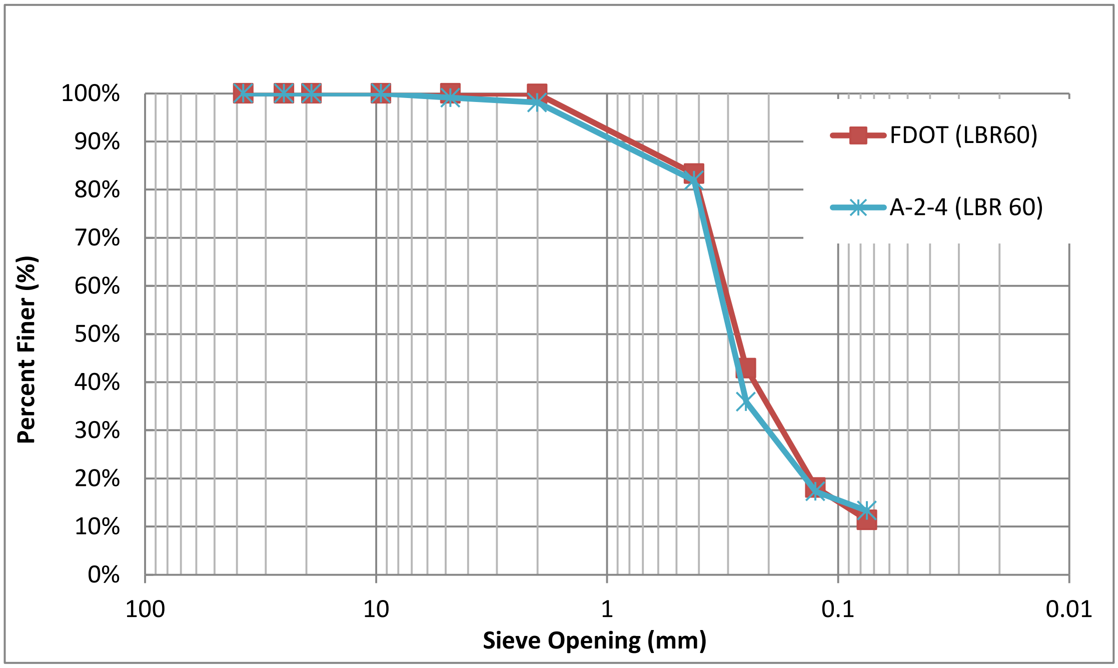

Figure A-1 Sieve Analysis for High LBR Material

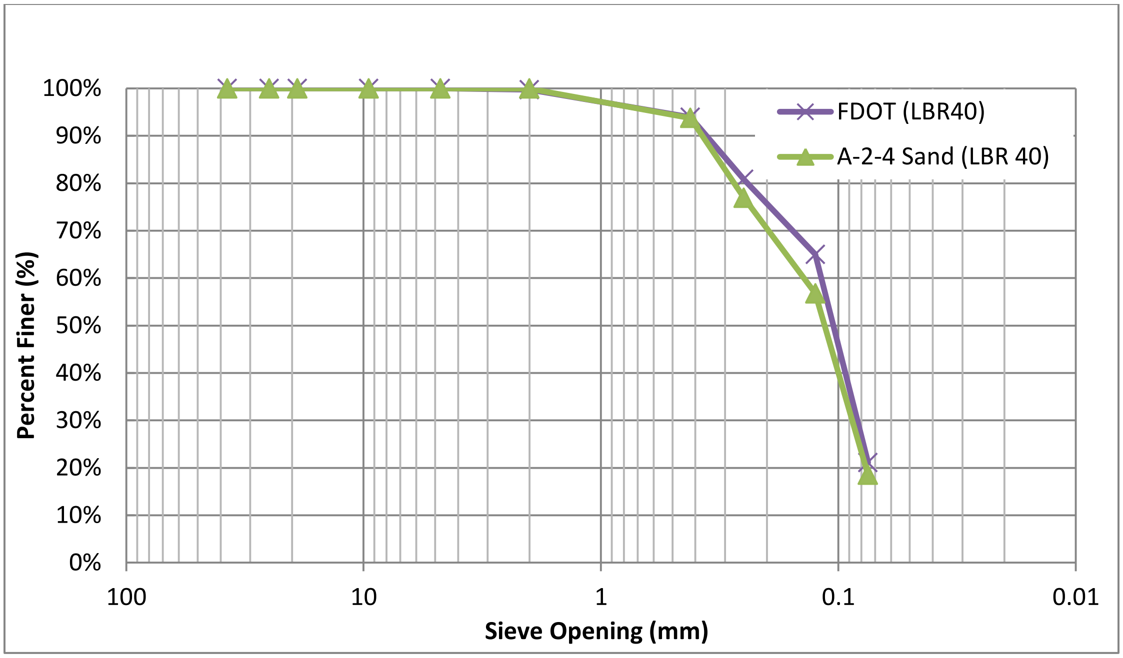

Figure A-2 Sieve Analysis for Medium LBR Material

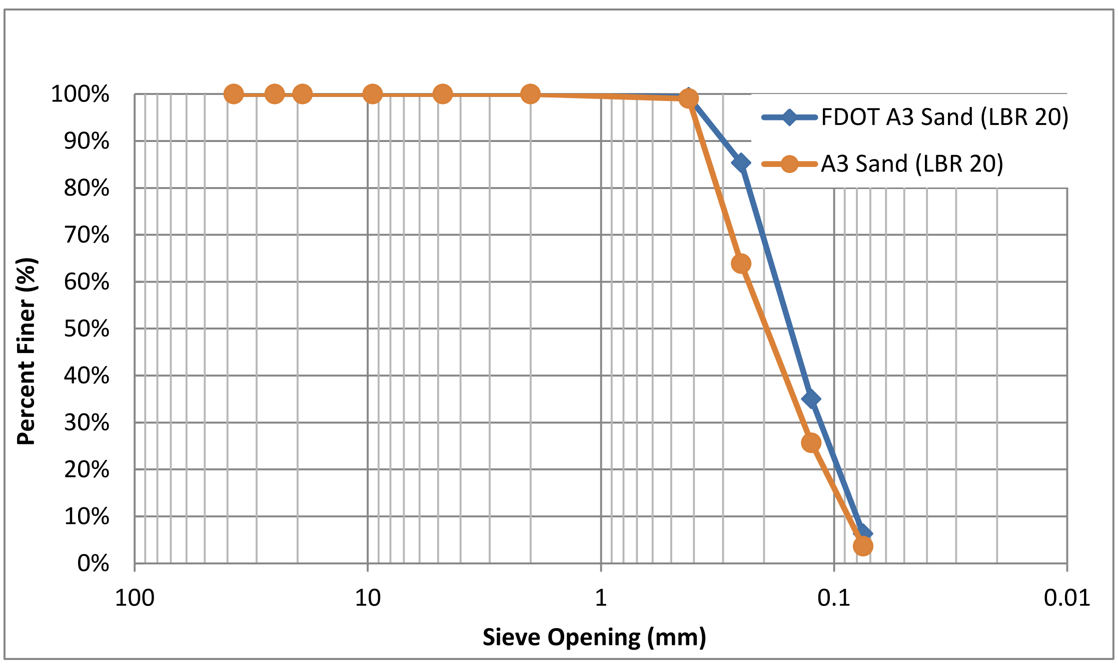

Figure A-3 Sieve Analysis for Low LBR Material

Appendix B – Moisture-Density Results

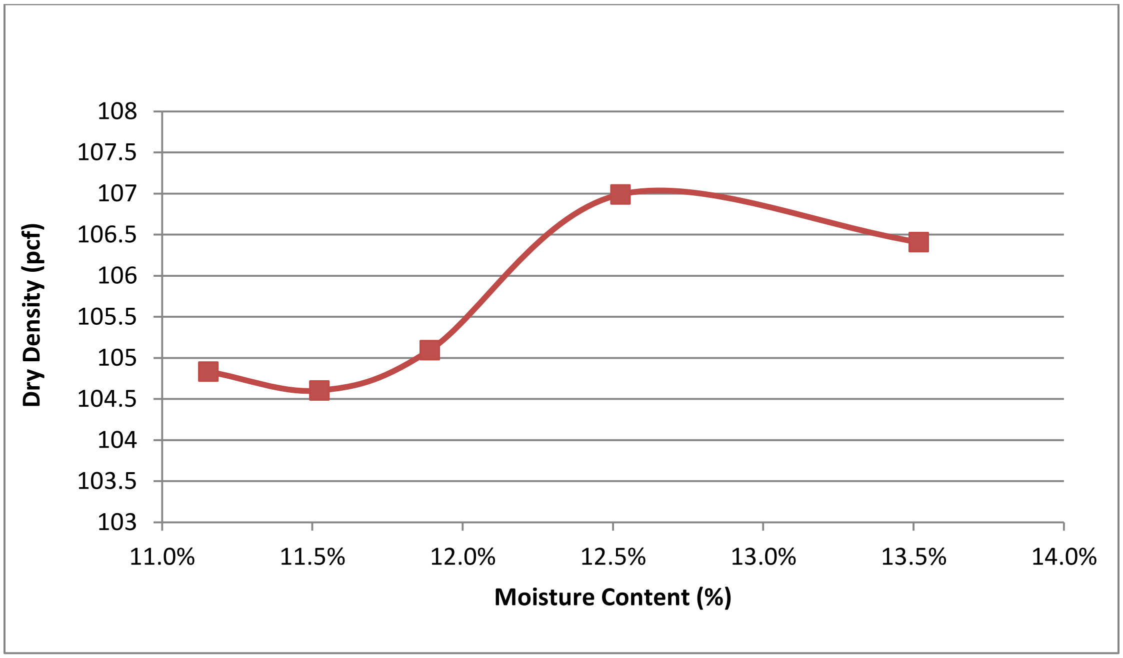

Figure B-1 Moisture Density Low LBR Material

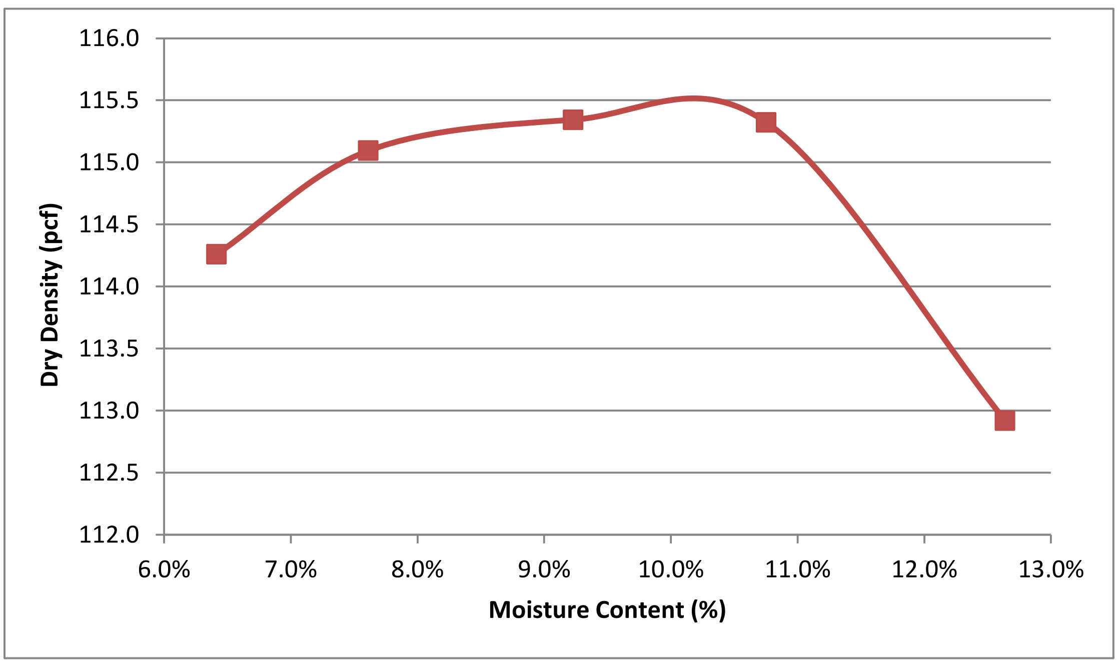

Figure B-2 Moisture Density Medium LBR Material

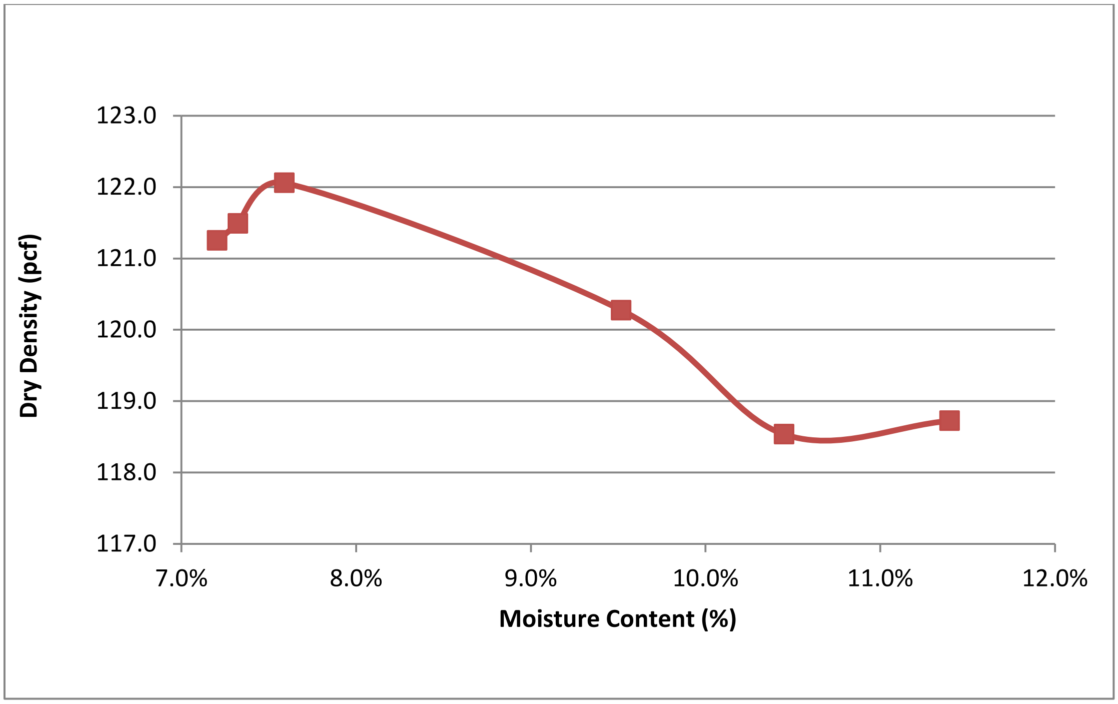

Figure B-3 Moisture Density High LBR Material

Appendix C – Limerock Bearing Ratio

C.1. Low LBR Soil

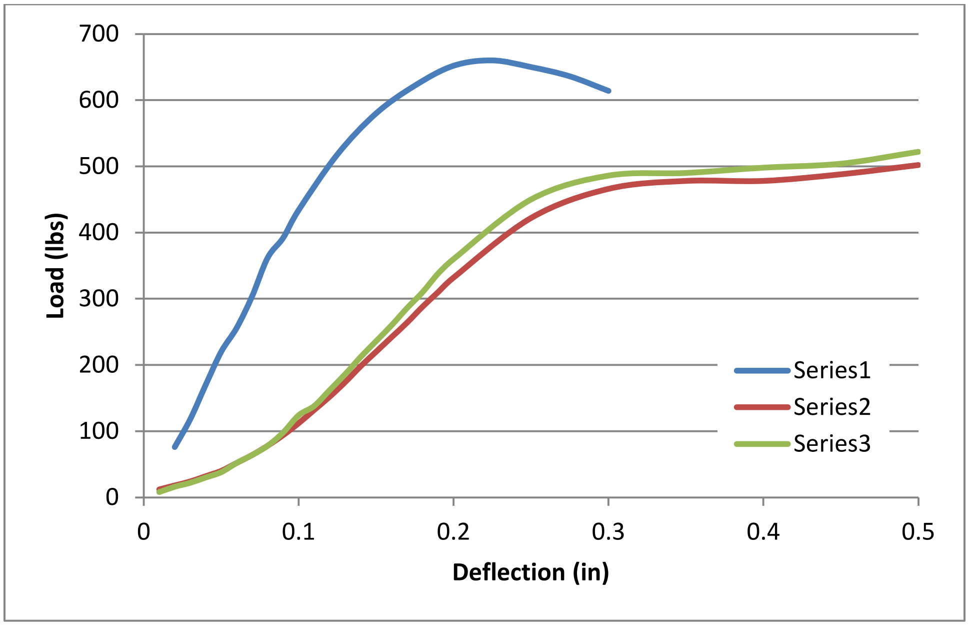

Figure C-1 Deflection versus Load for Low LBR Soil

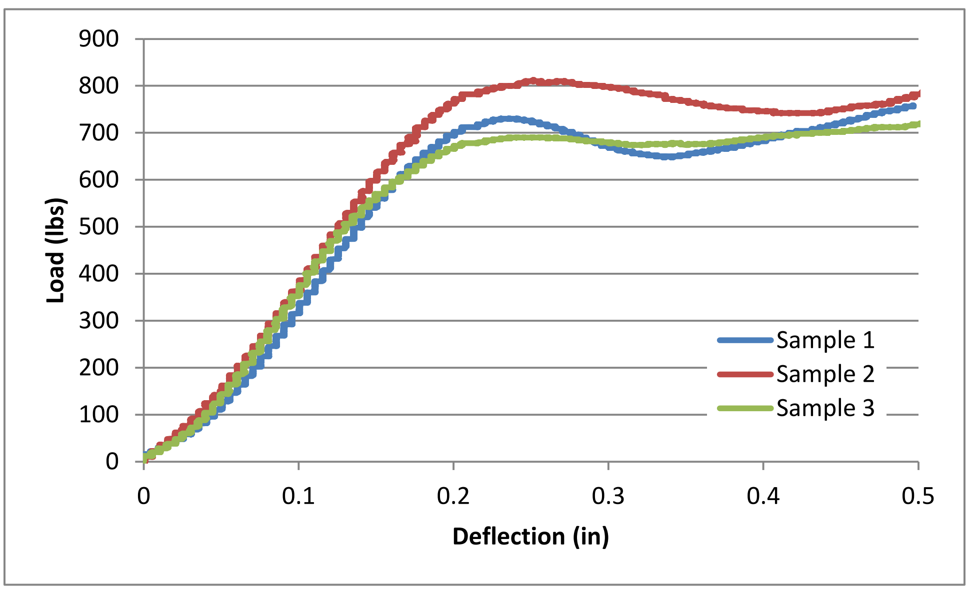

Figure C-2 Deflection versus Load for Low LBR Soil and 4% 1-inch GTR

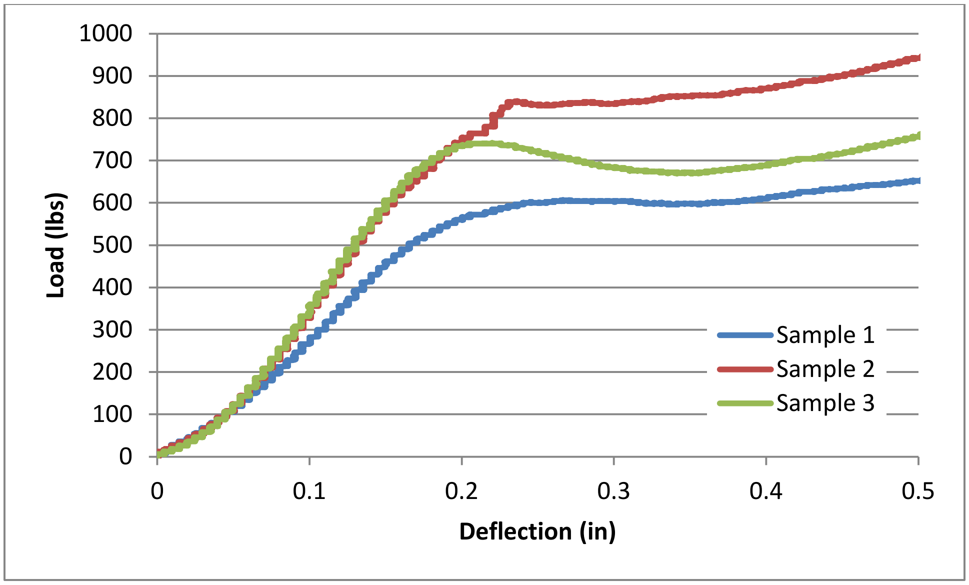

Figure C-3 Deflection versus Load for Low LBR Soil and 8% 1-inch GTR

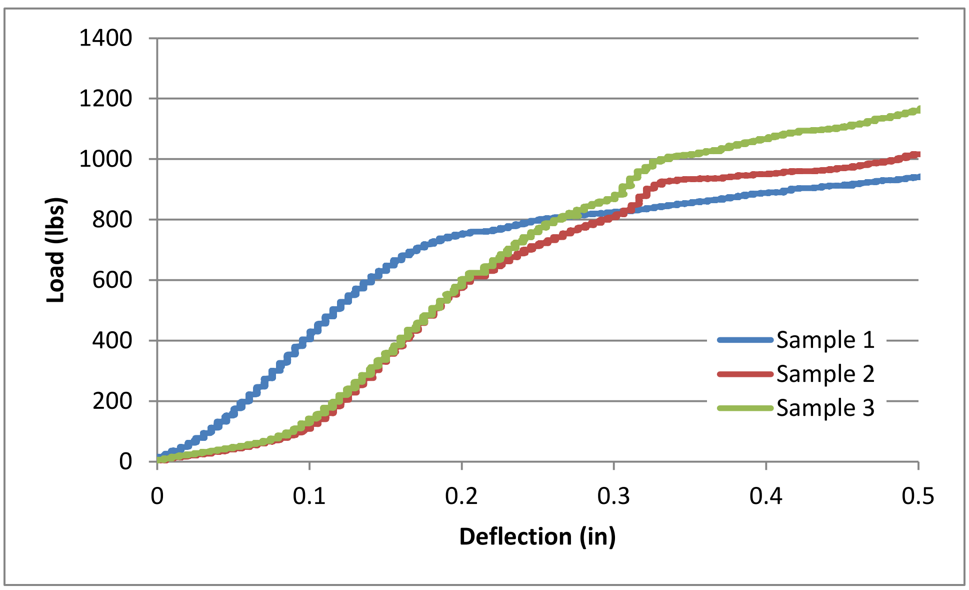

Figure C-4 Deflection versus Load for Low LBR Soil and 16% 1-inch GTR

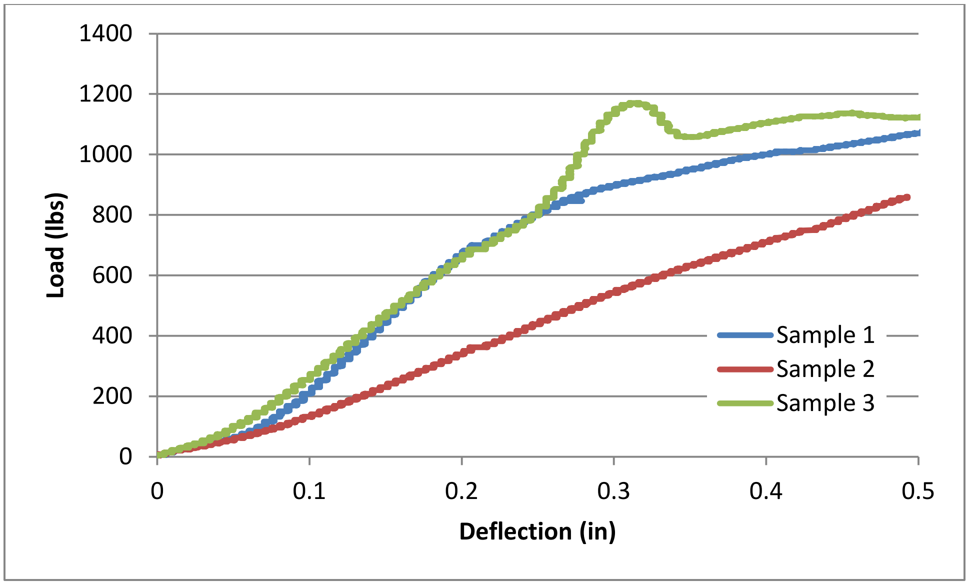

Figure C-5 Deflection versus Load for Low LBR Soil and 24% 1-inch GTR

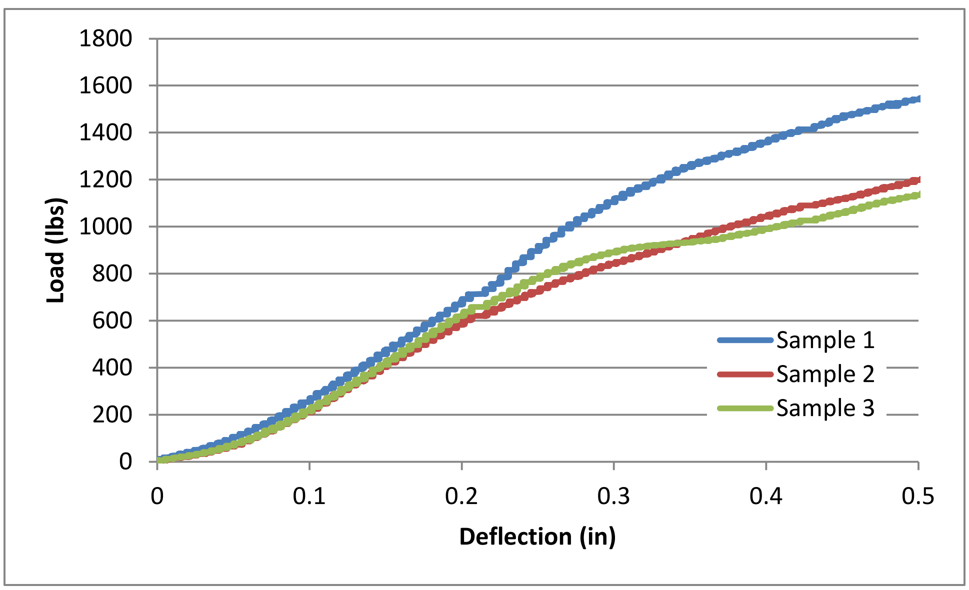

Figure C-6 Deflection versus Load for Low LBR Soil and 32% 1-inch GTR

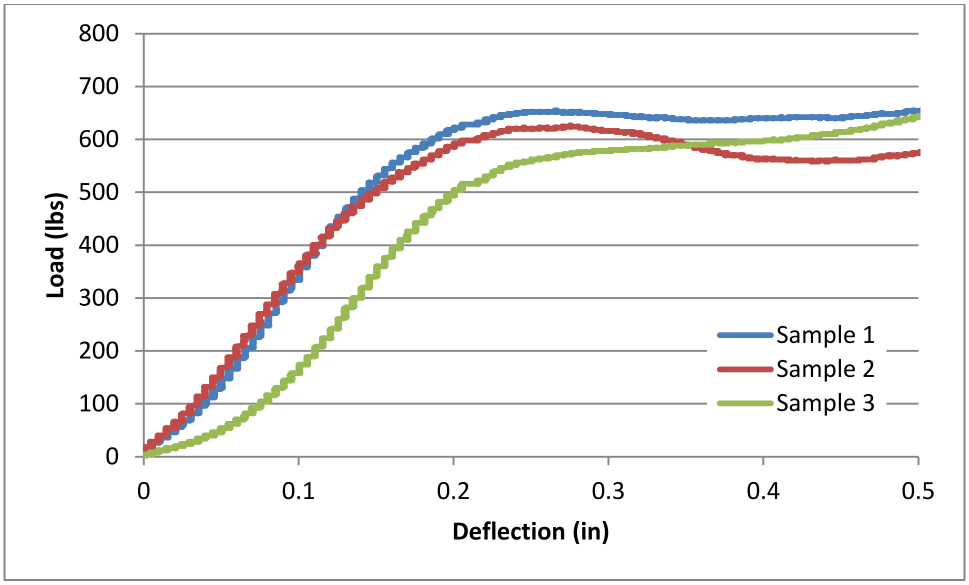

Figure C-7 Deflection versus Load for Low LBR Soil and 4% 3/8-inch GTR

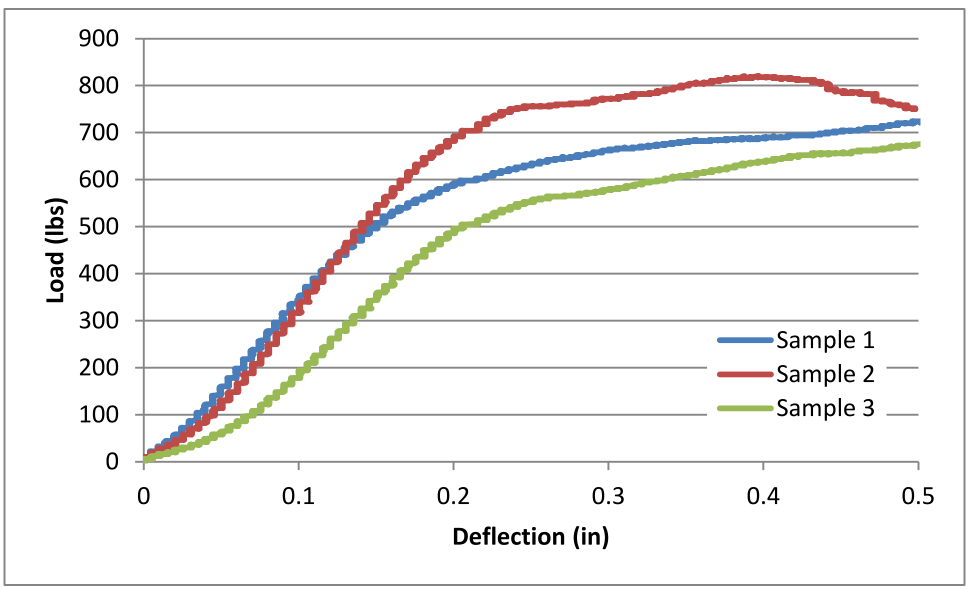

Figure C-8 Deflection versus Load for Low LBR Soil and 8% 3/8-inch GTR

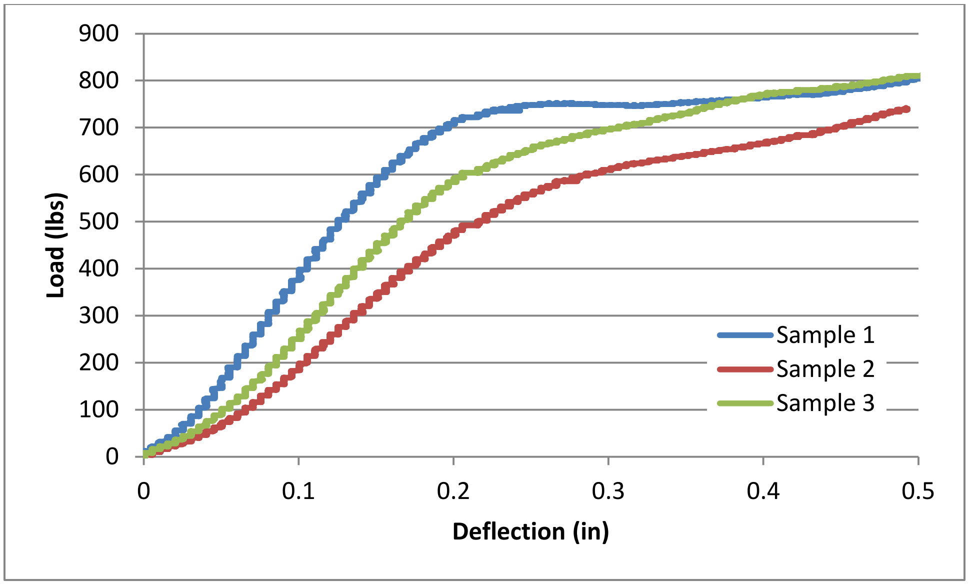

Figure C-9 Deflection versus Load for Low LBR Soil and 16% 3/8-inch GTR

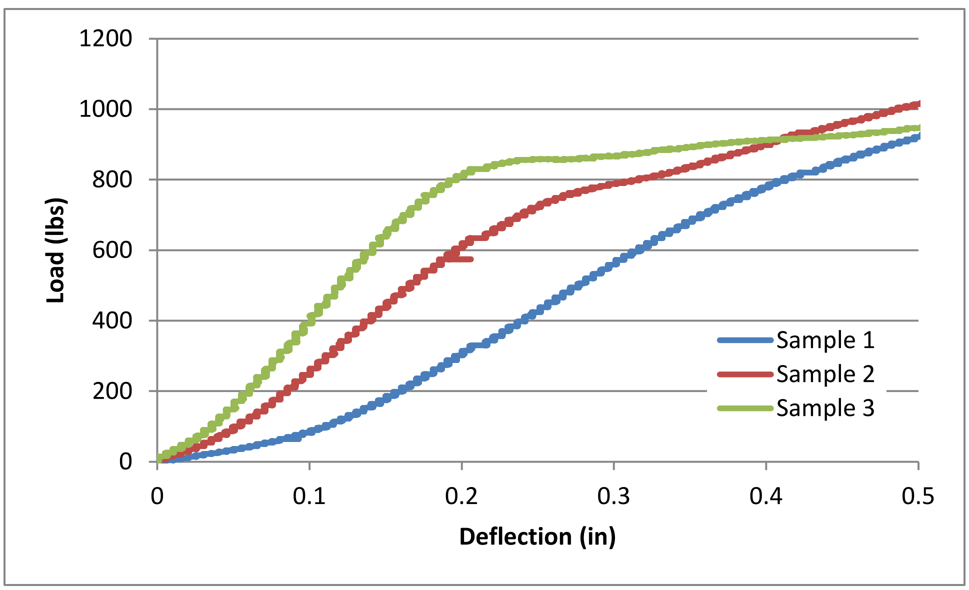

Figure C-10 Deflection versus Load for Low LBR Soil and 24% 3/8-inch GTR

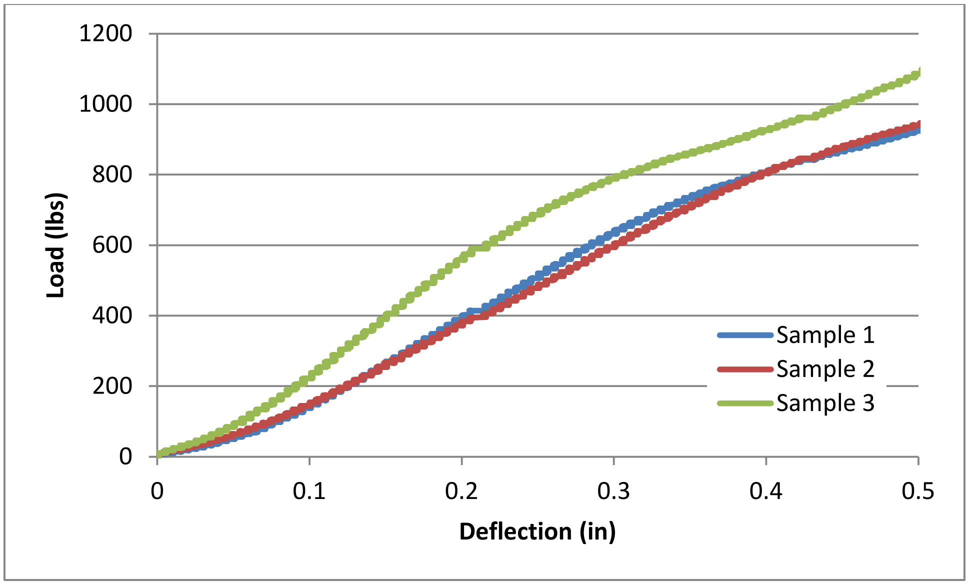

Figure C-11 Deflection versus Load for Low LBR Soil and 32% 3/8-inch GTR

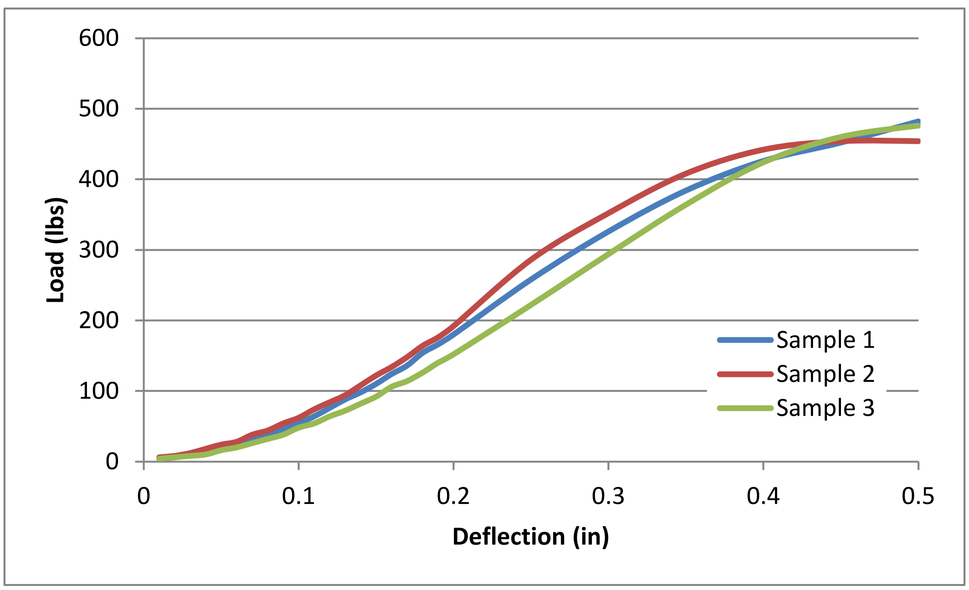

Figure C-12 Deflection versus Load for Low LBR Soil and 4% #40 mesh GTR

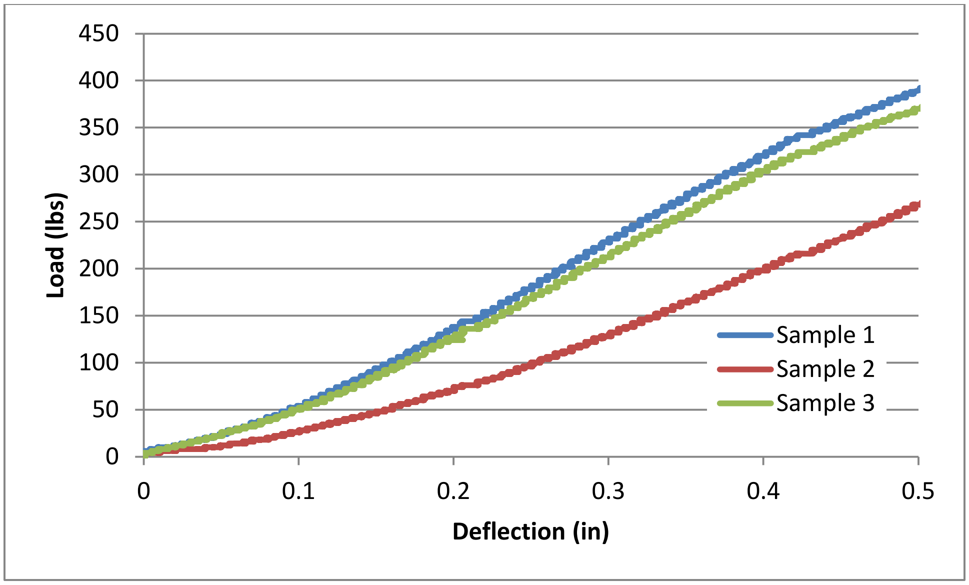

Figure C-13 Deflection versus Load for Low LBR Soil and 8% #40 mesh GTR

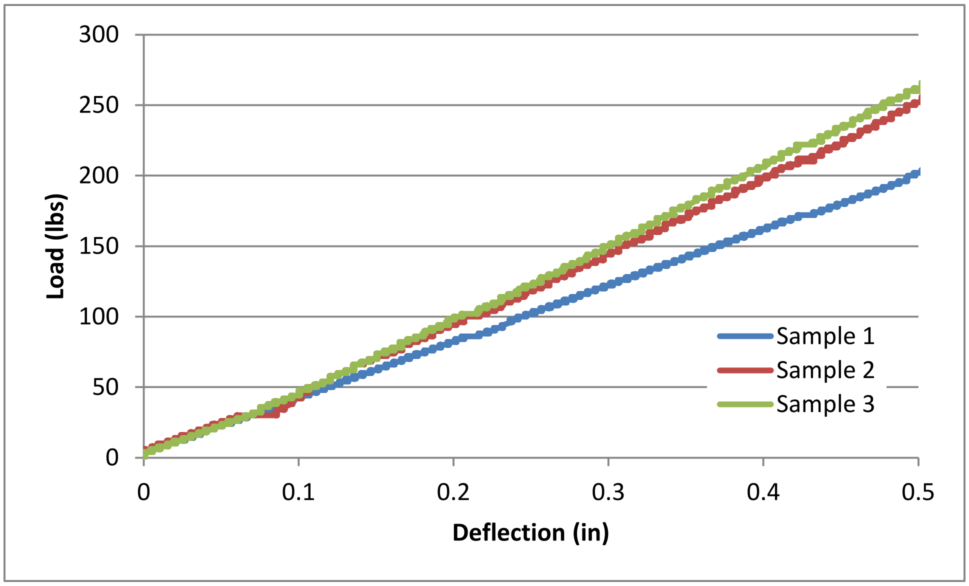

Figure C-14 Deflection versus Load for Low LBR Soil and 16% #40 mesh GTR

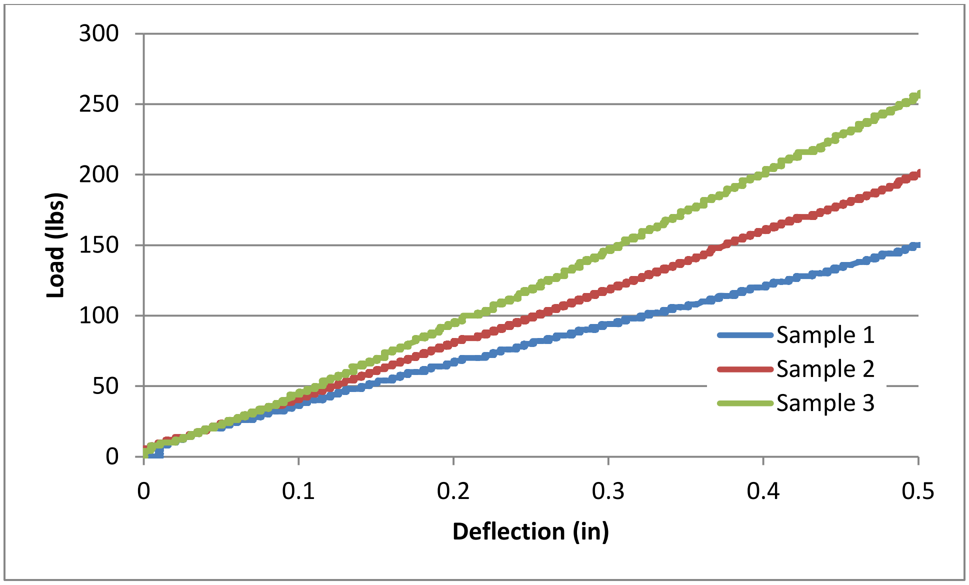

Figure C-15 Deflection versus Load for Low LBR Soil and 24% #40 mesh GTR

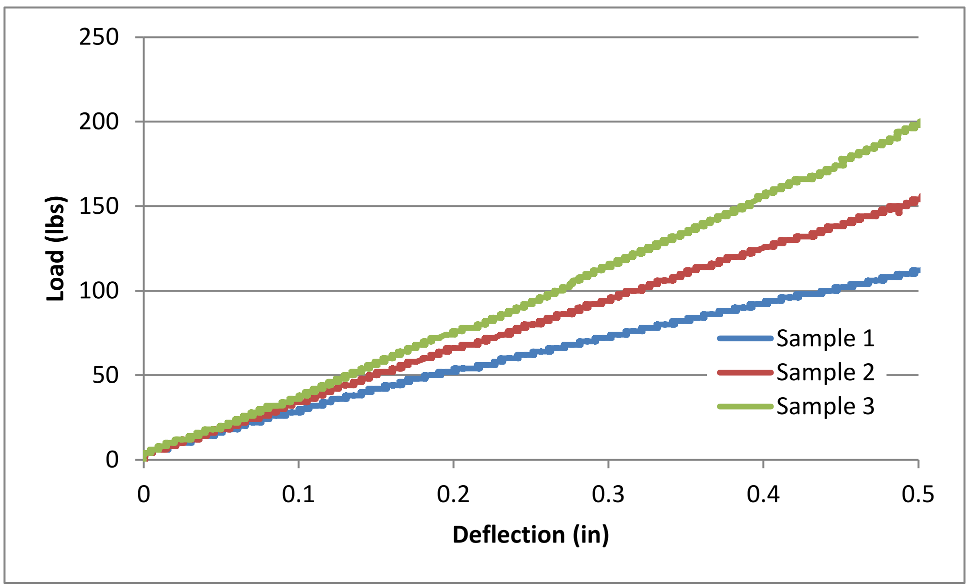

Figure C-16 Deflection versus Load for Low LBR Soil and 32% #40 mesh GTR

C.2. Medium LBR Soil

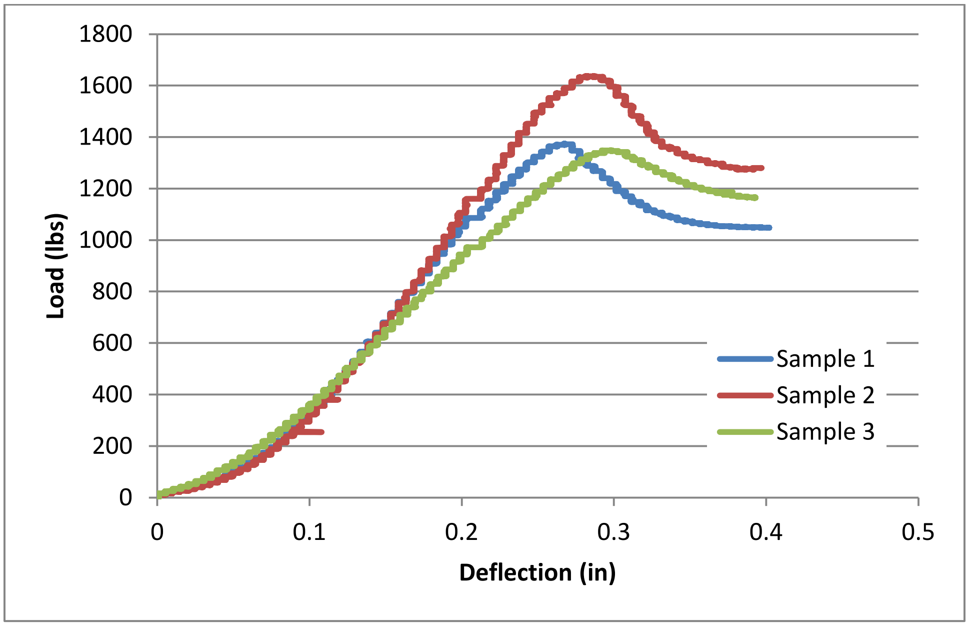

Figure C-17 Deflection versus Load for Medium LBR Soil

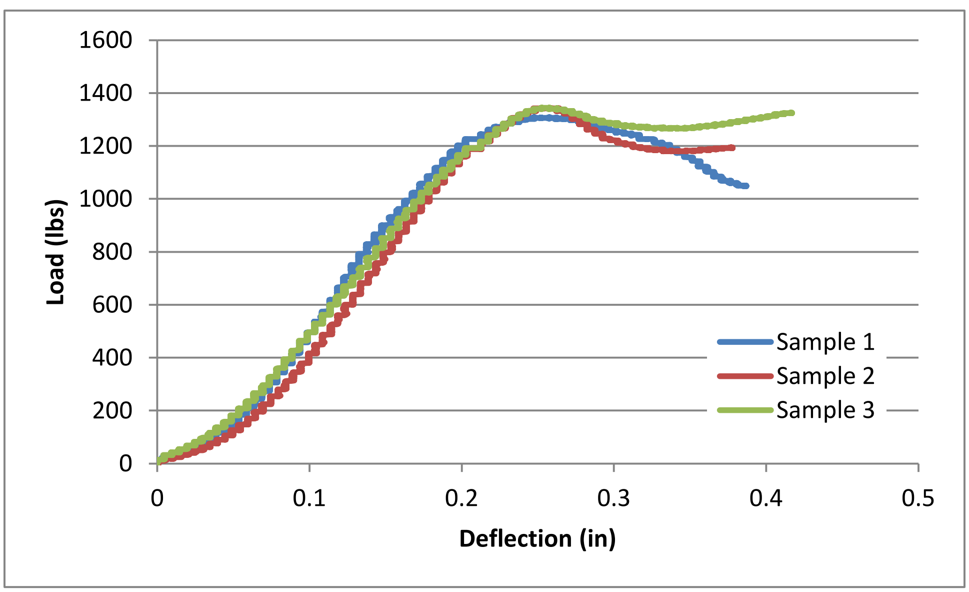

Figure C-18 Deflection versus Load for Medium LBR Soil and 4% 1-inch GTR

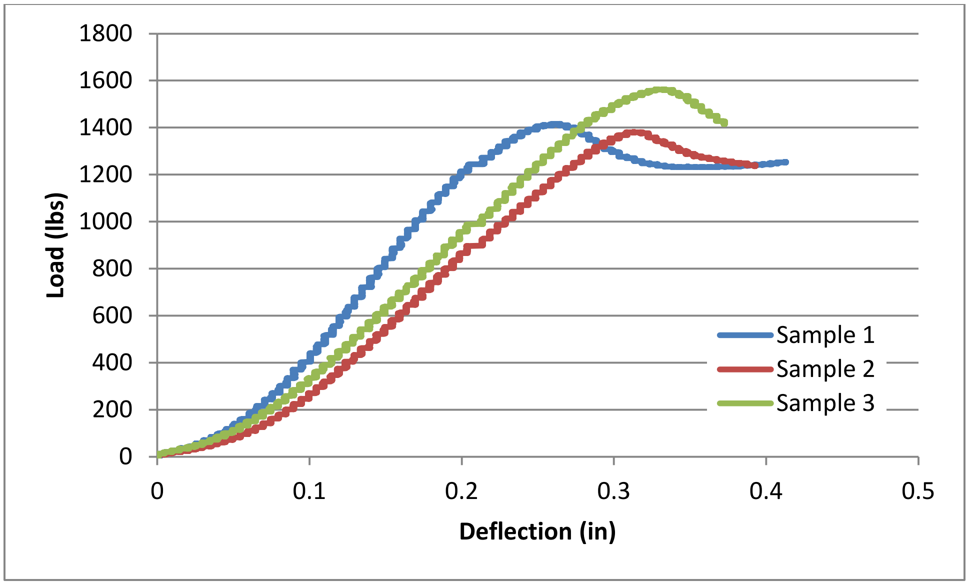

Figure C-19 Deflection versus Load for Medium LBR Soil and 8% 1-inch GTR

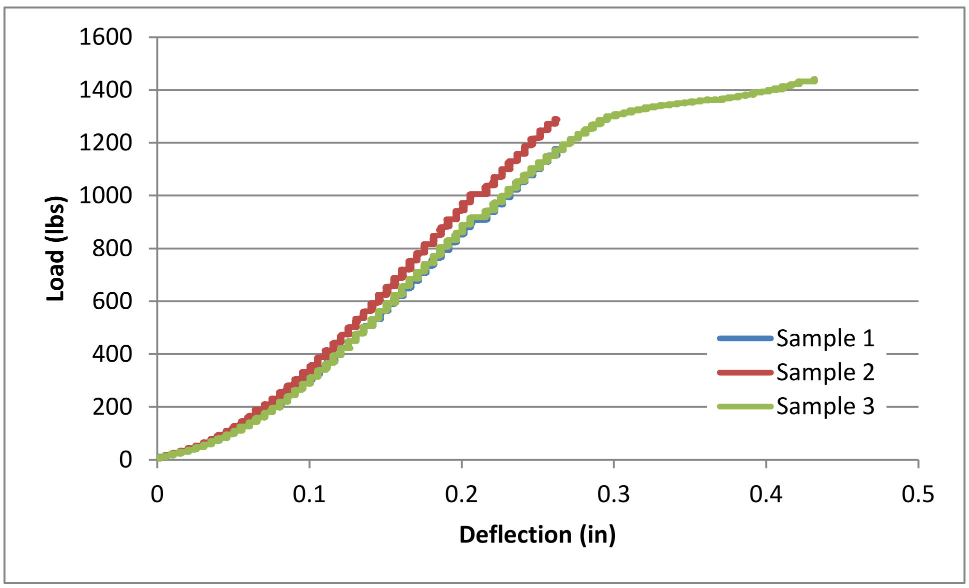

Figure C-20 Deflection versus Load for Medium LBR Soil and 16% 1-inch GTR

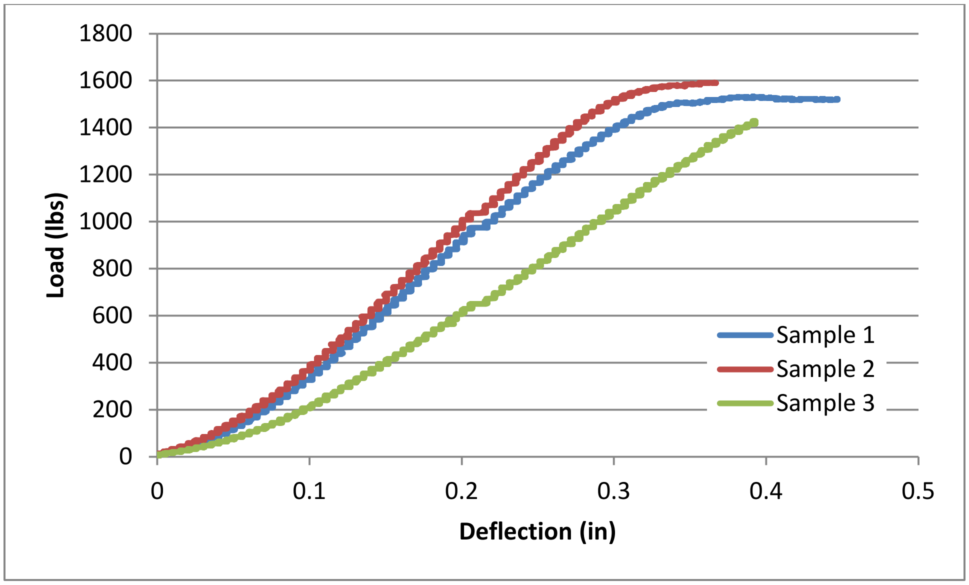

Figure C-21 Deflection versus Load for Medium LBR Soil and 24% 1-inch GTR

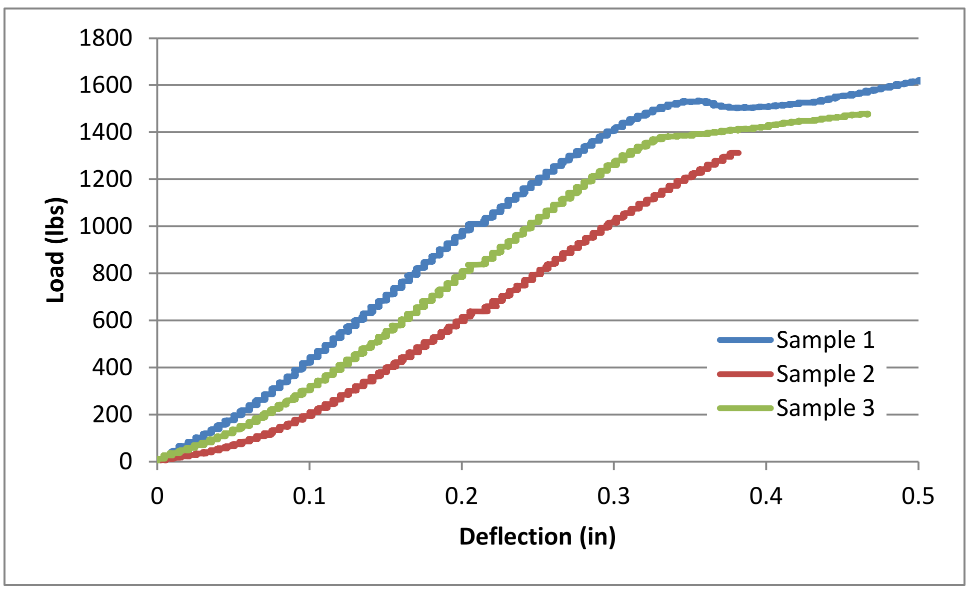

Figure C-22 Deflection versus Load for Medium LBR Soil and 32% 1-inch GTR

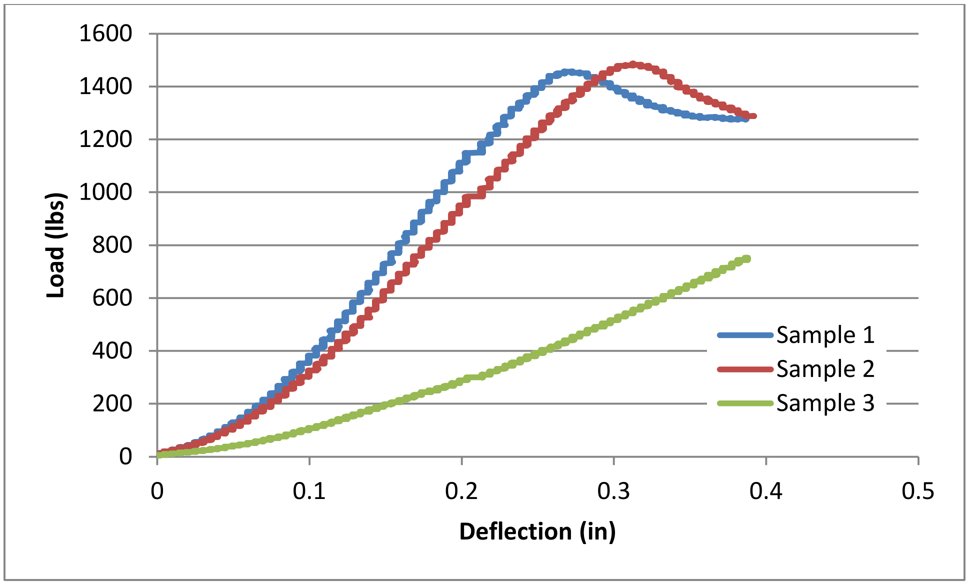

Figure C-23 Deflection versus Load for Medium LBR Soil and 4% 3/8-inch GTR

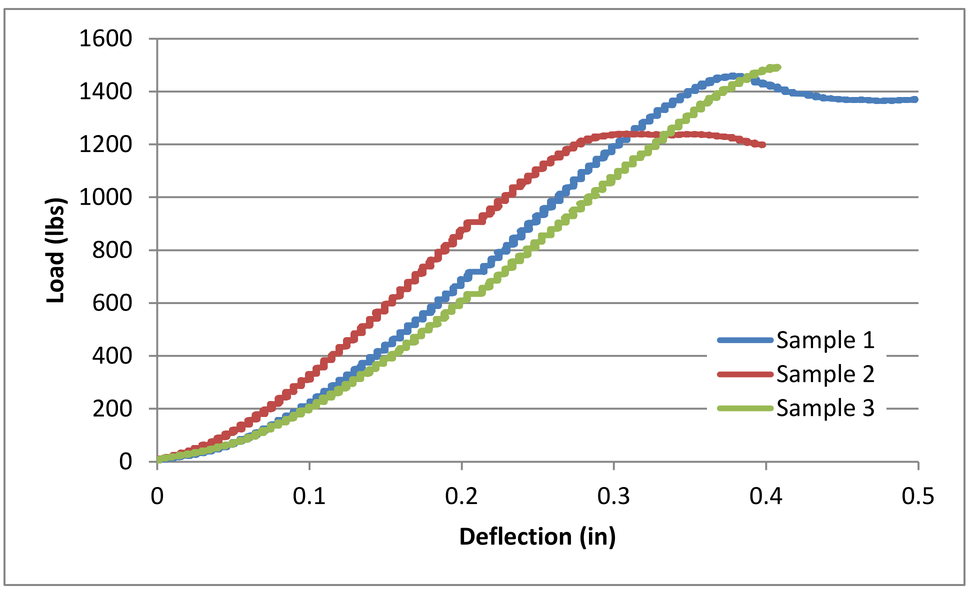

Figure C-24 Deflection versus Load for Medium LBR Soil and 8% 3/8-inch GTR

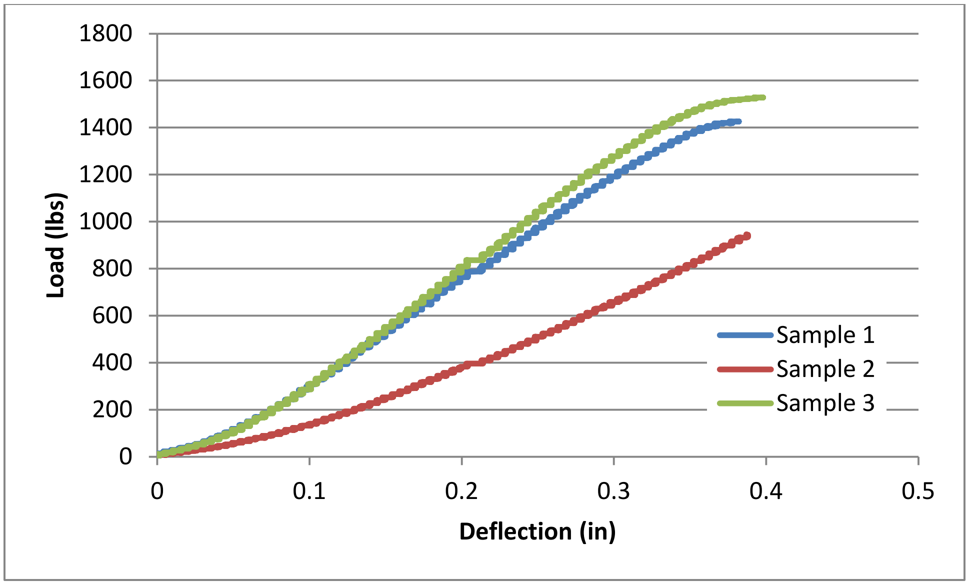

Figure C-25 Deflection versus Load for Medium LBR Soil and 16% 3/8-inch GTR

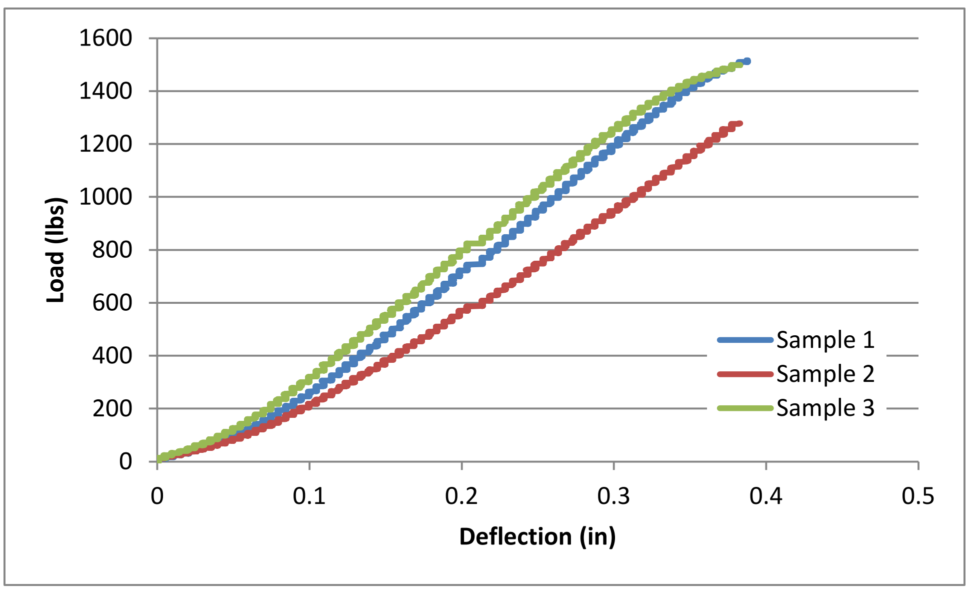

Figure C-26 Deflection versus Load for Medium LBR Soil and 24% 3/8-inch GTR

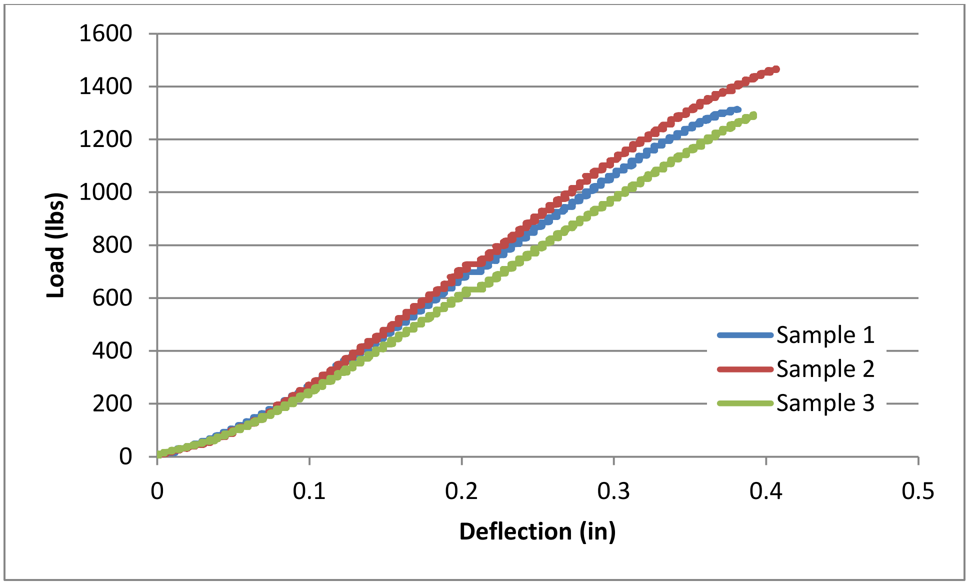

Figure C-27 Deflection versus Load for Medium LBR Soil and 32% 3/8-inch GTR

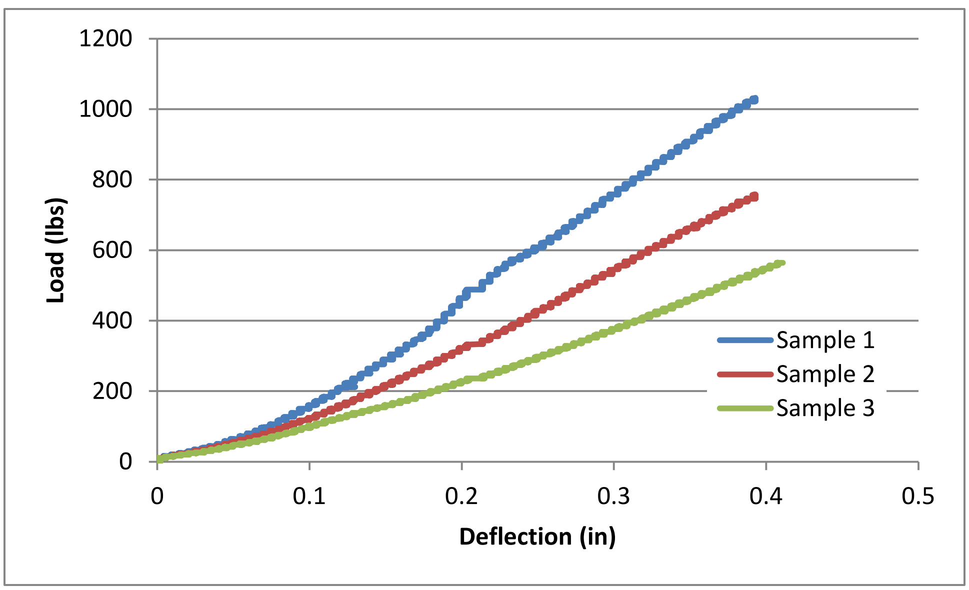

Figure C-28 Deflection versus Load for Medium LBR Soil and 4% #40 mesh GTR

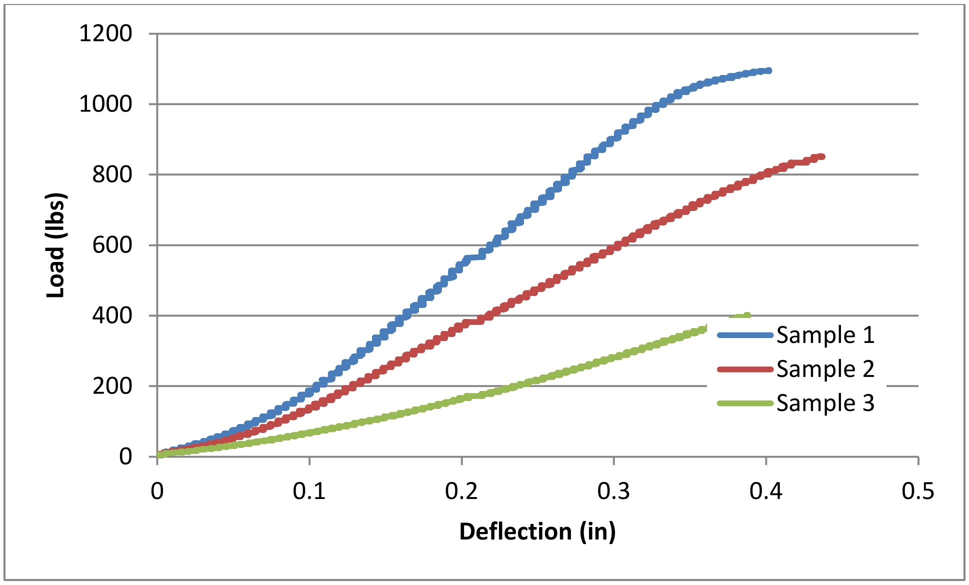

Figure C-29 Deflection versus Load for Medium LBR Soil and 8% #40 mesh GTR

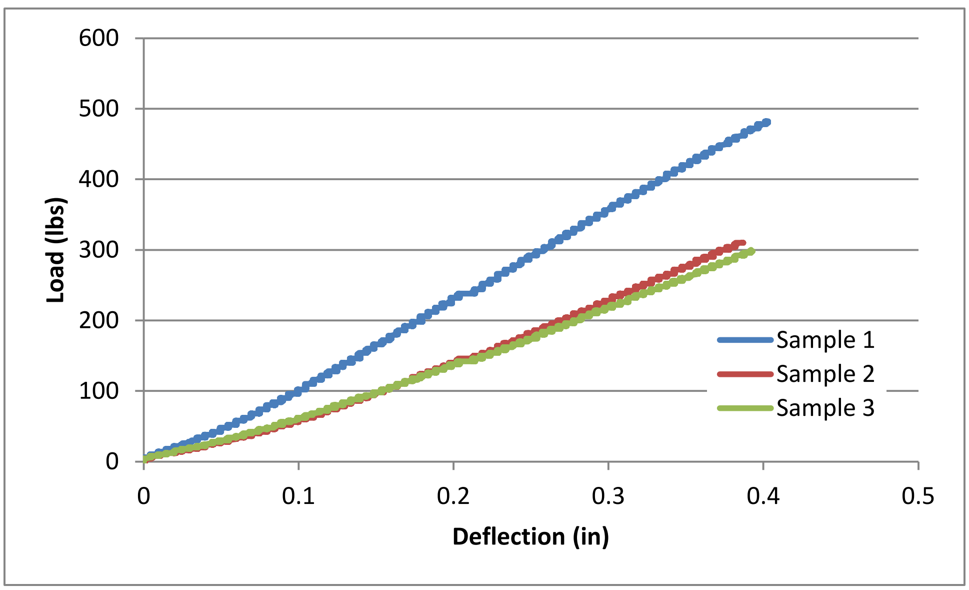

Figure C-30 Deflection versus Load for Medium LBR Soil and 16% #40 mesh GTR

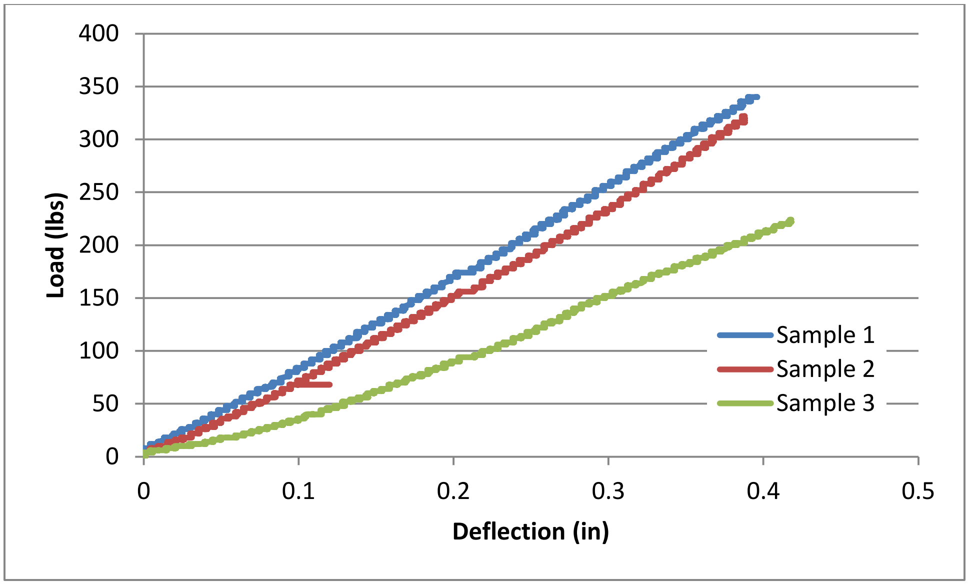

Figure C-31 Deflection versus Load for Medium LBR Soil and 24% #40 mesh GTR

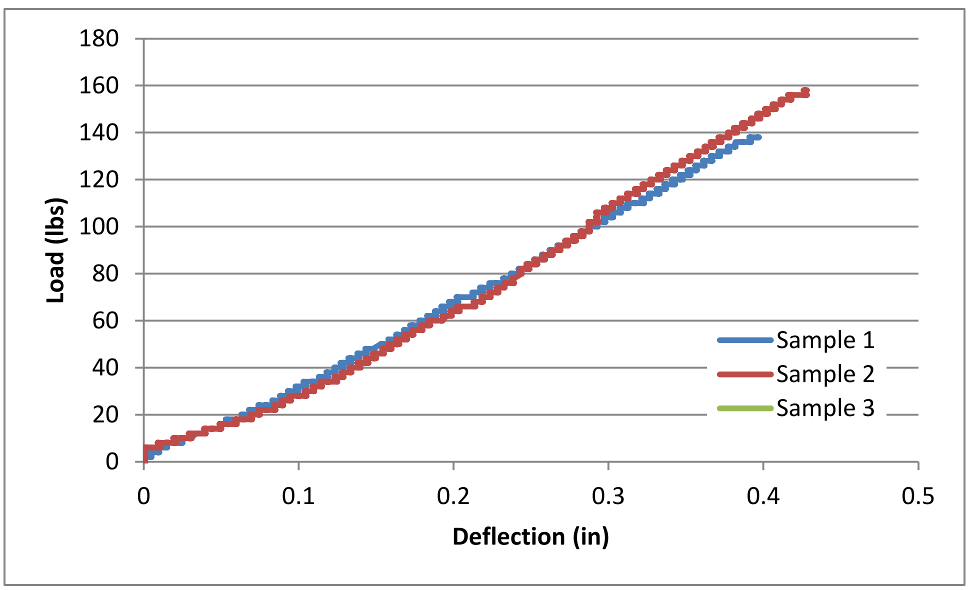

Figure C-32 Deflection versus Load for Medium LBR Soil and 32% #40 mesh GTR

C.3. High LBR Soil

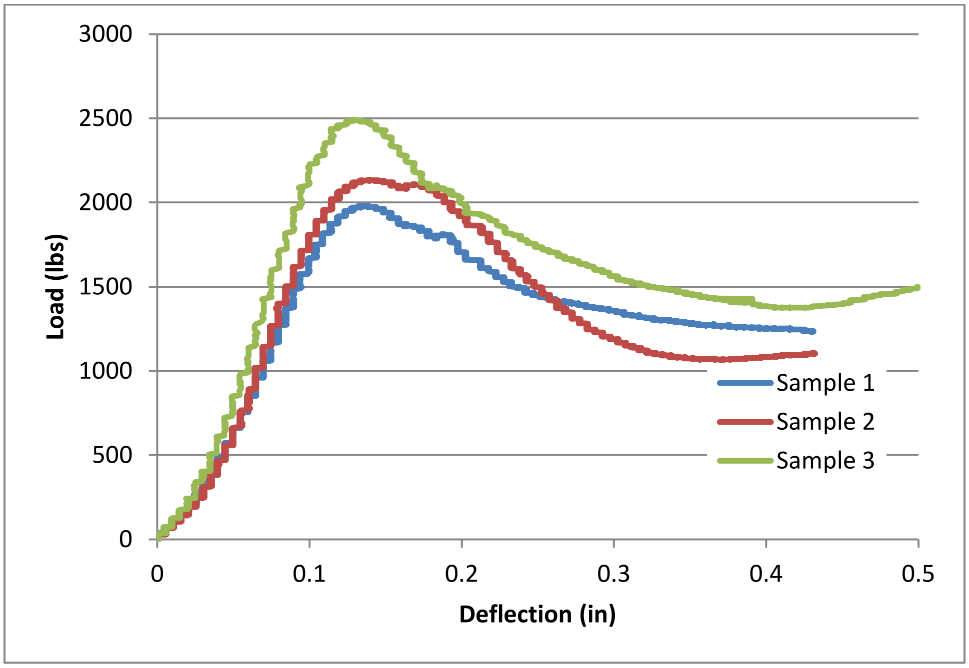

Figure C-33 Deflection versus Load for High LBR Soil

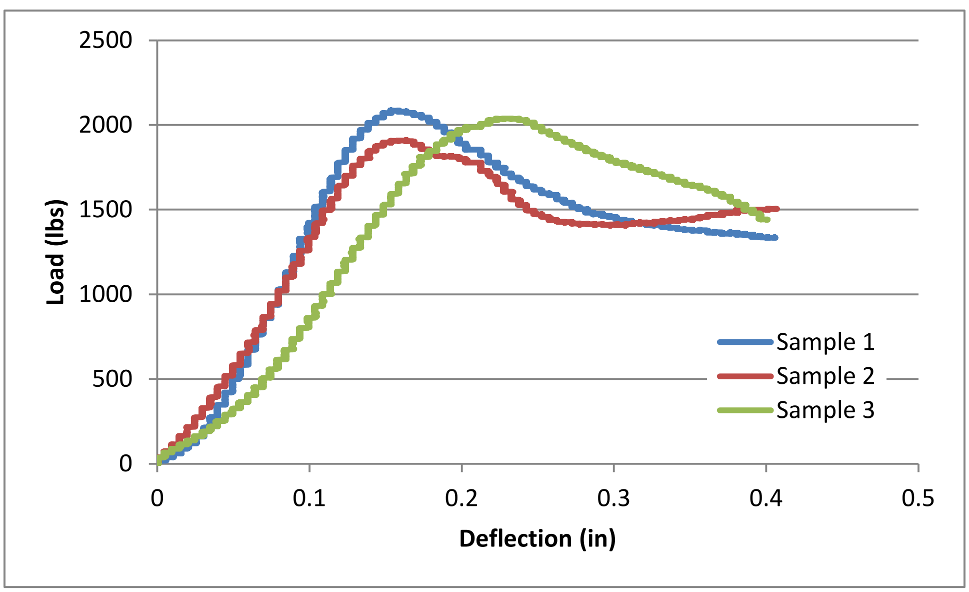

Figure C-34 Deflection versus Load for High LBR Soil and 4% 1-inch GTR

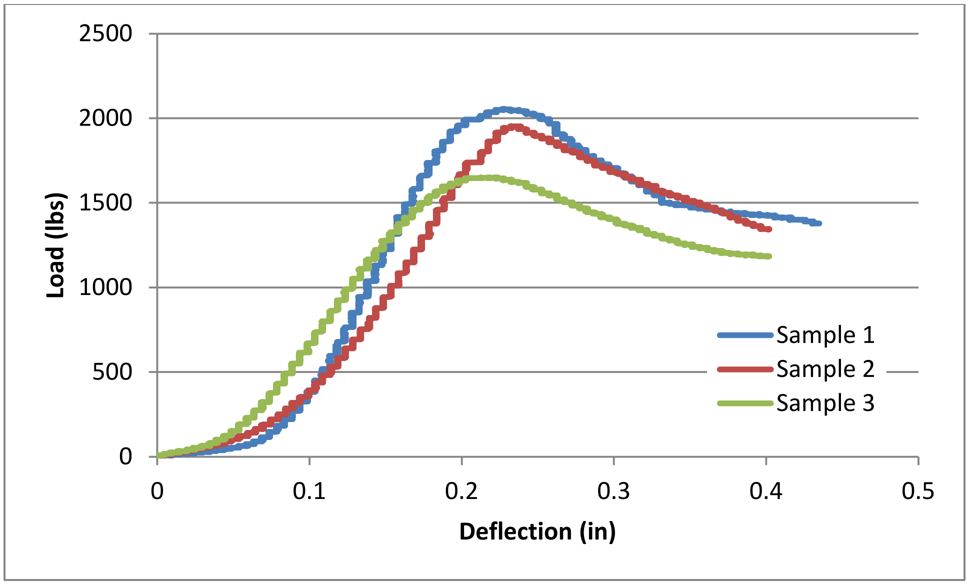

Figure C-35 Deflection versus Load for High LBR Soil and 8% 1-inch GTR

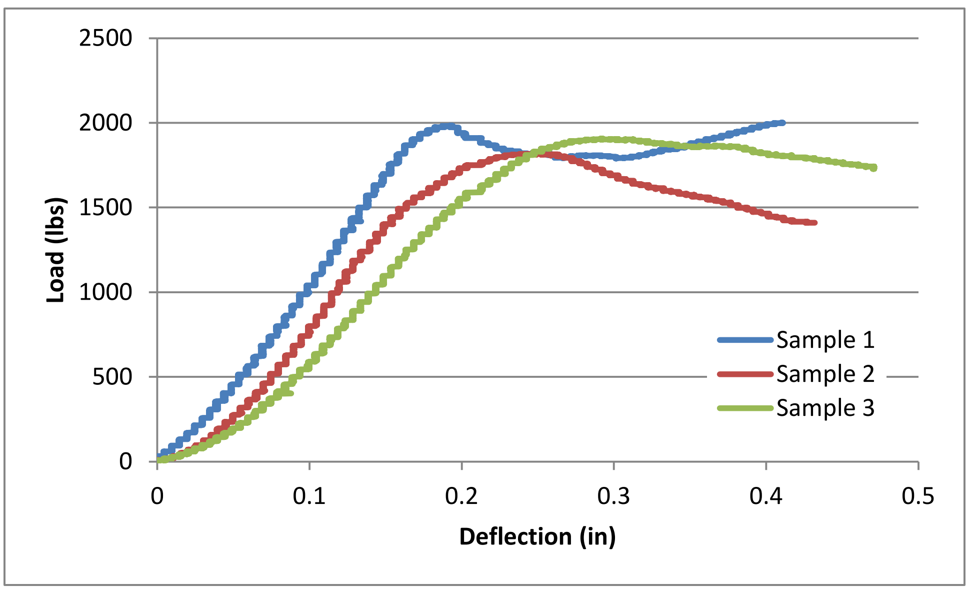

Figure C-36 Deflection versus Load for High LBR Soil and 16% 1-inch GTR

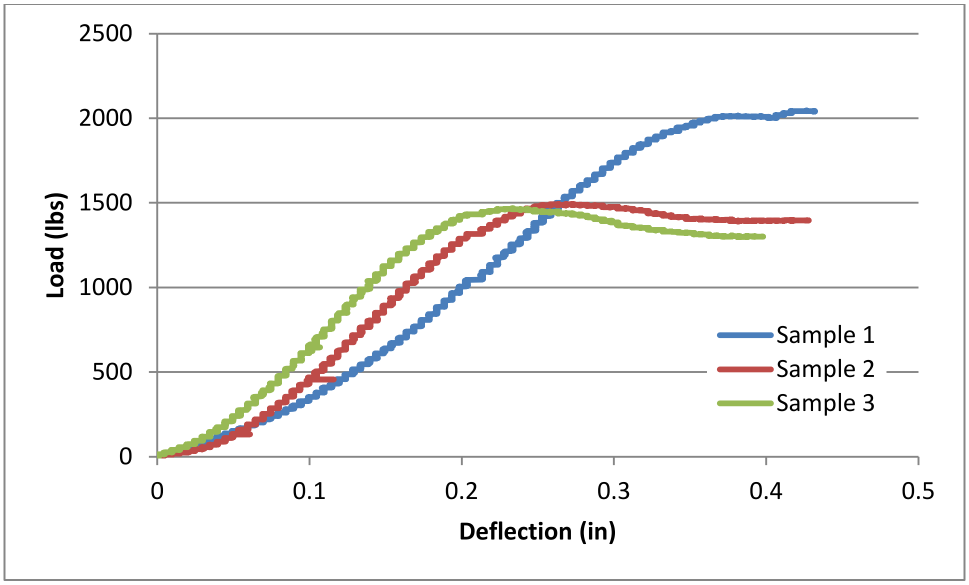

Figure C-37 Deflection versus Load for High LBR Soil and 24% 1-inch GTR

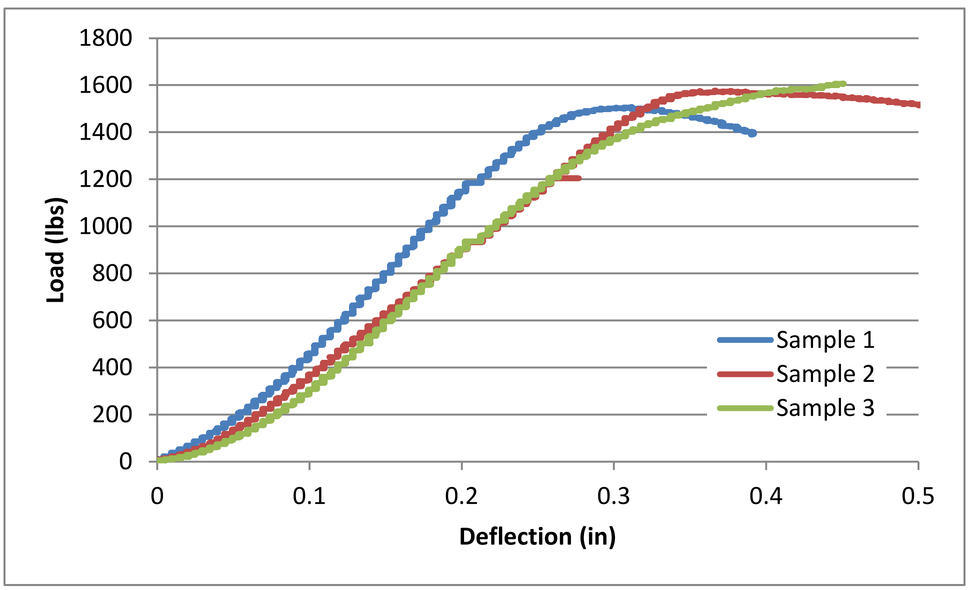

Figure C-38 Deflection versus Load for High LBR Soil and 32% 1-inch GTR

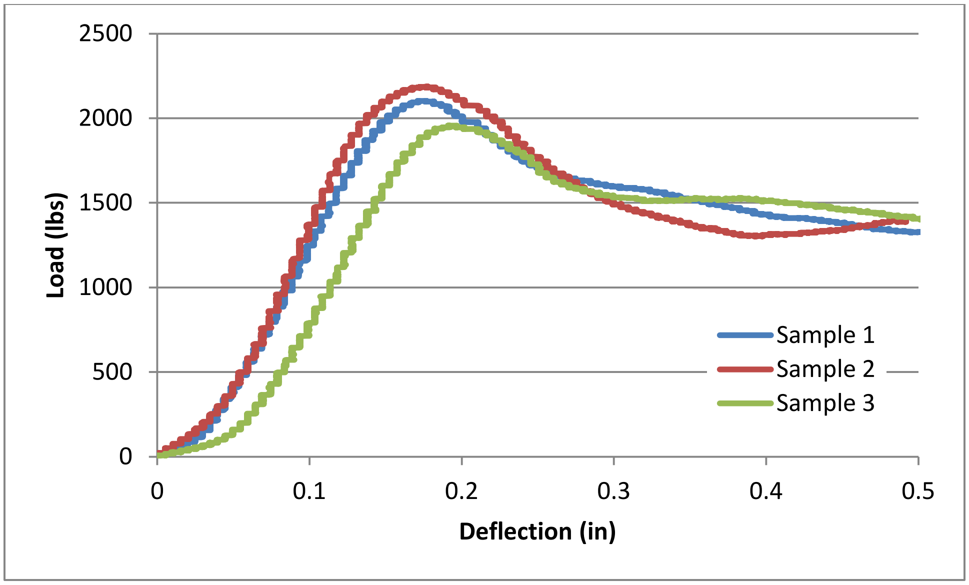

Figure C-39 Deflection versus Load for High LBR Soil and 4% 3/8-inch GTR

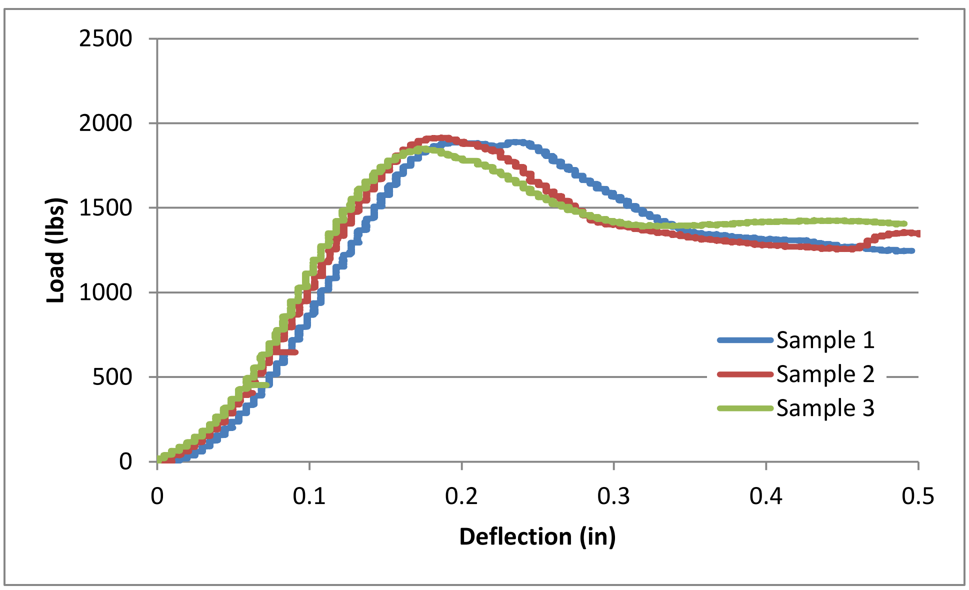

Figure C-40 Deflection versus Load for High LBR Soil and 8% 3/8-inch GTR

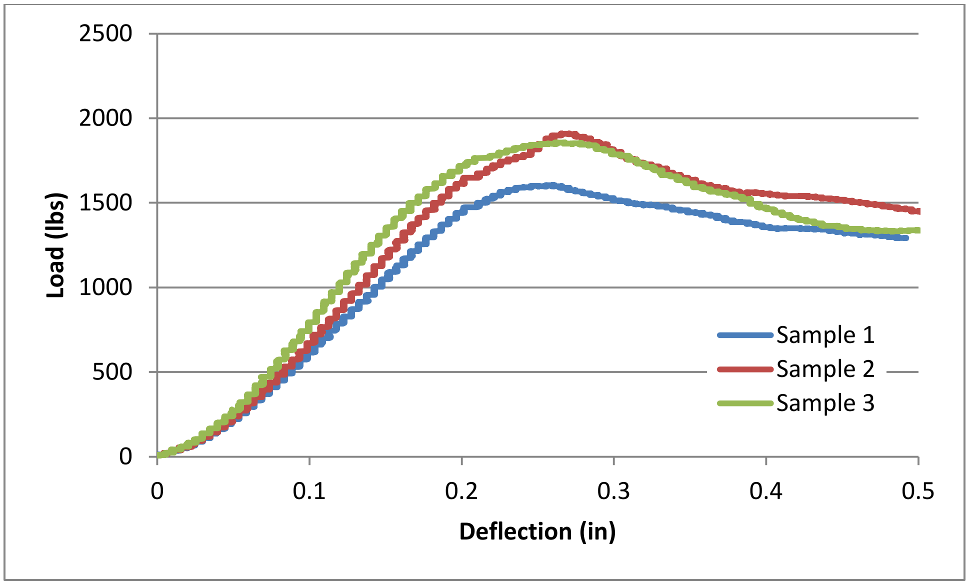

Figure C-41 Deflection versus Load for High LBR Soil and 16% 3/8-inch GTR

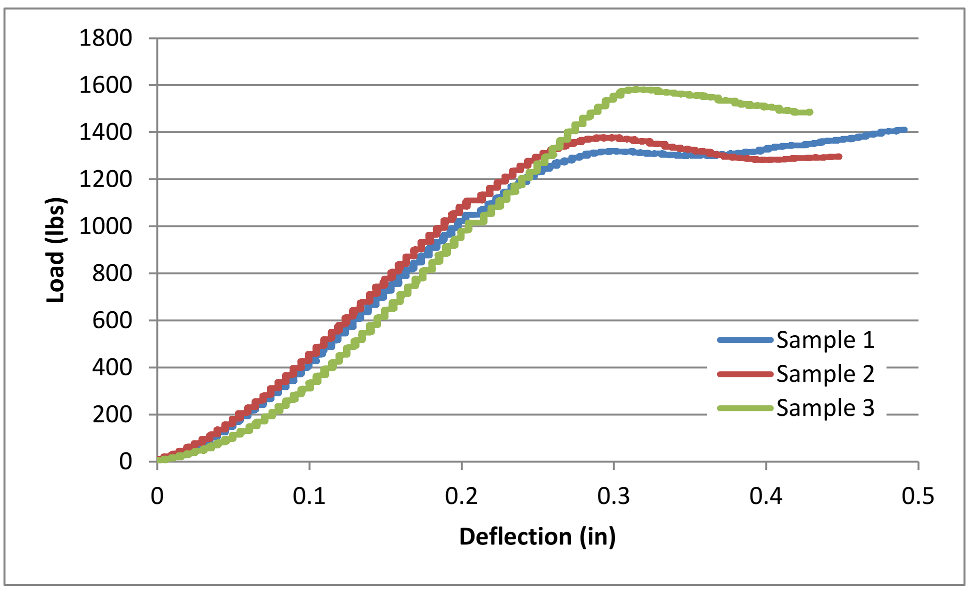

Figure C-42 Deflection versus Load for High LBR Soil and 24% 3/8-inch GTR

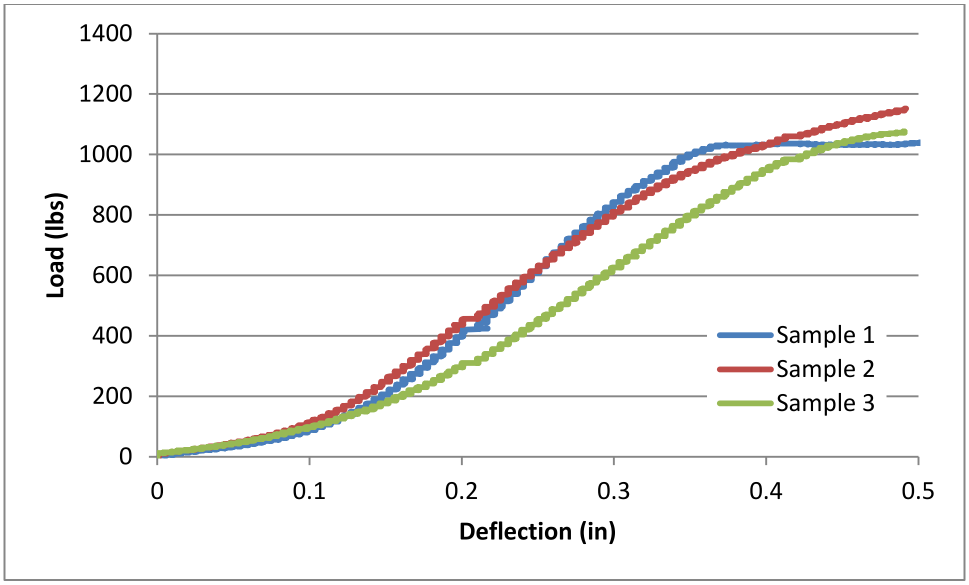

Figure C-43 Deflection versus Load for High LBR Soil and 32% 3/8-inch GTR

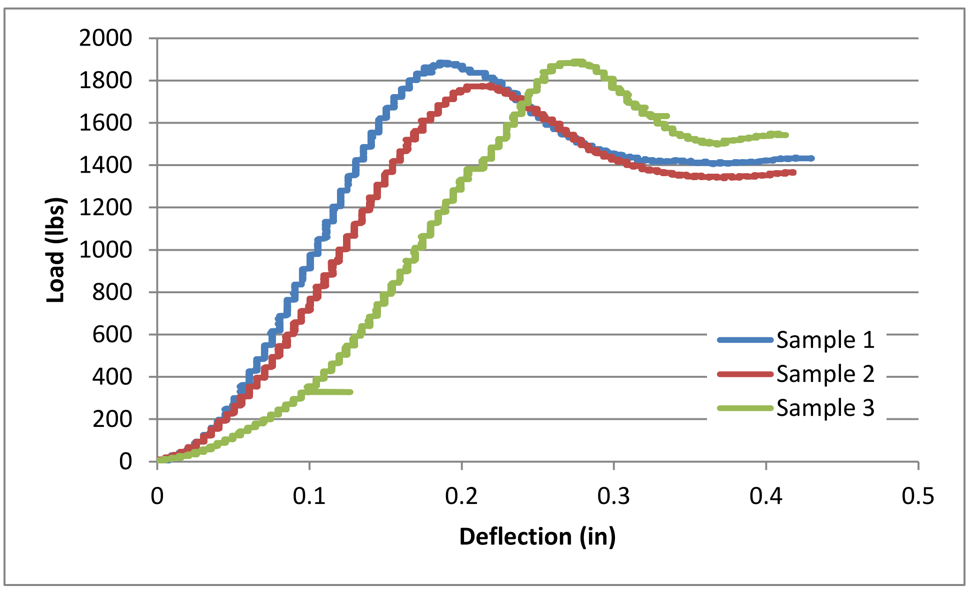

Figure C-44 Deflection versus Load for High LBR Soil and 4% #40 mesh GTR

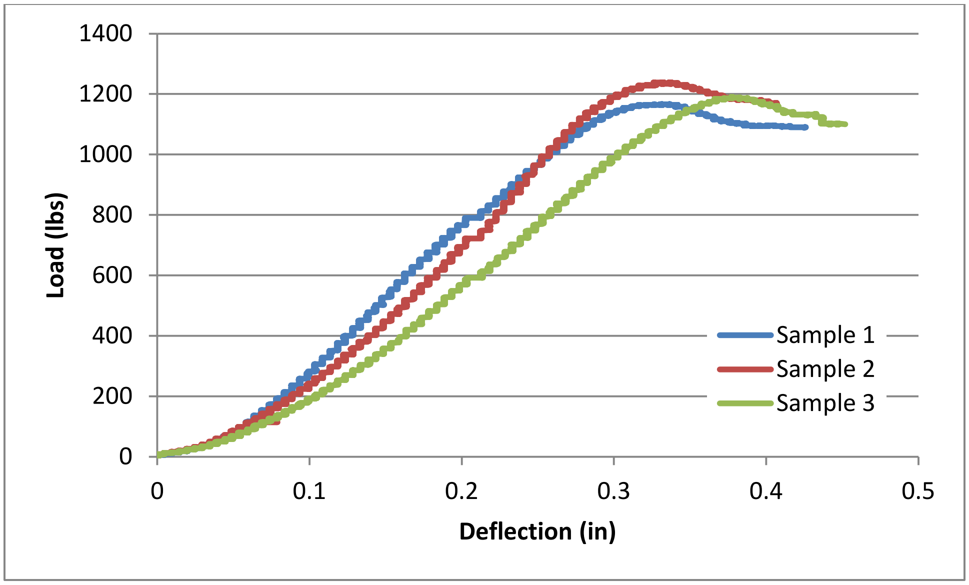

Figure C-45 Deflection versus Load for High LBR Soil and 8% #40 mesh GTR

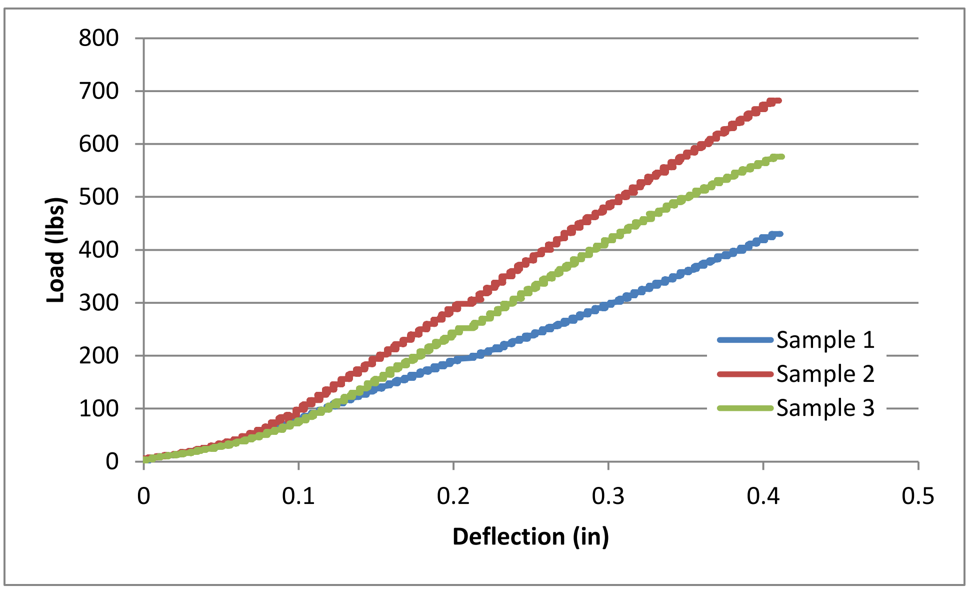

Figure C-46 Deflection versus Load for High LBR Soil and 16% #40 mesh GTR

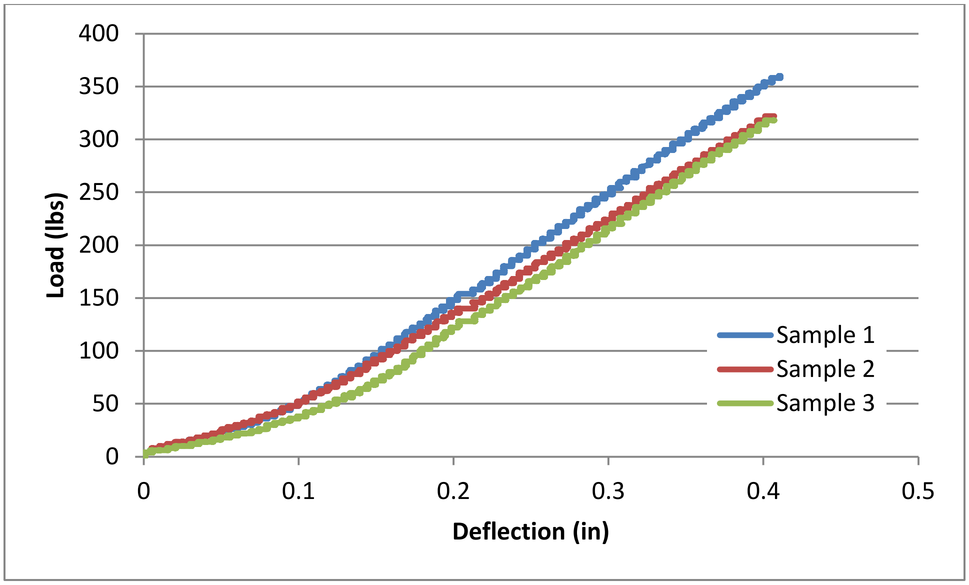

Figure C-47 Deflection versus Load for High LBR Soil and 24% #40 mesh GTR

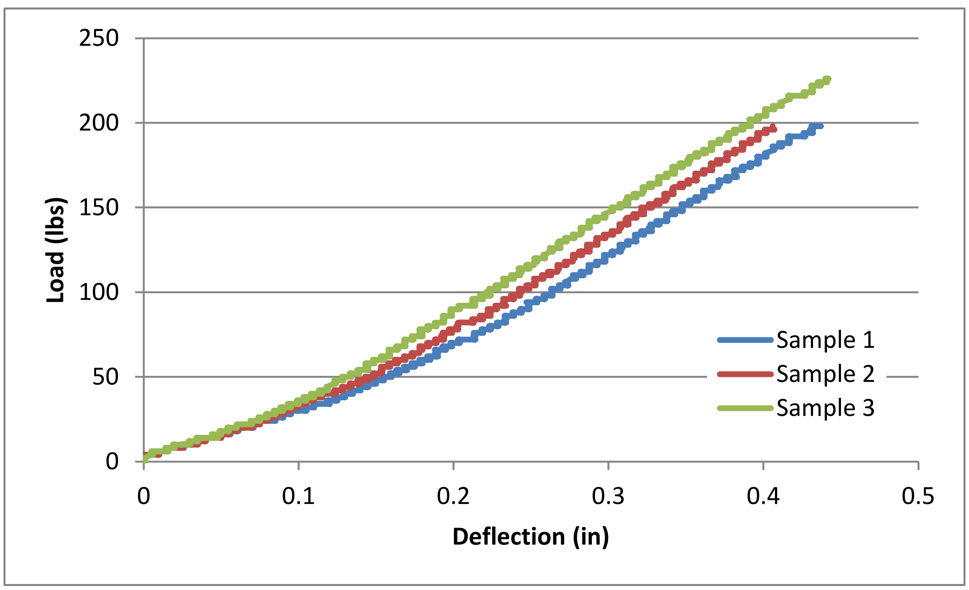

Figure C-48 Deflection versus Load for High LBR Soil and 32% #40 mesh GTR

Appendix D – Resilient Modulus

D.1. Low LBR Soil

Table D-1 Whitehurst (Low LBR Blend)

FLORIDA DEPARPTMENT OF TRANSPORTAION
FOUNDATIONS LABORATORY
F.I.T. SOIL RUBBER BLEND MR SUMMARY
WHITEHURST LOW LBR BLEND
JULY 2013 DATA SUMMARY

SAMPLE NUMBER	MAX DENSITY	OPT % W	ACTUAL DENSITY	ACTUAL MOIST	% MAX	4x8 SAMPLES--INSTRON Bulk Stress (psi)				15 psi AVG	K1	K2	R^2
	6 INCH T180					2	9	11	15				
100% SAND	108.0	12.0%	107.7	11.5	99.7	5,668	12,552	13,957	16,443	16,719	3929.2	0.5286	0.9309
			108.2	11.4	100.2	6,624	13,384	14,701	16,995		4790.6	0.4676	0.939
#40 2%	108.0	12.0%	105.5	11.3	97.7	5,936	12,227	13,464	15,628	15,589	4255	0.4804	0.9587
			106.0	11.2	98.1	6,106	12,269	13,467	15,551		4426.4	0.464	0.9516
#40 4%	108.0	12.0%	103.3	11.6	95.6	5,014	10,811	11,978	14,035	14,351	3519.3	0.5108	0.918
			103.6	11.4	95.9	5,276	11,318	12,531	14,666		3711.7	0.5074	0.9187
#40 8%	108.0	12.0%	100.0	11.0	92.6	3,184	8,393	9,552	11,666	11,028	2036.7	0.6445	0.9037
			99.1	11.4	91.8	2,597	7,311	8,394	10,390		1612	0.6881	0.9009
#40 12%	108.0	12.0%	95.8	11.3	88.7	1,317	5,224	6,278	8,342	8,245	697.6	0.9163	0.6363
			96.8	11.5	89.6	1,096	4,900	5,983	8,148		550.0	0.9954	0.805
#40 16%	108.0	12.0%	94.4	11.7	87.4	382	2,603	3,362	4,995	5,403	157.7	1.2761	0.7669
			94.4	11.4	87.4	464	3,061	3,938	5,810		194.5	1.2544	0.6594
3/8" 2%	108.0	12.0%	107.1	11.5	99.2	6,163	12,911	14,249	16,596	16,422	4383.7	0.4916	0.9271
			106.4	11.8	98.5	5,791	12,509	13,863	16,248		4061.2	0.512	0.9485
3/8" 4%	108.0	12.0%	106.1	11.6	98.3	5,231	11,830	13,190	15,607	15,426	3591.7	0.5425	0.9039
			106.8	11.3	98.9	5,289	11,656	12,952	15,245		3674.5	0.5254	0.9348
3/8" 8%	108.0	12.0%	104.3	11.2	96.6	4,087	9,619	10,783	12,864	12,709	2755.3	0.569	0.8862
			104.5	11.6	96.8	3,735	9,232	10,417	12,554		2461.1	0.6017	0.8941
3/8" 12%	108.0	12.0%	102.5	11.5	95.0	3,056	7,978	9,068	11,052	11,066	1963.8	0.6380	0.8387
			101.5	11.2	94.0	2,715	7,757	8,924	11,081		1673.6	0.6980	0.8119
3/8" 16%	108.0	12.0%	97.8	11.8	90.6	2,359	6,642	7,625	9,440	9,338	1464.1	0.6882	0.7655
			98.0	11.7	90.7	2,089	6,336	7,347	9,236		1253.10	0.7376	0.7538
1" 2%	108.0	12.0%	107.1	11.0	99.2	5,444	11,471	12,671	14,776	15,379	3861.8	0.4955	0.931
			106.2	11.7	98.3	6,404	12,675	13,884	15,983		4675.5	0.4539	0.8593
1" 4%	108.0	12.0%	106.5	11.0	98.6	4,394	10,159	11,361	13,505	13,529	2985.8	0.5573	0.9586
			105	11.6	97.2	4,170	10,052	11,304	13,552		2780.4	0.5849	0.9199
1" 8%	108.0	12.0%	104.5	11.4	96.7	3,730	9,461	10,712	12,978	12,704	2429.1	0.6188	0.8871
			103.5	11.4	95.9	3,671	9,123	10,302	12,429		2413	0.6053	0.8206
1" 12%	108.0	12.0%	99.4	11.6	92.1	2,843	7,461	8,486	10,354	10,572	1822.9	0.6414	0.7922
			100.9	11.4	93.4	2,930	7,753	8,829	10,791		1870.7	0.6471	0.7939
1" 16%	108.0	12.0%	97.9	11.6	90.6	2,170	6,015	6,892	8,504	8,847	1356.3	0.6779	0.7082
			99.6	11.0	92.2	2,437	6,564	7,491	9,189		1543.8	0.6587	0.7001

D.2. Medium LBR Soil

Table D-2 Orange Heights PIT (Medium LBR Blend)

FLORIDA DEPARPTMENT OF TRANSPORTAION
FOUNDATIONS LABORATORY
F.I.T. SOIL RUBBER BLEND MR SUMMARY
40 LBR SAND(ORANGE HEIGHTS PIT)
MAY 2013 DATA SUMMARY

SAMPLE NUMBER	MAX DENSITY	OPT % W	ACTUAL DENSITY	ACTUAL MOIST	% MAX	4x8 SAMPLES--INSTRON Bulk Stress (psi)				15 psi AVG	K1	K2	R^2
6 INCH T180						2	9	11	15				
100% SAND	117.3	10.2%	116.8	10.3	99.6	4,901	11,108	12,389	14,666	14,634	3361.4	0.544	0.9286
			116.9	10.3	99.7	4,980	11,116	12,373	14,601		3439.3	0.5339	0.9359
#40 2%	117.3	10.2%	115.0	10.6	98.0	3,262	8,032	9,058	10,907	10,638	2153.4	0.5991	0.946
			114.0	10.2	97.2	2,991	7,566	8,563	10,369		1949.8	0.6171	0.9297
#40 4%	117.3	10.2%	112.6	10.4	96.0	1,814	5,869	6,864	8,745	9,247	1055.8	0.7807	0.9036
			110.7	10.1	94.4	2,545	6,935	7,928	9,749		1603.1	0.6666	0.8764
#40 8%	117.3	10.2%	109.4	10.4	93.2	1,143	4,225	5,030	6,587	7,424	625.43	0.8694	0.8167
			108.9	10.2	92.8	1,569	5,422	6,398	8,261		886.33	0.8243	0.8918
#40 12%	117.3	10.2%	105.1	10.5	89.6	704	3,372	4,156	5,741	5,780	342.2	1.0413	0.7381
			105.6	10.4	90.1	651	3,339	4,153	5,819		306.3	1.0873	0.788
#40 16%	117.3	10.2%	102.2	10.2	87.2	387	2,325	2,953	4,275	4,391	169.4	1.1921	0.7881
			102.3	10.5	87.2	412	2,458	3,119	4,508		181.1	1.1870	0.7669
3/8" 2%	117.3	10.2%	115.4	10.2	98.4	4,297	9,790	10,926	12,948	12,935	2940.5	0.5474	0.9336
			115.7	10.3	98.6	4,110	9,665	10,833	12,922		2771.6	0.5685	0.9206
3/8" 4%	117.3	10.2%	114.3	10.3	97.5	3,723	9,001	10,127	12,149	11,968	2478.4	0.587	0.9115
			114	10.4	97.2	3,432	8,621	9,748	11,787		2245.3	0.6123	0.8795
3/8" 8%	117.3	10.2%	111.1	10.0	94.7	2,646	6,695	7,577	9,176	9,217	1725.3	0.6171	0.897
			110.3	10.2	94.1	2,331	6,527	7,488	9,259		1450.6	0.6845	0.8881
3/8" 12%	117.3	10.2%	107.7	10.3	91.8	1,598	4,993	5,812	7,351	8,311	945.6	0.7573	0.8431
			108.2	10.3	92.3	2,248	6,473	7,454	9,271		1380.4	0.7033	0.8608
3/8" 16%	117.3	10.2%	105.2	10.8	89.7	1,468	4,453	5,164	6,492	7,130	880.5	0.7377	0.8208
			106.9	10.3	91.1	1,759	5,331	6,180	7,767		1055.60	0.7370	0.8112
1" 2%	117.3	10.2%	115.5	10.1	98.4	3,964	9,333	10,463	12,483	12,770	2671.6	0.5693	0.934
			115.5	10.5	98.5	3,972	9,657	10,872	13,058		2638	0.5906	0.9175
1" 4%	117.3	10.2%	113.7	10.0	96.9	3,291	7,986	8,989	10,792	11,334	2186.8	0.5895	0.9059
			113.2	10.6	96.5	3,356	8,621	9,777	11,876		2172.9	0.6272	0.895
1" 8%	117.3	10.2%	111.3	10.7	94.9	2,416	6,665	7,631	9,407	9,407	1513.7	0.6746	0.8546
			110.6	10.6	94.3	2,289	6,574	7,568	9,408		1407.5	0.7015	0.8397
1" 12%	117.3	10.2%	108.4	10.6	92.4	1,886	5,660	6,554	8,221	7,806	1136.4	0.7307	0.837
			107.9	10.7	92.0	1,805	5,170	5,949	7,391		1111.2	0.6997	0.8552
1" 16%	117.3	10.2%	106.2	10.6	90.6	1,592	4,898	5,690	7,173	7,137	948.8	0.7470	0.7595
			105.0	10.7	89.5	1,596	4,863	5,643	7,101		954.9	0.7409	0.8112

D.3. High LBR Soil

Table D-3 FDOT Maintenance PIT (High LBR Blend)

FLORIDA DEPARPTMENT OF TRANSPORTAION
FOUNDATIONS LABORATORY
F.I.T. SOIL RUBBER BLEND MR SUMMARY

FEBRUARY 2012 DATA SUMMARY

SAMPLE NUMBER	MAX DENSITY	OPT % W	ACTUAL DENSITY	ACTUAL MOIST	% MAX	4x8 SAMPLES--INSTRON Bulk Stress (psi)				15 psi AVG	K1	K2	R^2
6 INCH T180						2	9	11	15				
100% SAND	122.8	7.5%	121.4	7.9	98.8	7,279	13,995	15,271	17,474	17,220	5386.0	0.4346	0.8626
			121.6	7.3	99.0	7,980	14,013	15,107	16,967		6155.6	0.3744	0.7863
#40 2%	122.8	7.5%	121.9	7.5	99.3	5,370	10,995	12,097	14,024	14,193	3859.9	0.4764	0.8077
			122.5	7.4	99.8	5,775	11,400	12,483	14,362		4220.8	0.4522	0.8236
#40 4%	122.8	7.5%	118.4	7.8	96.4	2,812	7,865	9,022	11,154	11,101	1750.2	0.6839	0.8483
			118.1	7.1	96.2	2,889	7,864	8,988	11,049		1820.9	0.6658	0.8704
#40 8%	122.8	7.5%	114.0	7.8	92.9	835	3,821	4,681	6,406	6,284	414.1	1.0114	0.7774
			113.8	7.9	92.7	812	3,687	4,511	6,163		404.5	1.0058	0.8076
#40 12%	122.8	7.5%	111.9	7.4	91.1	515	2,580	3,199	4,460	4,459	245.2	1.0712	0.7797
			110.8	7.6	90.3	513	2,576	3,195	4,457		243.7	1.0732	0.7926
#40 16%	122.8	7.5%	107.4	7.6	87.5	465	1,983	2,406	3,244	3,070	238.4	0.9640	0.6171
			106.7	7.6	86.9	346	1,690	2,089	2,897		166.6	1.0546	0.7256
3/8" 2%	122.8	7.5%	121.5	7.5	98.9	6,232	11,945	13,029	14,899	14,837	4617.3	0.4326	0.7983
			120.3	7.3	98.0	5,547	11,525	12,707	14,775		3960.1	0.4862	0.8480
3/8" 4%	122.8	7.5%	119.5	7.9	97.4	4,352	10,110	11,314	13,462	12,383	2951.3	0.5604	0.8599
			118.2	8.0	96.3	3,286	8,264	9,347	11,305		2148.2	0.6132	0.8566
3/8" 8%	122.8	7.5%	116.0	7.7	94.5	2,819	7,531	8,586	10,514	10,650	1792.4	0.6533	0.8485
			116.2	7.7	94.6	3,029	7,817	8,871	10,786		1956.9	0.6303	0.8203
3/8" 12%	122.8	7.5%	112.9	7.4	92.0	1,281	4,709	5,602	7,326	7,301	703.2	0.8654	0.8588
			114.0	7.7	92.8	1,291	4,693	5,575	7,275		712.4	0.8580	0.8612
3/8" 16%	122.8	7.5%	110.6	6.8	90.1	887	3,566	4,293	5,719	5,542	467.5	0.9247	0.8639
			111.5	7.0	90.8	715	3,219	3,934	5,365		357.7	0.9999	0.8702
1" 2%	122.8	7.5%	120.4	7.3	98.1	6,059	12,063	13,223	15,241	14,531	4411.5	0.4578	0.8255
			119.9	7.3	97.7	4,733	10,533	11,719	13,821		3273.3	0.5319	0.8612
1" 4%	122.8	7.5%	117.2	8.0	95.4	3,625	9,117	10,311	12,471	12,726	2369.8	0.6132	0.8701
			118.5	7.9	96.5	4,305	9,812	10,953	12,981		2944.7	0.5478	0.8920
1" 8%	122.8	7.5%	115.7	8.0	94.3	2,336	6,922	8,002	10,011	10,004	1416.1	0.7222	0.8973
			115.3	7.5	93.9	2,336	6,915	7,993	9,997		1416.5	0.7216	0.9010
1" 12%	122.8	7.5%	113.7	6.9	92.6	1,961	6,031	7,006	8,832	9,419	1168.8	0.7468	0.8936
			114.7	7.2	93.4	2,711	7,186	8,185	10,007		1729.7	0.6482	0.8907
1" 16%	122.8	7.5%	112.0	7.6	91.2	1,251	4,411	5,219	6,767	7,017	700.0	0.8378	0.8680
			112.1	7.4	91.3	1,162	4,566	5,480	7,267		618.5	0.9098	0.8429

Appendix E – Consolidation

E.1. Low LBR Soil

Table E-1 – C_v values for Low LBR Soil

	Pressure	Cv (in^2/sec)	Cv (in^2/sec)	Cv (in^2/sec)	Cv (in^2/sec)	Cv (in^2/sec)	Cv (in^2/sec)	Cv (in^2/sec)
Trial	tsf	Virgin Soil	1" GTR 16%	1" GTR 32%	3/8" GTR 16%	3/8" GTR 32%	#40" GTR 16%	#40 GTR 32%
A	0.125	0.156	0.325	0.325	0.325	0.325	0.091	0.263
A	0.5	0.217	0.408	0.408	0.409	0.408	0.261	0.402
A	1	0.323	0.407	0.405	0.725	0.530	0.404	0.516
A	2	0.216	0.530	0.715	0.722	0.718	0.524	0.686
A	4	0.322	1.032	1.020	0.529	0.715	0.519	
A	8	0.406	0.713	0.702	0.716	0.400	0.513	
A	16	0.404	0.707	1.003	1.026	0.519	0.690	
B	0.125	0.134	0.156	0.263	0.263	0.263	0.217	0.263
B	0.5	0.325	0.410	0.322	0.262	0.323	0.180	0.525
B	1	0.410	0.534	0.407	0.534	0.532	0.317	0.396
B	2	0.262	0.725	0.405	0.408	0.720	0.398	0.995
B	4	0.408	1.040	0.716	0.723	1.032	0.699	0.972
B	8	0.322	0.528	0.713	0.722	0.712	0.690	0.657
B	16	0.529	0.526	1.020	0.721	1.019	0.981	0.639

E.1.1. Virgin Material

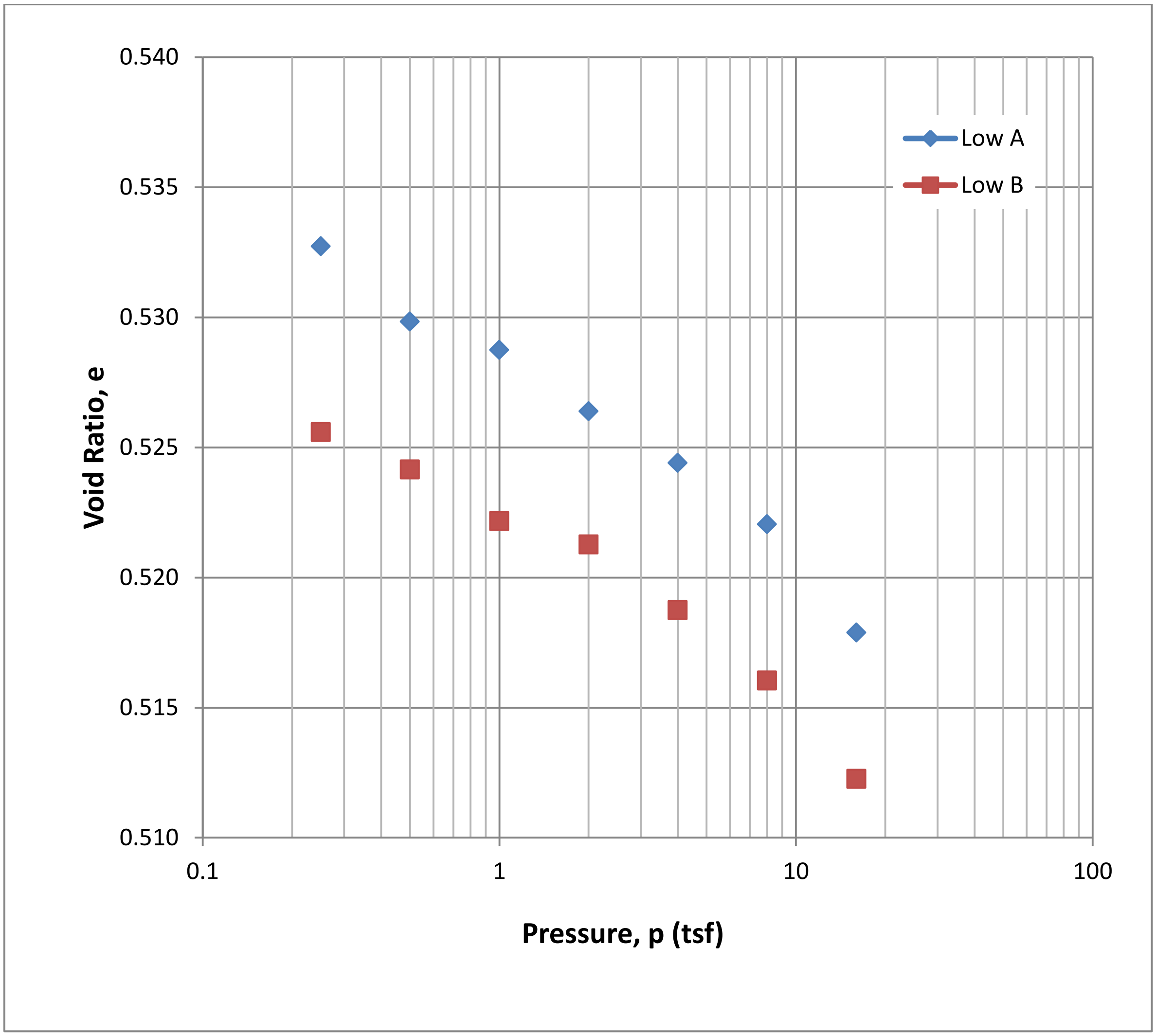

Figure E-1 – Void Ratio versus log-Pressure Curves for Low LBR Soil

E.1.2. 1" GTR

E.1.2.1. 1" GTR 16%

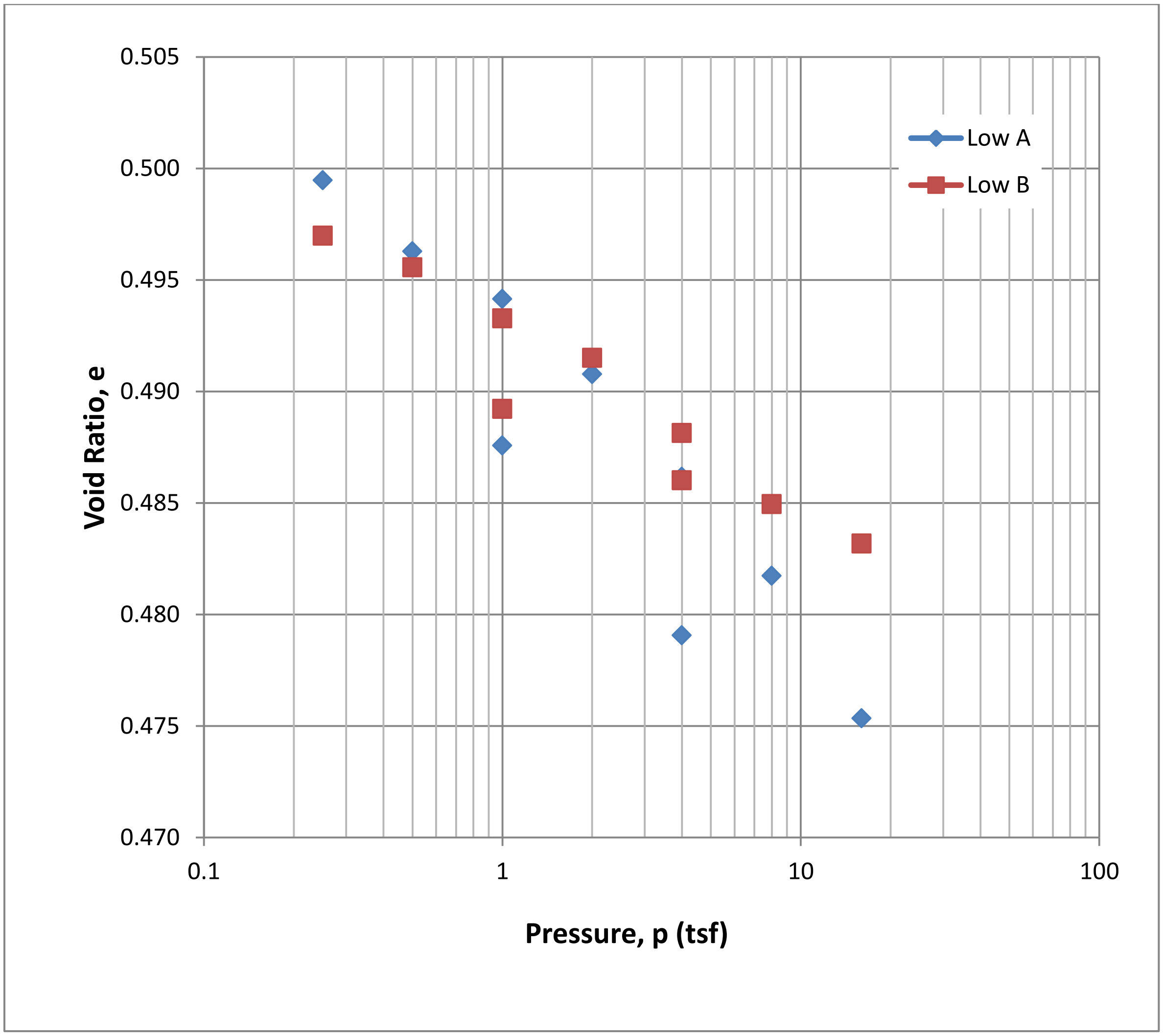

Figure E-2 – Void Ratio versus log-Pressure Curves for Low LBR Soil and 16% 1-inch GTR

E.1.2.2. 1” GTR 32%

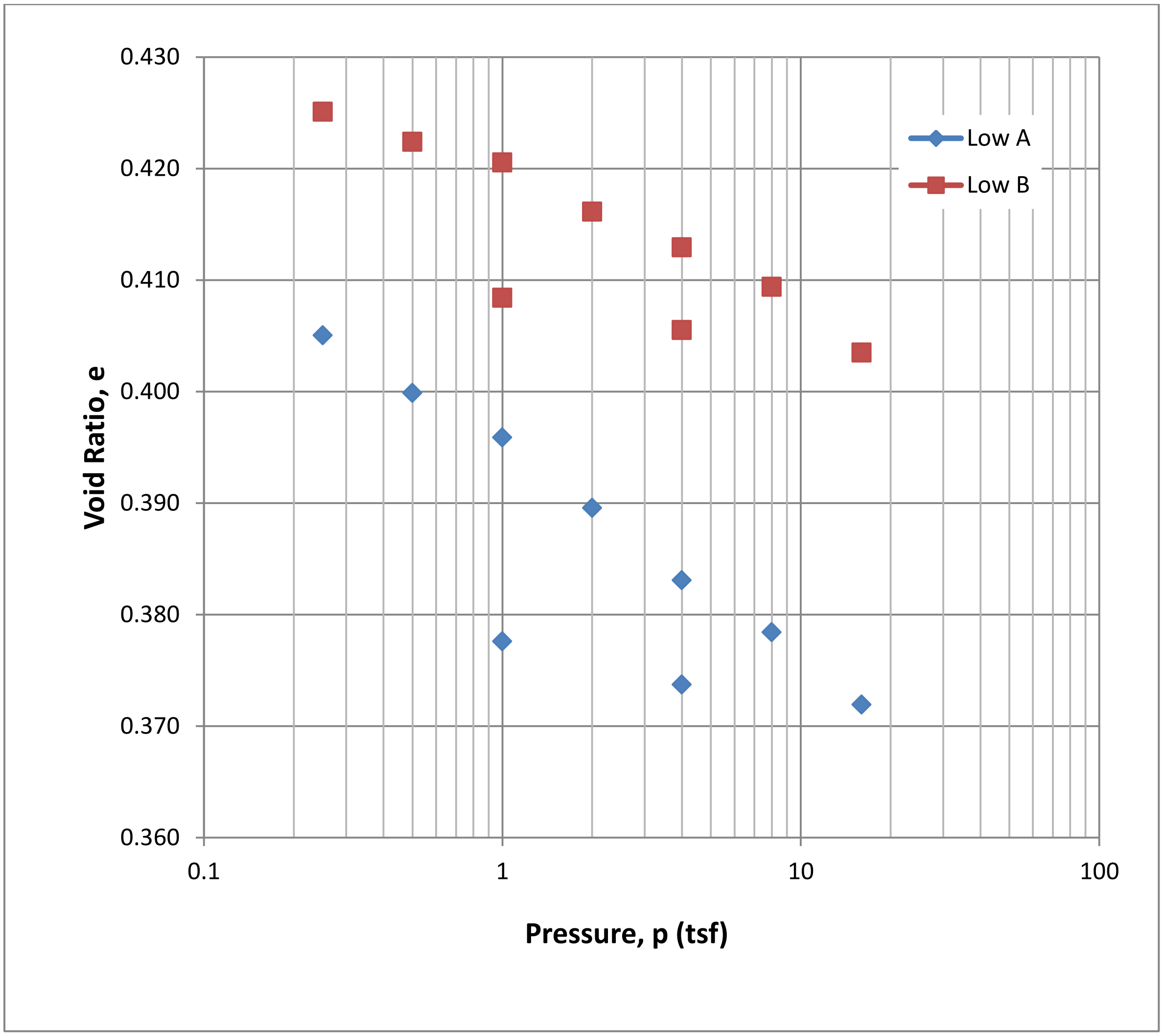

Figure E-3 – Void Ratio versus log-Pressure Curves for Low LBR Soil and 32% 1-inch GTR

E.1.3. 3/8" GTR

E.1.3.1. 3/8" GTR 16%

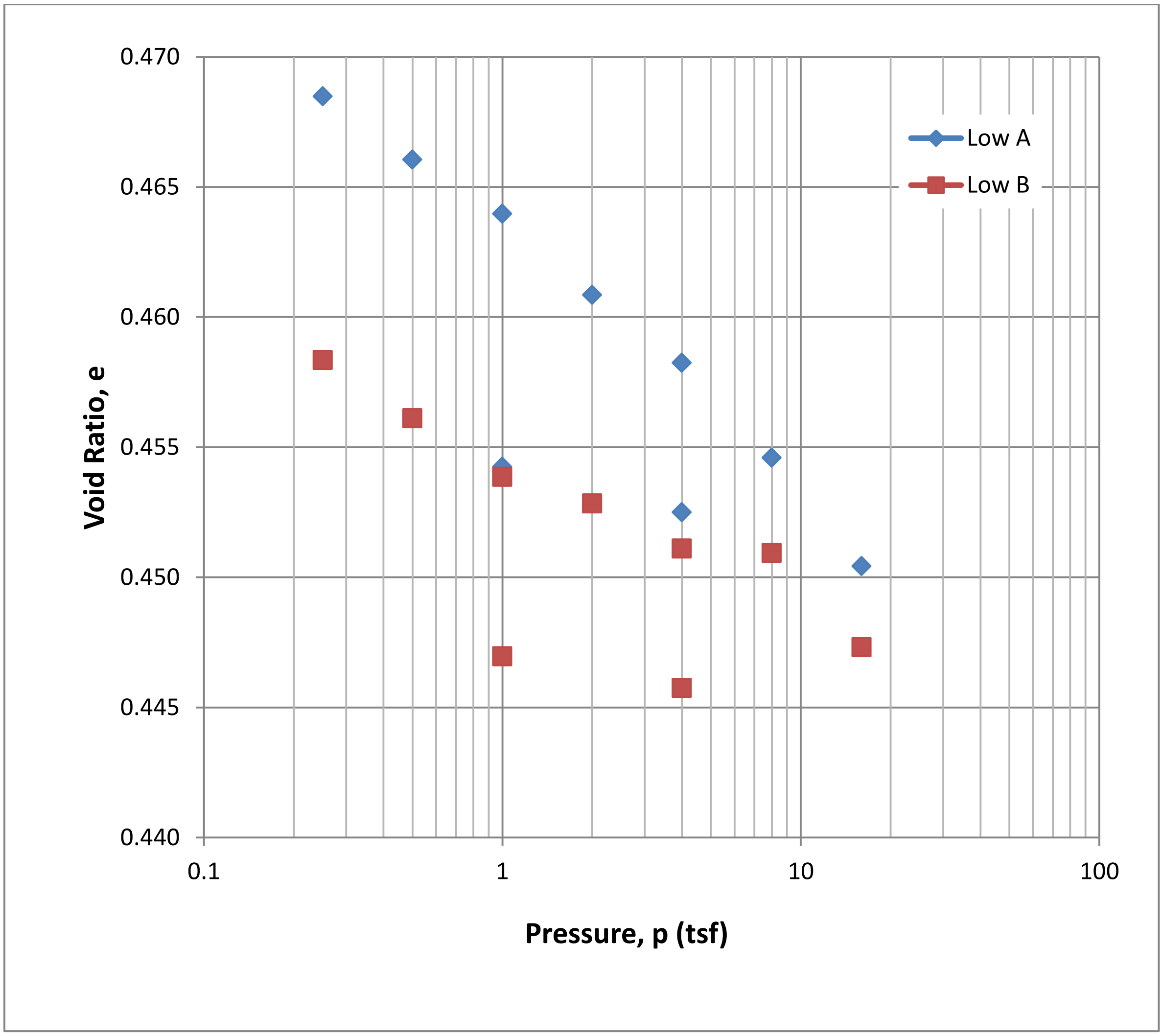

Figure E-4 – Void Ratio versus log-Pressure Curves for Low LBR Soil and 16% 3/8-inch GTR

E.1.3.2. 3/8" GTR 32%

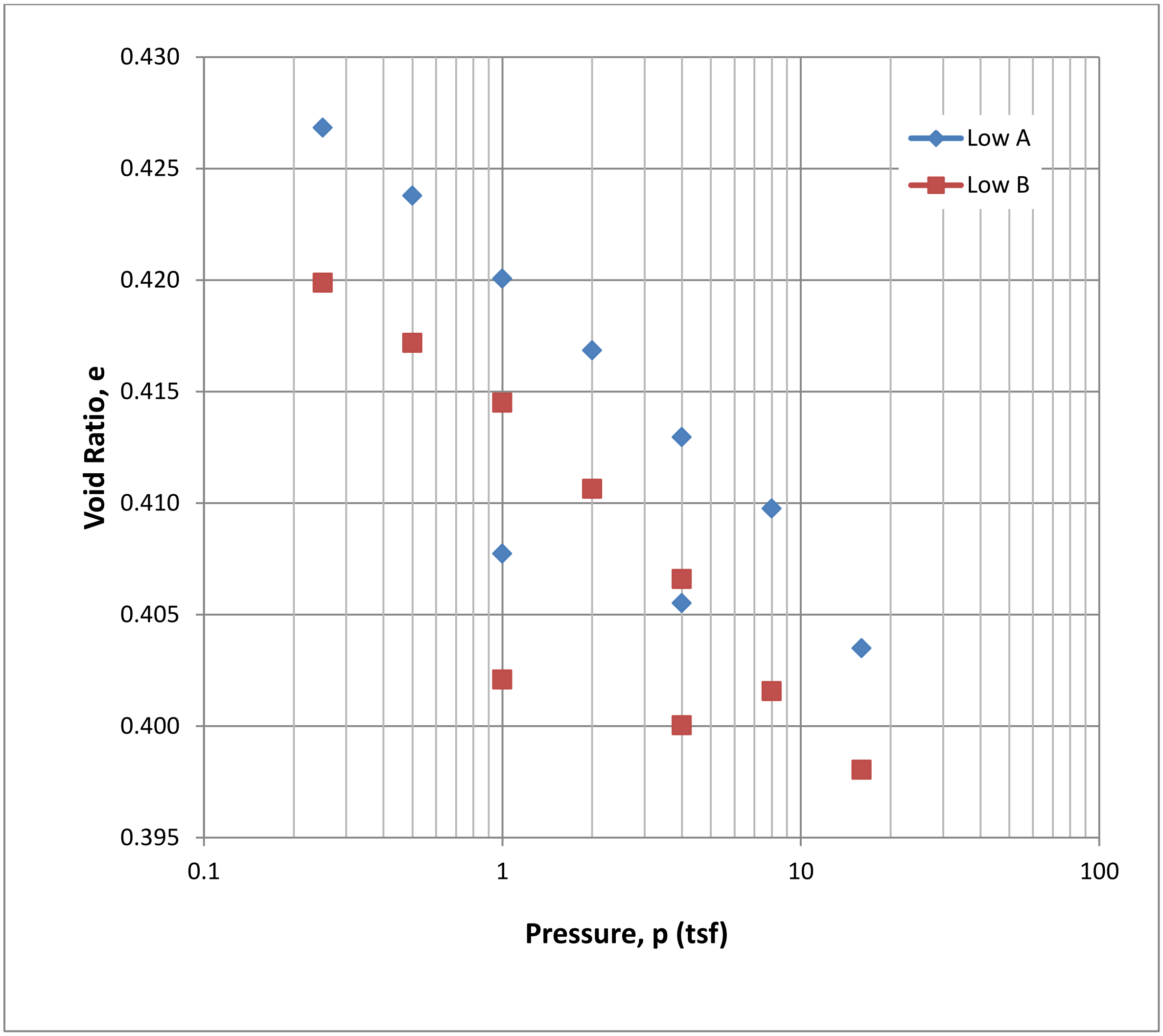

Figure E-5 – Void Ratio versus log-Pressure Curves for Low LBR Soil and 32% 3/8-inch GTR

E.1.4. #40 mesh GTR

E.1.4.1. #40 mesh GTR 16%

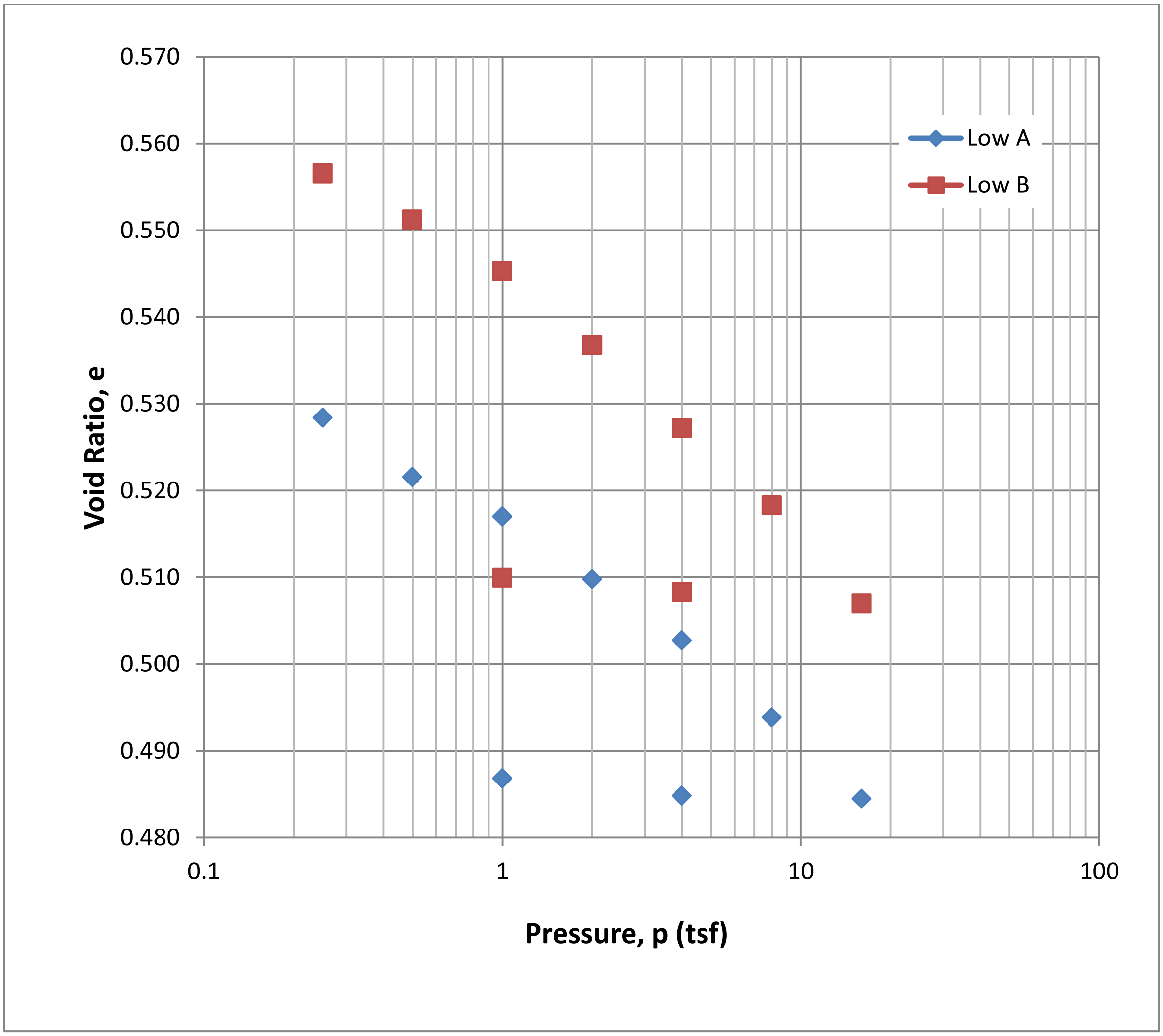

Figure E-6 – Void Ratio versus log-Pressure Curves for Low LBR Soil and 16% #40 mesh GTR

E.1.4.2. #40 mesh GTR 32%

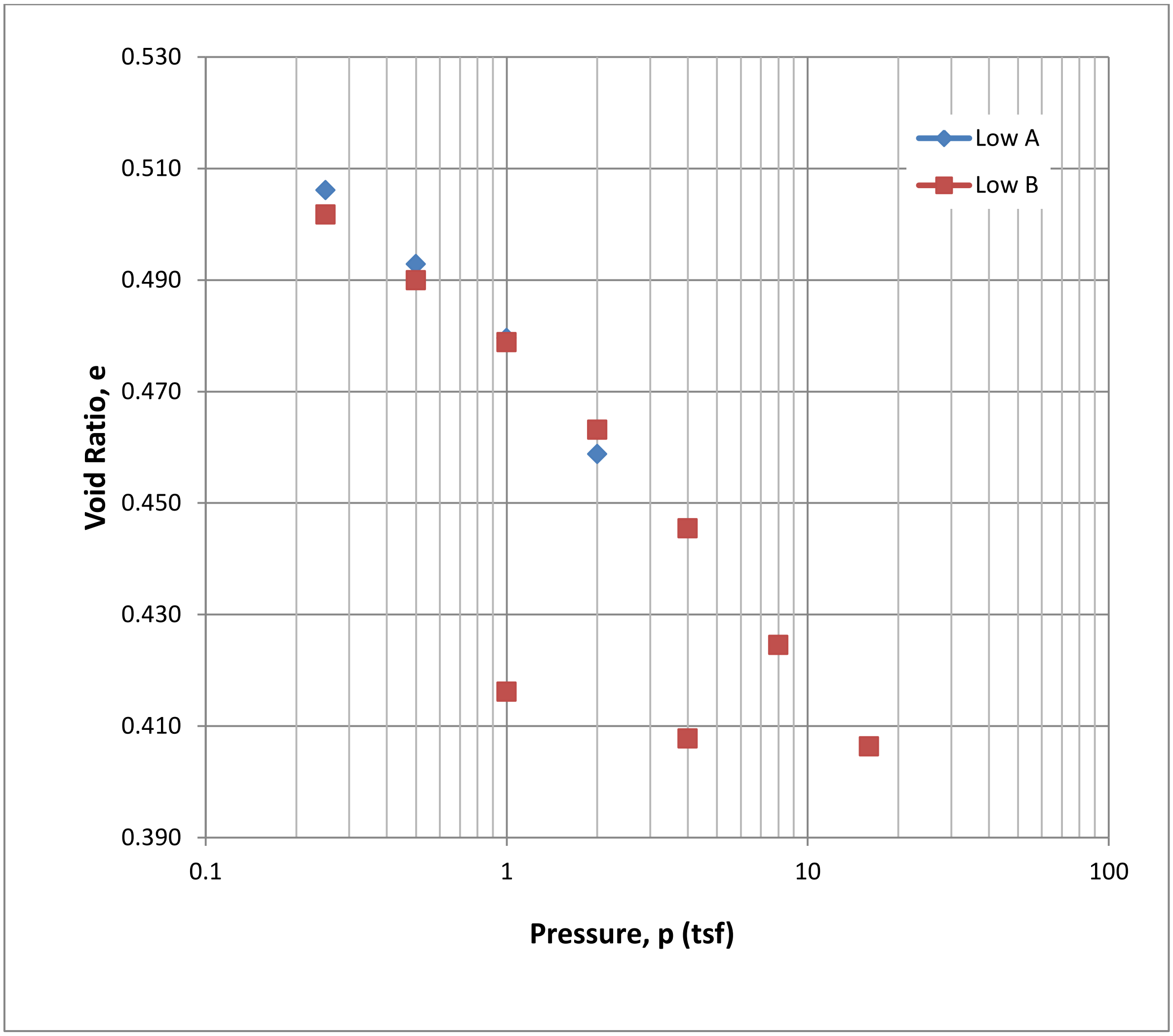

Figure E-7 – Void Ratio versus log-Pressure Curves for Low LBR Soil and 32% #40 mesh GTR

E.2. Medium LBR Soil

Table E-2 – C_v values for Medium LBR Soil

	Pressure	Cv (in²/sec)	Cv (in²/sec)	Cv (in²/sec)	Cv (in²/sec)	Cv (in²/sec)	Cv (in²/sec)	Cv (in²/sec)
Trial	tsf	Virgin Soil	1" GTR 16%	1" GTR 32%	3/8" GTR 16%	3/8" GTR 32%	#40" GTR 16%	#40 GTR 32%
A	0.125	0.183	0.263	0.263	0.103	0.537	0.325	0.183
A	0.5	0.182	0.397	0.323	0.262	0.261	0.533	0.405
A	1	0.117	0.312	0.260	0.323	0.723	0.719	0.400
A	2	0.323	0.393	0.405	0.531	1.036	0.525	0.700
A	4	0.409		0.718	0.528	0.716	0.521	0.689
A	8	0.323		1.027	0.403	0.713	0.703	0.676
A	16	0.723		0.710	0.715	1.021	0.392	0.950
B	0.125	0.411	0.325	0.263	0.156	0.731	0.134	0.217
B	0.5	0.409	0.216	0.408	0.262	0.726	0.260	0.404
B	1	0.323	0.321	0.259	0.407	0.531	0.402	0.711
B	2	0.532	0.721	0.526	0.530	0.718	0.399	0.701
B	4	0.405	0.403	0.523	0.718	0.525	0.704	0.691
B	8	0.527	0.713	0.398	0.525	1.022	0.697	0.977
B	16	0.713	0.709	1.013	0.710	1.013	0.689	1.497

E.2.1. Virgin Material

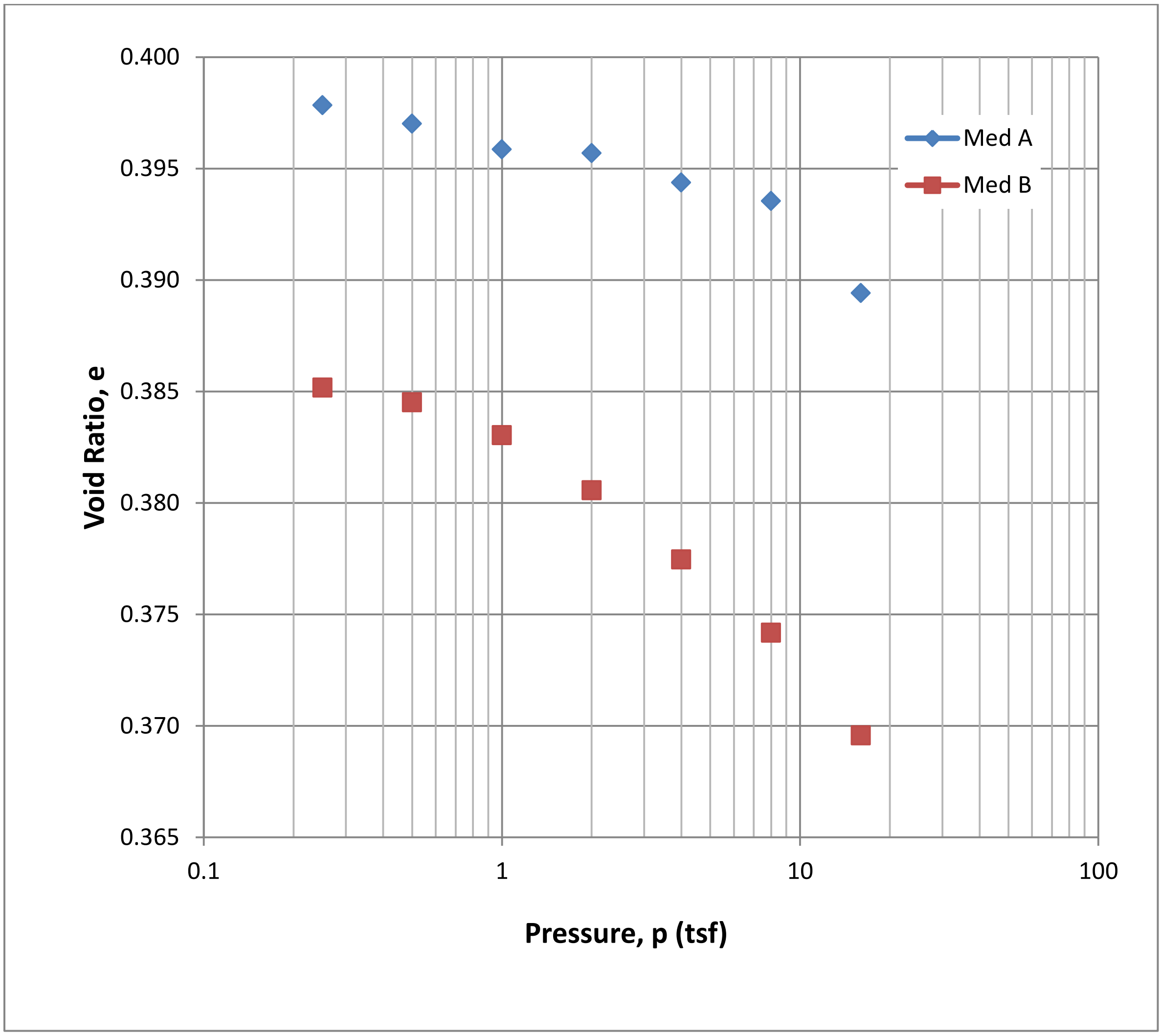

Figure E-8 – Void Ratio versus log-Pressure Curves for Medium LBR Soil

E.2.2. 1” GTR

E.2.2.1. 1” GTR 16%

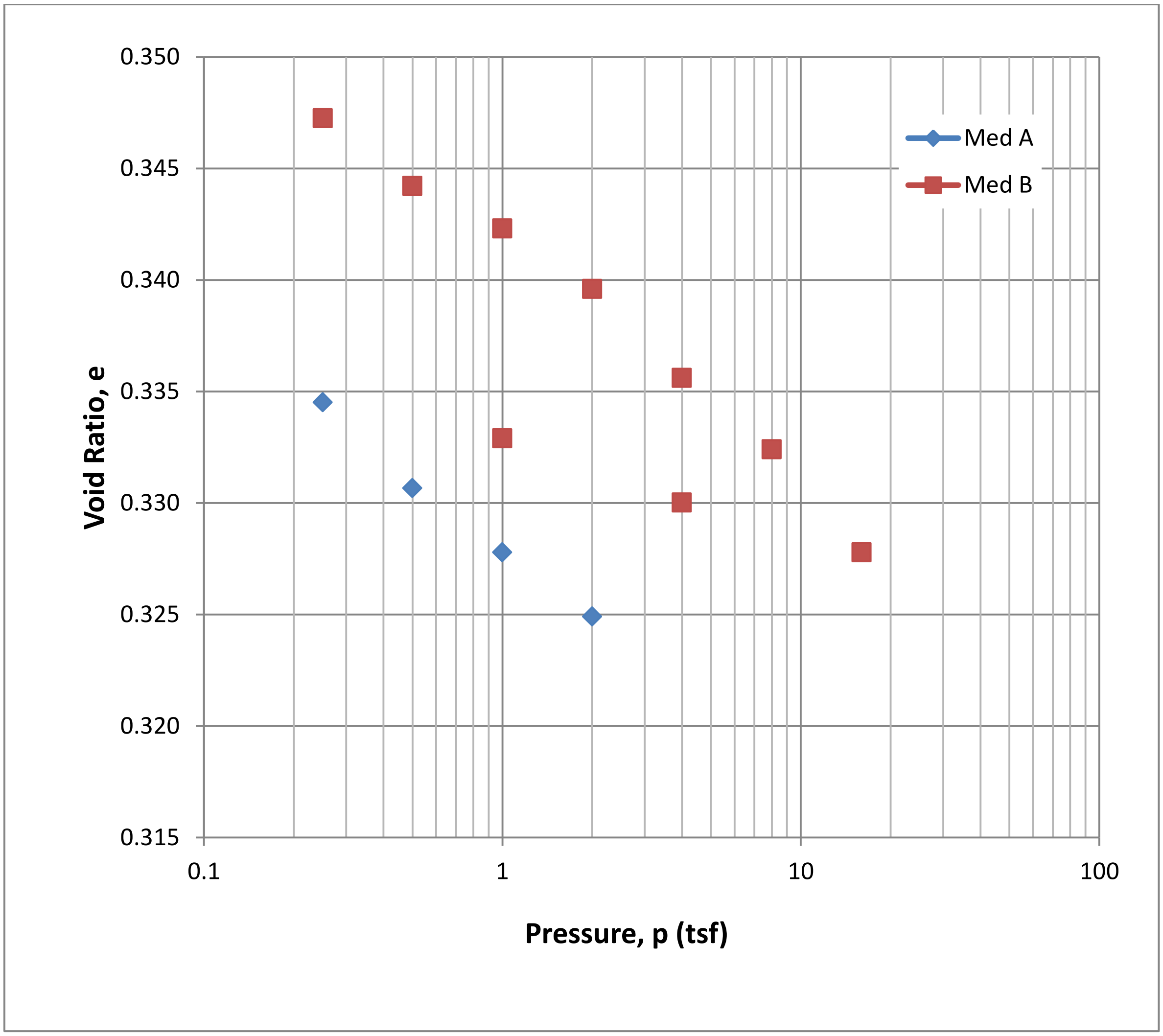

Figure E-9 – Void Ratio versus log-Pressure Curves for Medium LBR Soil and 16% 1-inch GTR

E.2.2.2. 1" GTR 32%

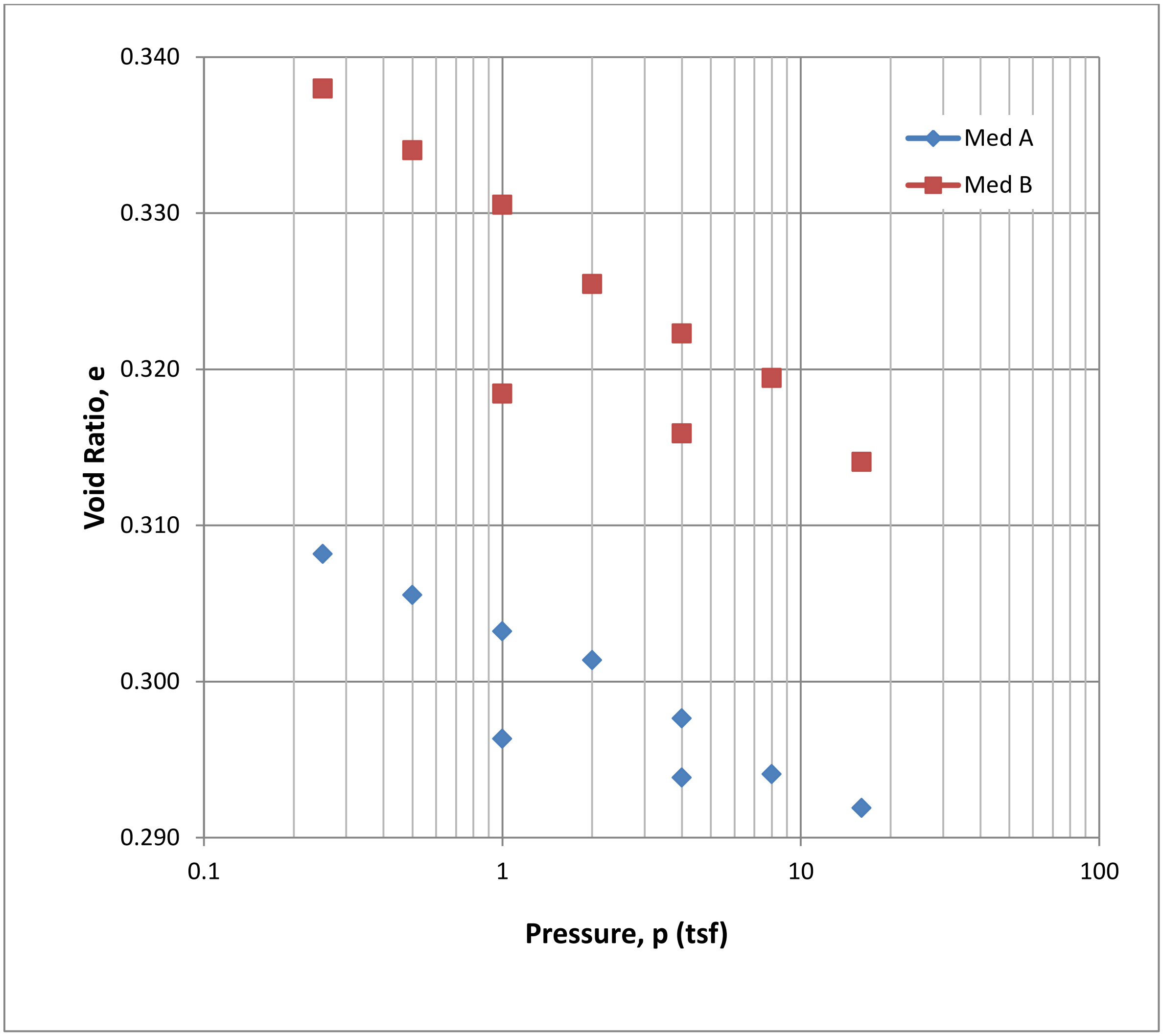

Figure E-10 – Void Ratio versus log-Pressure Curves for Medium LBR Soil and 32% 1-inch GTR

E.2.3. 3/8" GTR

E.2.3.1. 3/8" GTR 16%

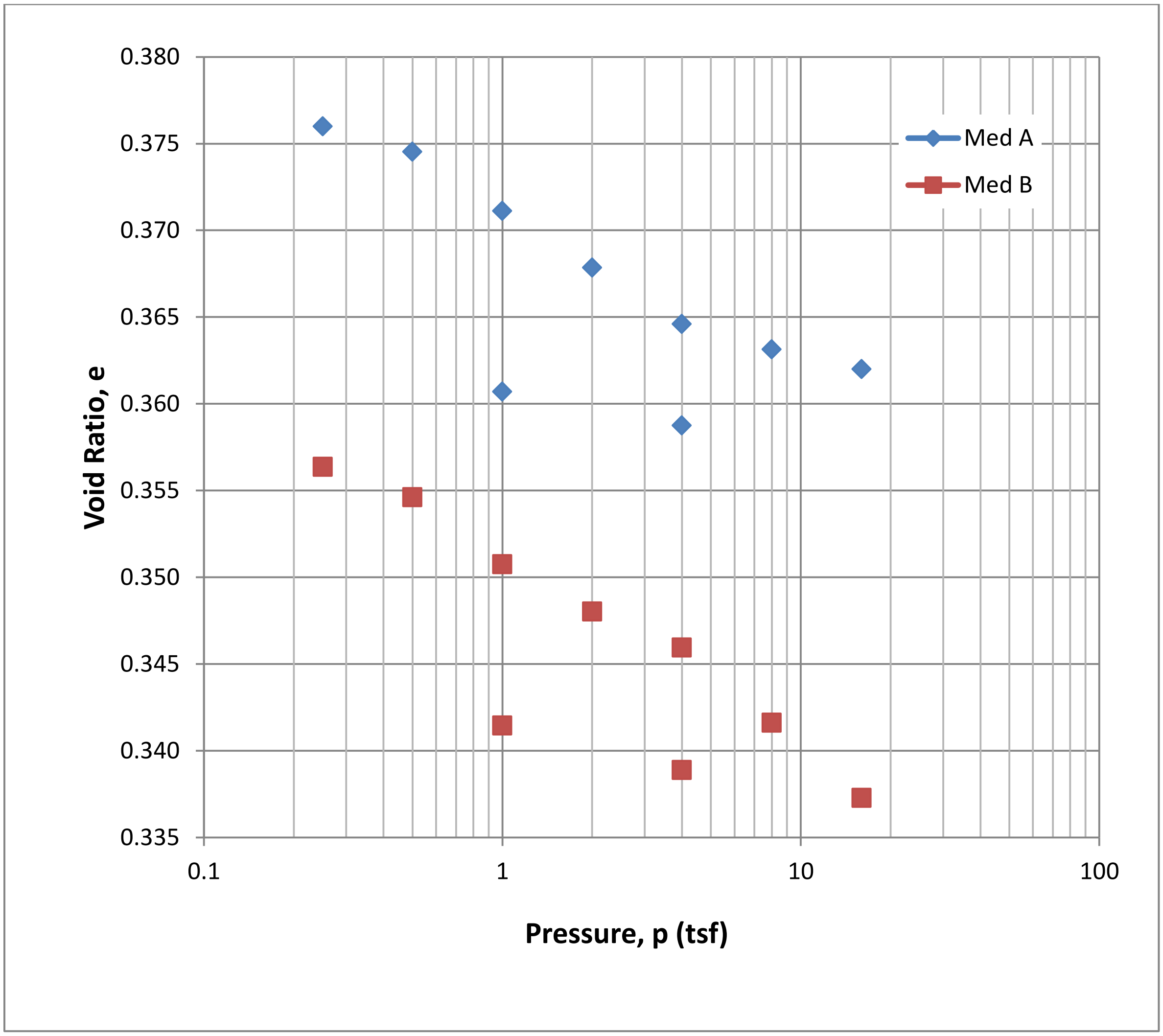

Figure E-11 – Void Ratio versus log-Pressure Curves for Medium LBR Soil and 16% 3/8-inch GTR

E.2.3.2. 3/8” GTR 32%

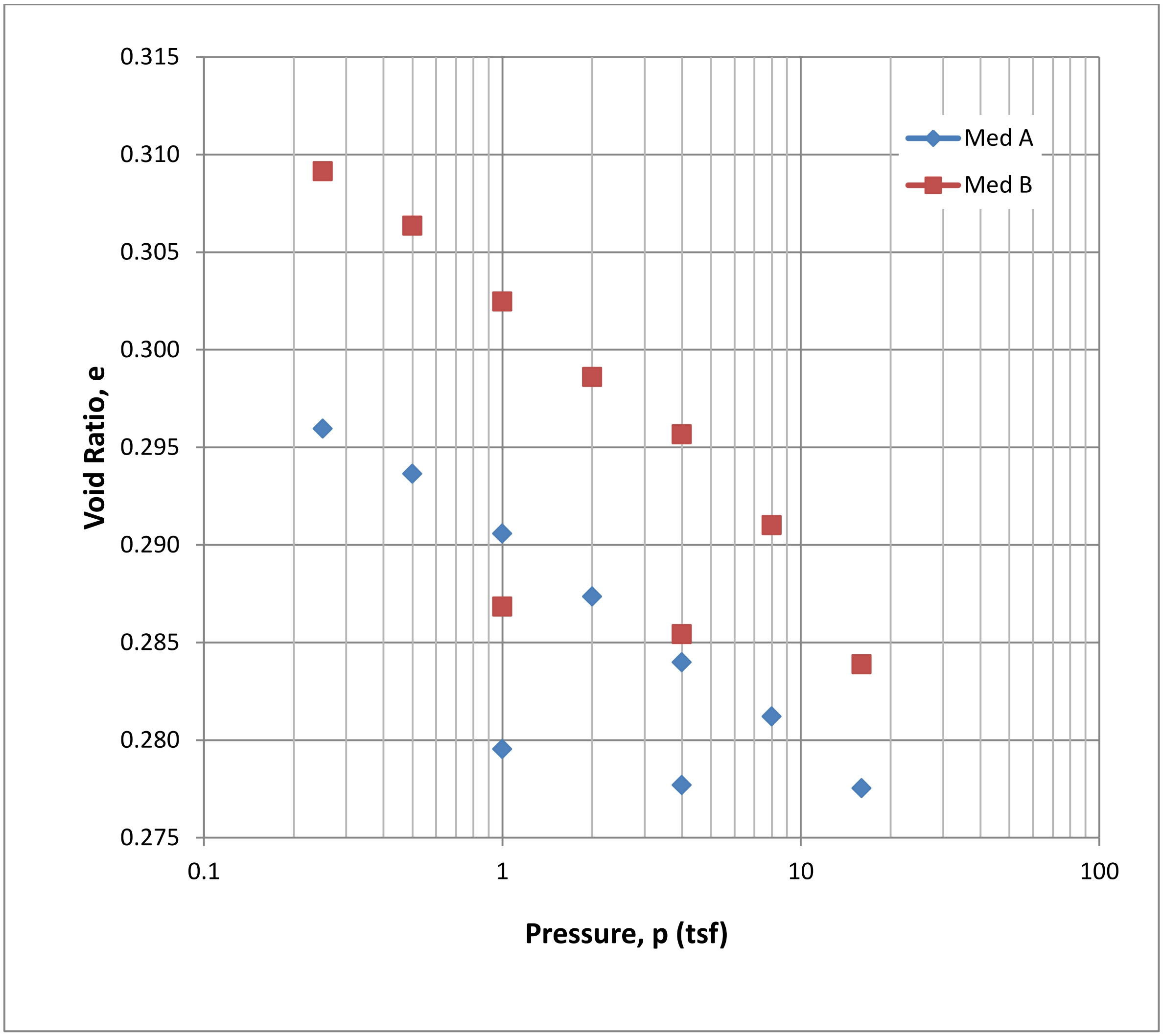

Figure E-12 – Void Ratio versus log-Pressure Curves for Medium LBR Soil and 32% 3/8-inch GTR

E.2.4. #40 mesh GTR

E.2.4.1. #40 mesh GTR 16%

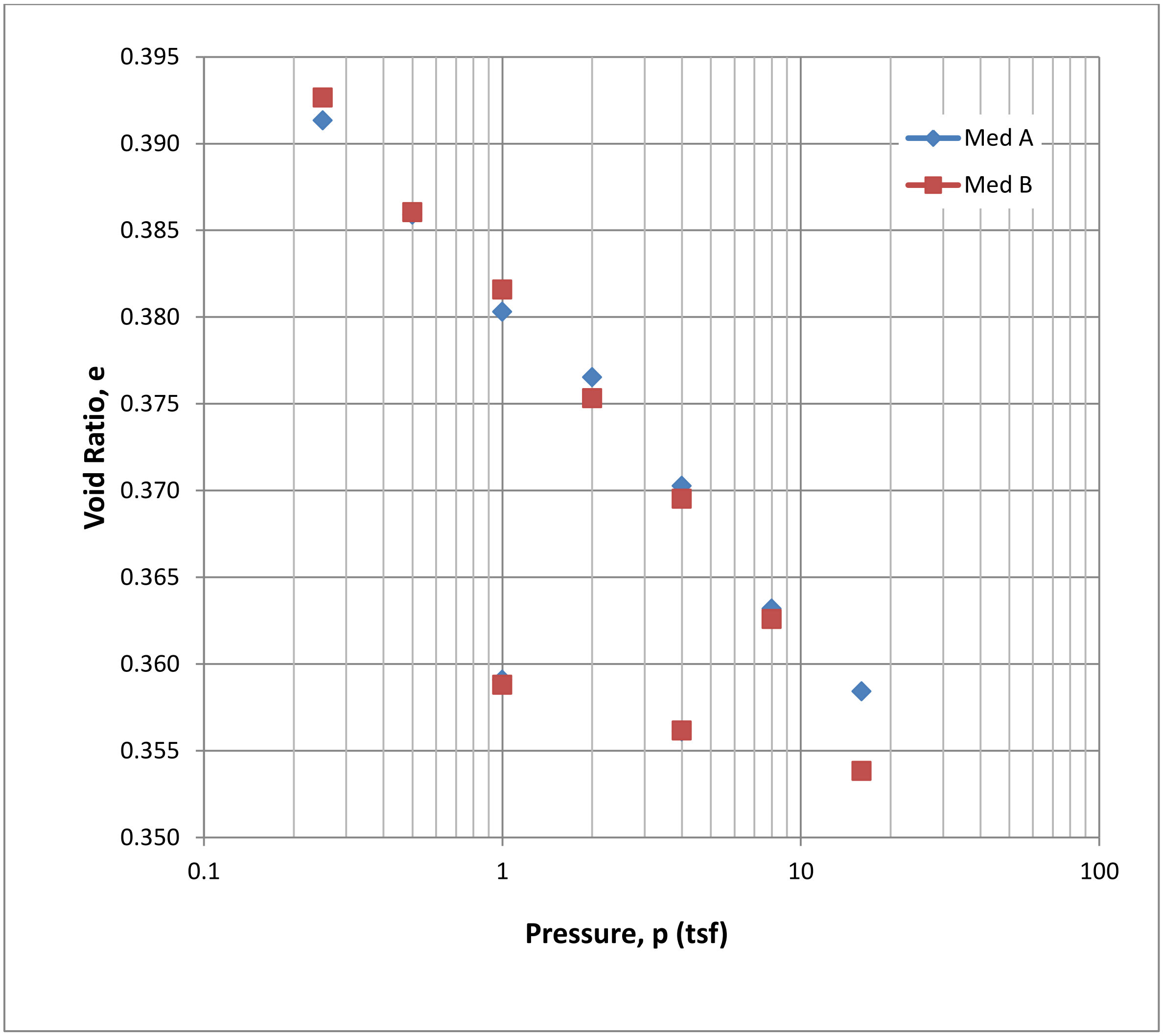

Figure E-13 – Void Ratio versus log-Pressure Curves for Medium LBR Soil and 16% #40 mesh GTR

E.2.4.2. #40 mesh GTR 32%

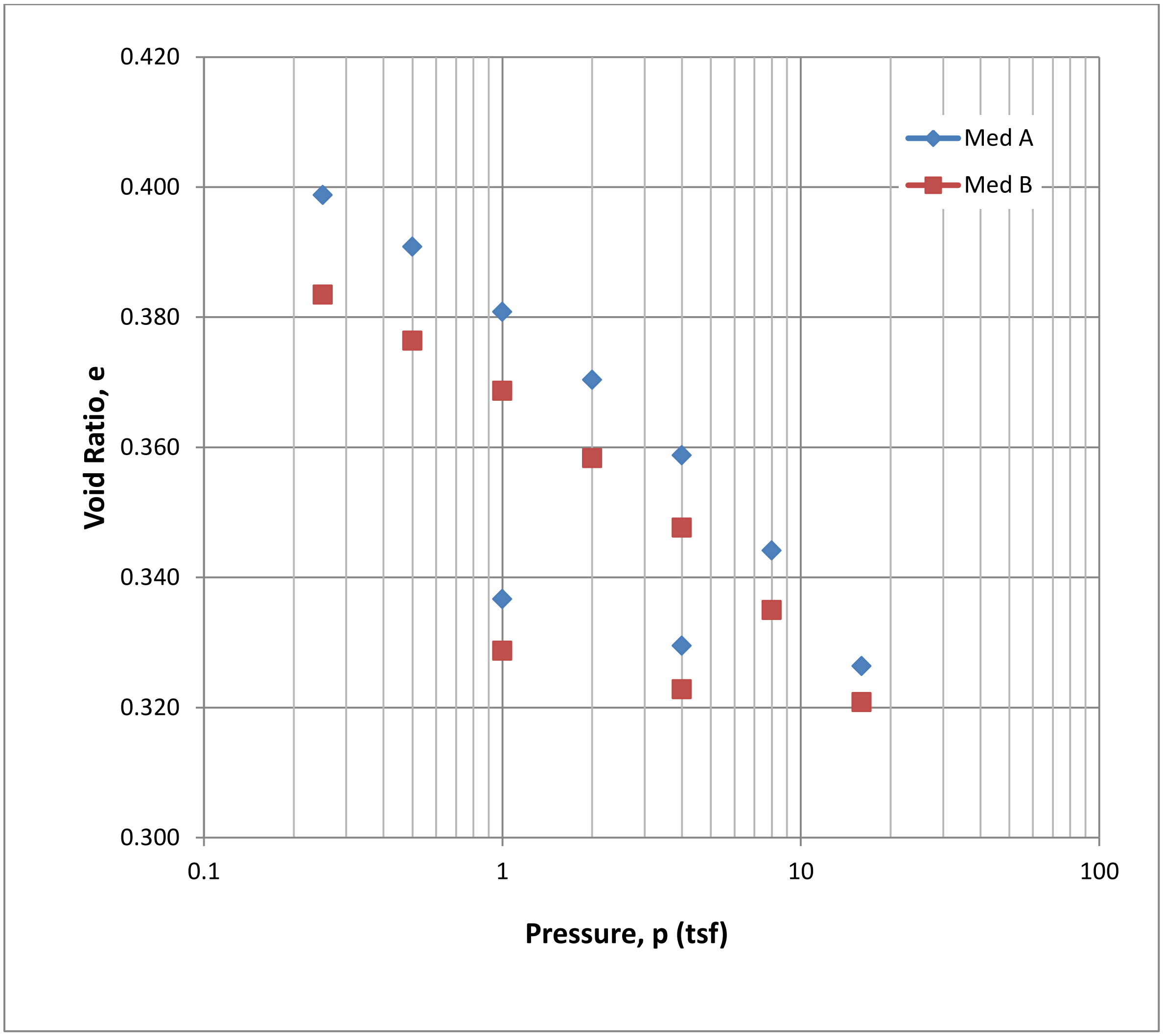

Figure E-14 – Void Ratio versus log-Pressure Curves for Medium LBR Soil and 32% #40 mesh GTR

E.3. High LBR Soil

Table E-3 – C_v values for High LBR Soil

	Pressure	Cv (in^2/sec)	Cv (in^2/sec)	Cv (in^2/sec)	Cv (in^2/sec)	Cv (in^2/sec)	Cv (in^2/sec)	Cv (in^2/sec)	Cv (in^2/sec)
Trial	tsf	Virgin Soil	1" GTR 1%	1" GTR 16%	1" GTR 32%	3/8" GTR 16%	3/8" GTR 32%	#40" GTR 16%	#40 GTR 32%
A	0.125	1.053	1.053	0.263	0.411	0.263	0.411	0.263	0.325
A	0.5	0.262	1.640	0.262	0.323	0.323	0.216	0.322	0.322
A	1	0.408	1.047	0.181	0.260	0.261	0.133	0.320	0.259
A	2	0.406	1.041	0.407	0.320	0.321	0.319	0.317	0.400
A	4	0.719	1.035	0.406	0.527	0.320	0.401	0.520	0.515
A	8	0.318	1.607	0.405	0.715	0.526	0.315	0.701	0.688
A	16	1.027	1.594	1.031	0.711	0.401	0.395	0.390	0.675
B	0.125	0.117	0.263	0.117	0.325	0.217	0.117	0.217	0.217
B	0.5	0.325	0.325	0.262	0.407	0.262	0.102	0.154	0.181
B	1	0.324	0.183	0.182	0.259	0.261	0.102	0.179	0.214
B	2	0.533	0.535	0.406	0.318	0.530	0.321	0.256	0.317
B	4	0.406	1.046	0.404	0.710	0.403	0.180	0.396	0.702
B	8	1.033	1.042	0.525	0.704	0.713	0.402	0.393	0.504
B	16	1.603	1.621	0.709	0.698	0.520	0.400	0.389	0.966

E.3.1. Virgin Material

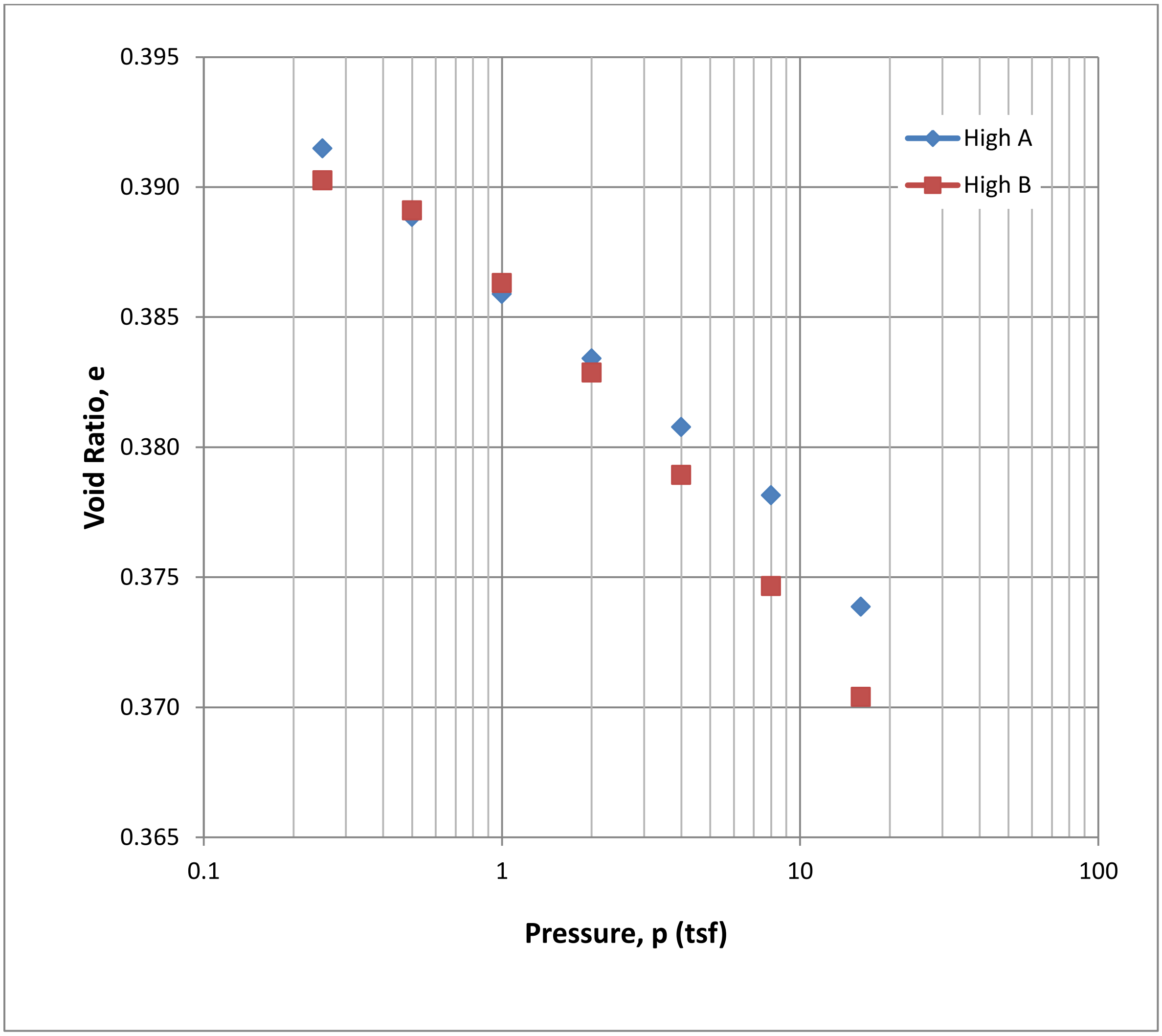

Figure E-15 – Void Ratio versus log-Pressure Curves for High LBR Soil

E.3.2. 1" GTR

E.3.2.1. 1" GTR 16%

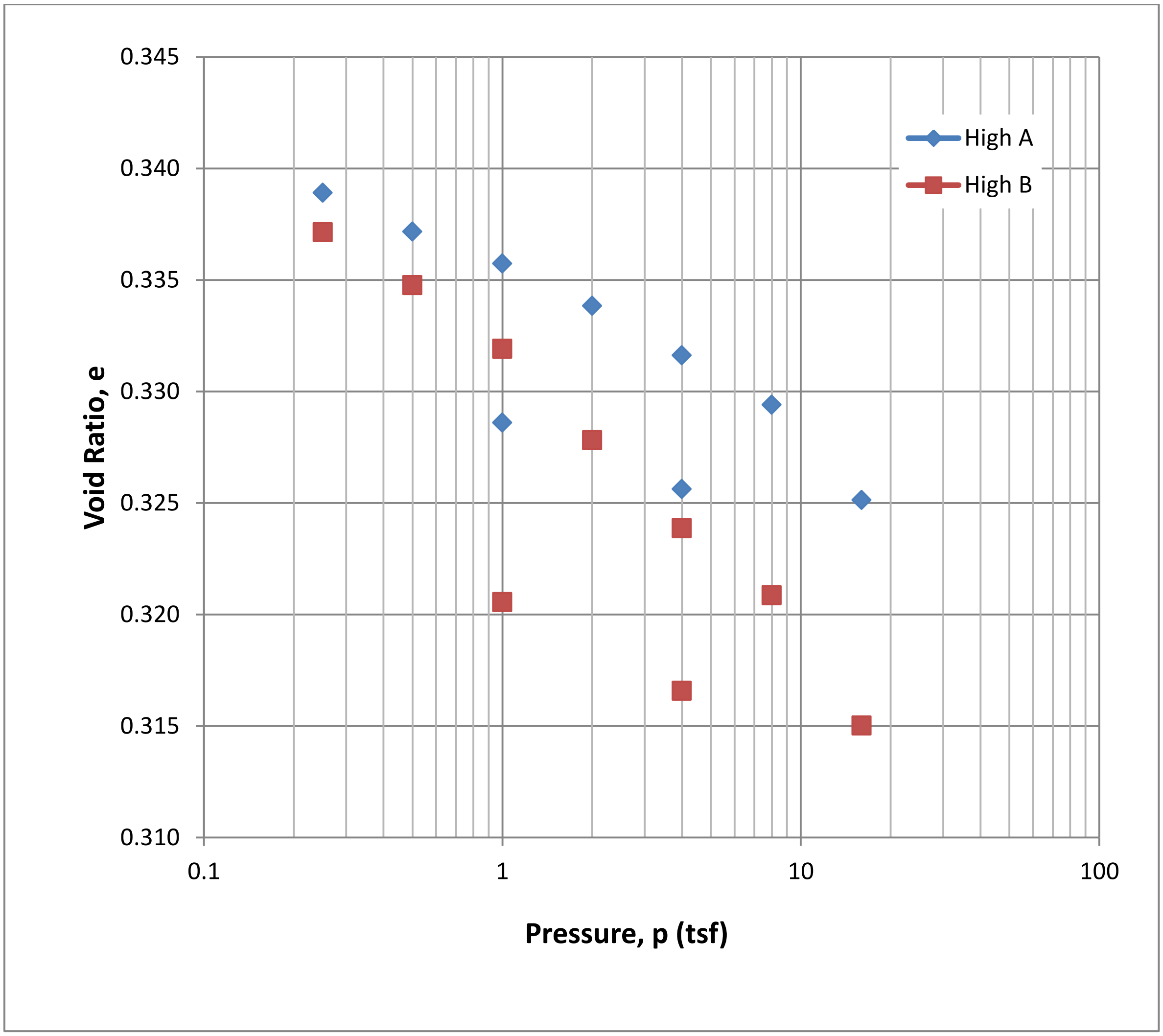

Figure E-16 – Void Ratio versus log-Pressure Curves for High LBR Soil and 16% 1-inch GTR

E.3.2.2. 1” GTR 32%

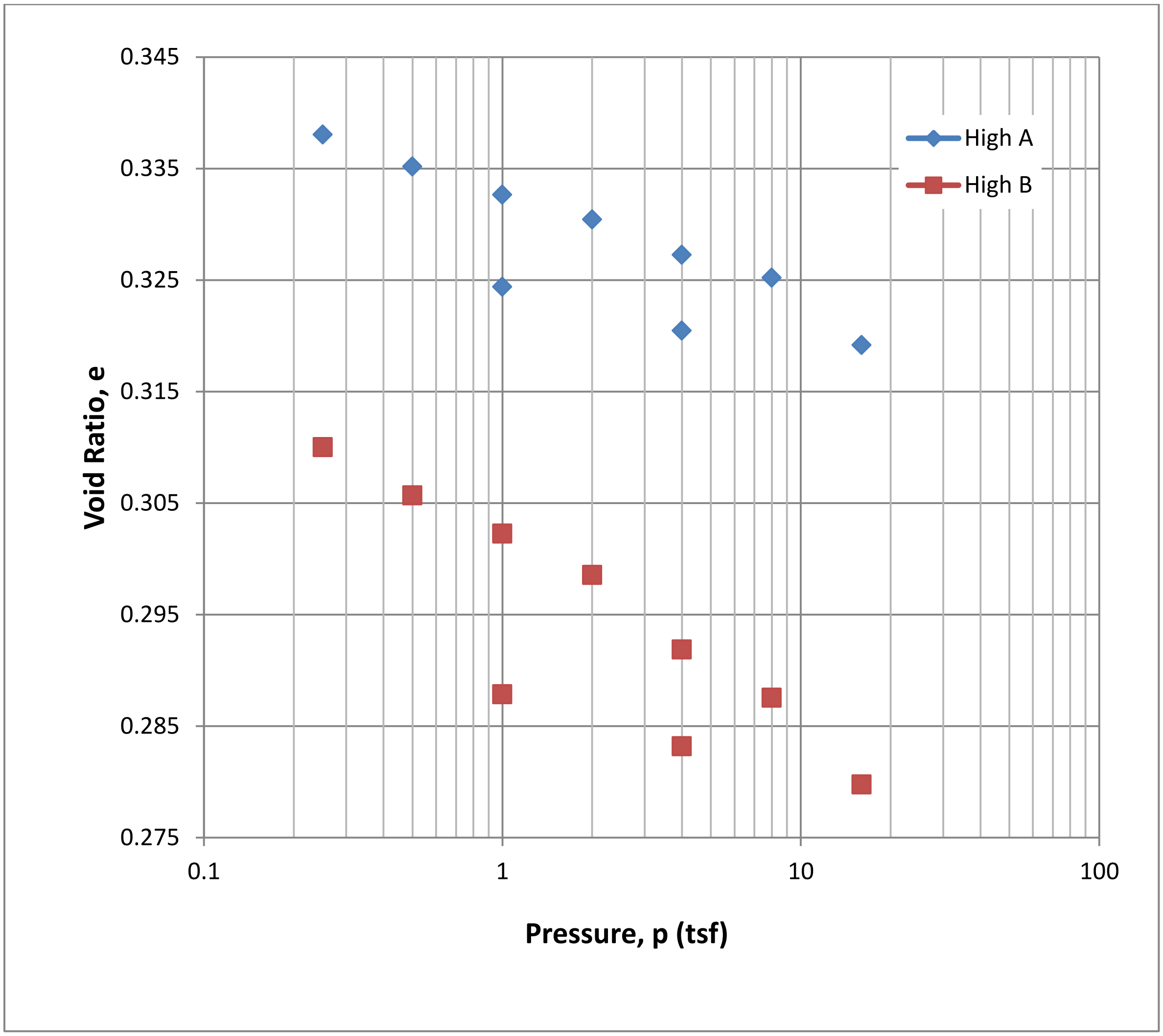

Figure E-17 – Void Ratio versus log-Pressure Curves for High LBR Soil and 32% 1-inch GTR

E.3.3. 3/8" GTR

E.3.3.1. 3/8" GTR 16%

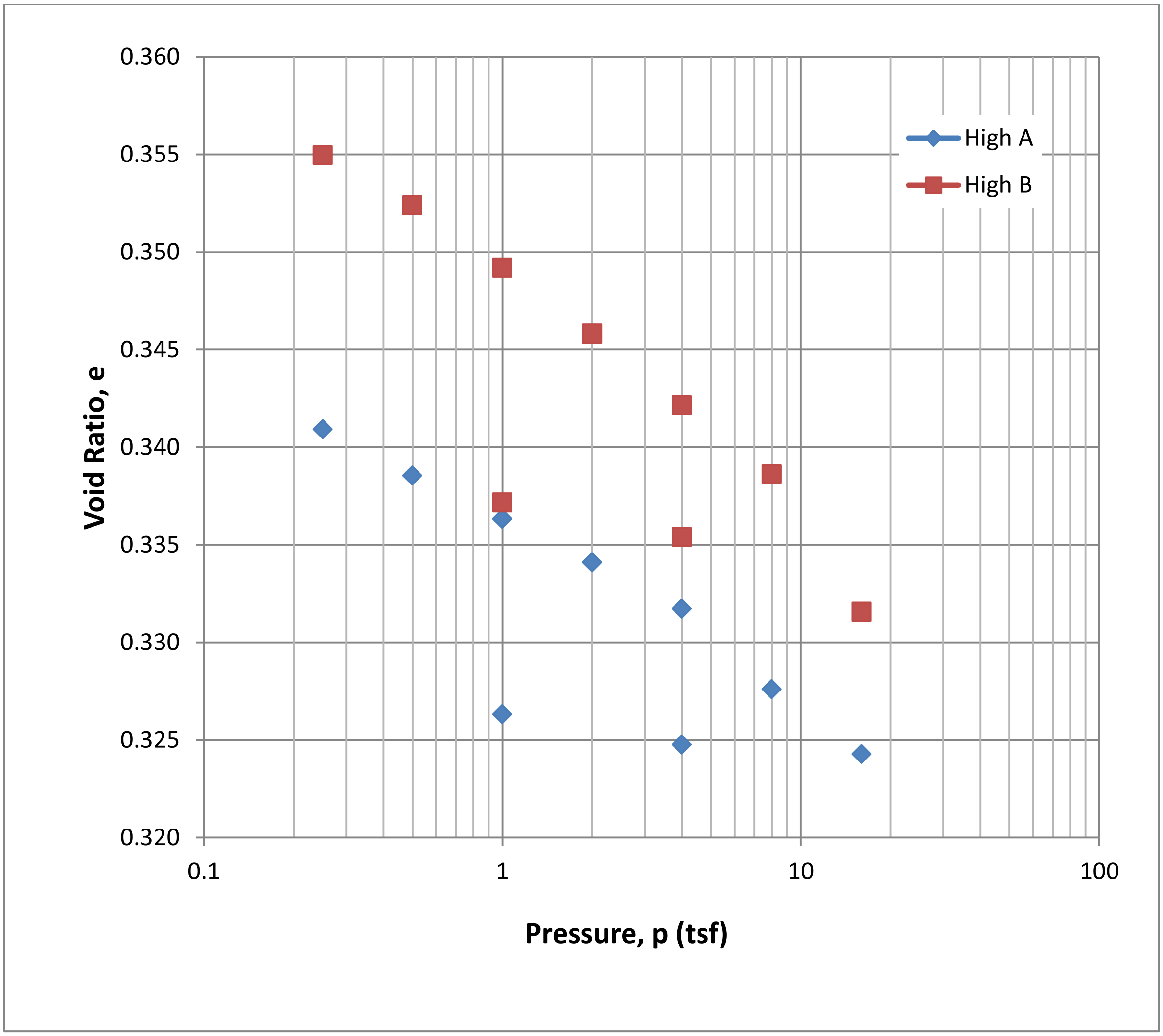

Figure E-18 – Void Ratio versus log-Pressure Curves for High LBR Soil and 16% 3/8-inch GTR

E.3.3.2. 3/8" GTR 32%

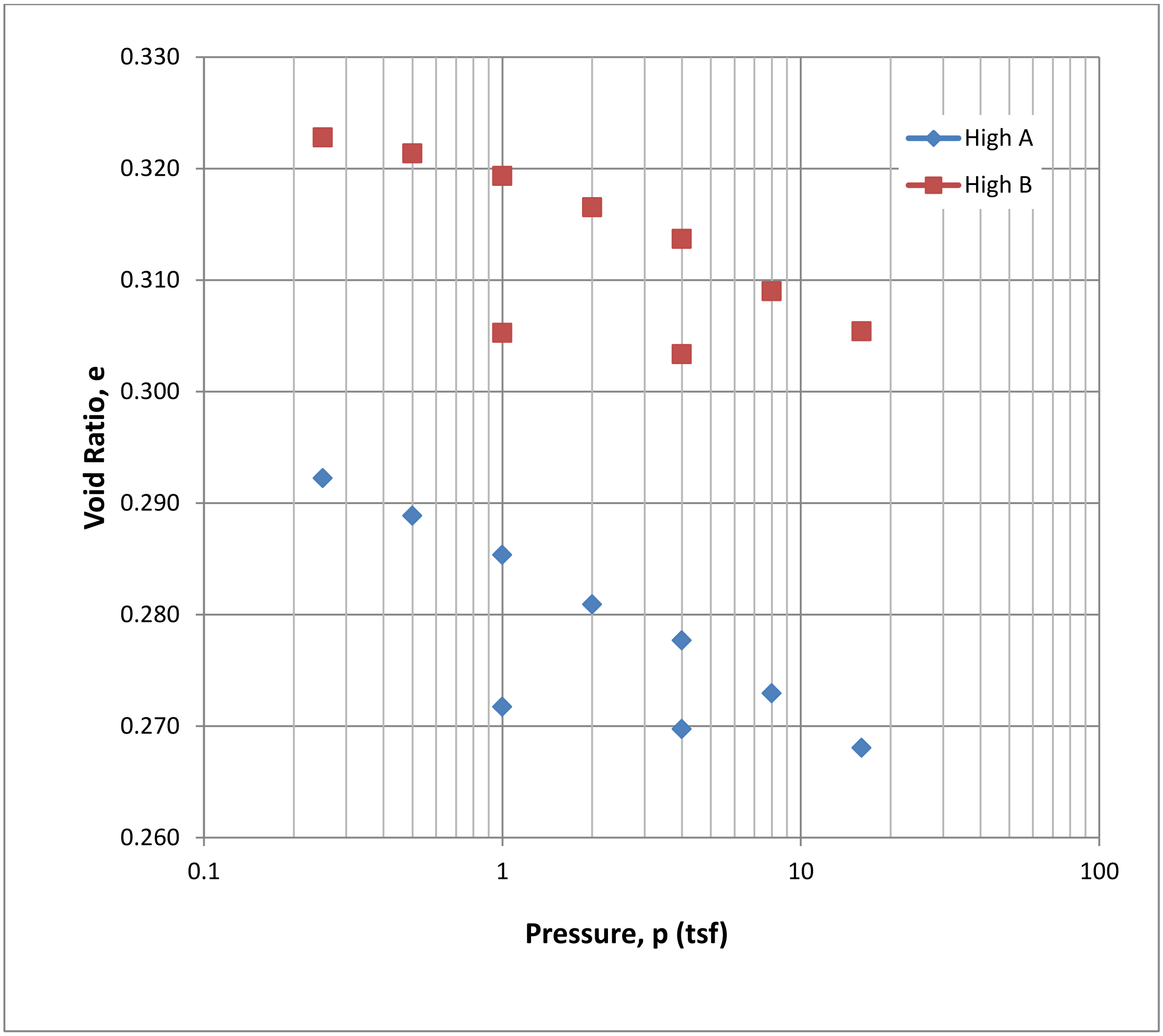

Figure E-19 – Void Ratio versus log-Pressure Curves for High LBR Soil and 32% 3/8-inch GTR

E.3.4. #40 mesh GTR

E.3.4.1. #40 mesh GTR 16%

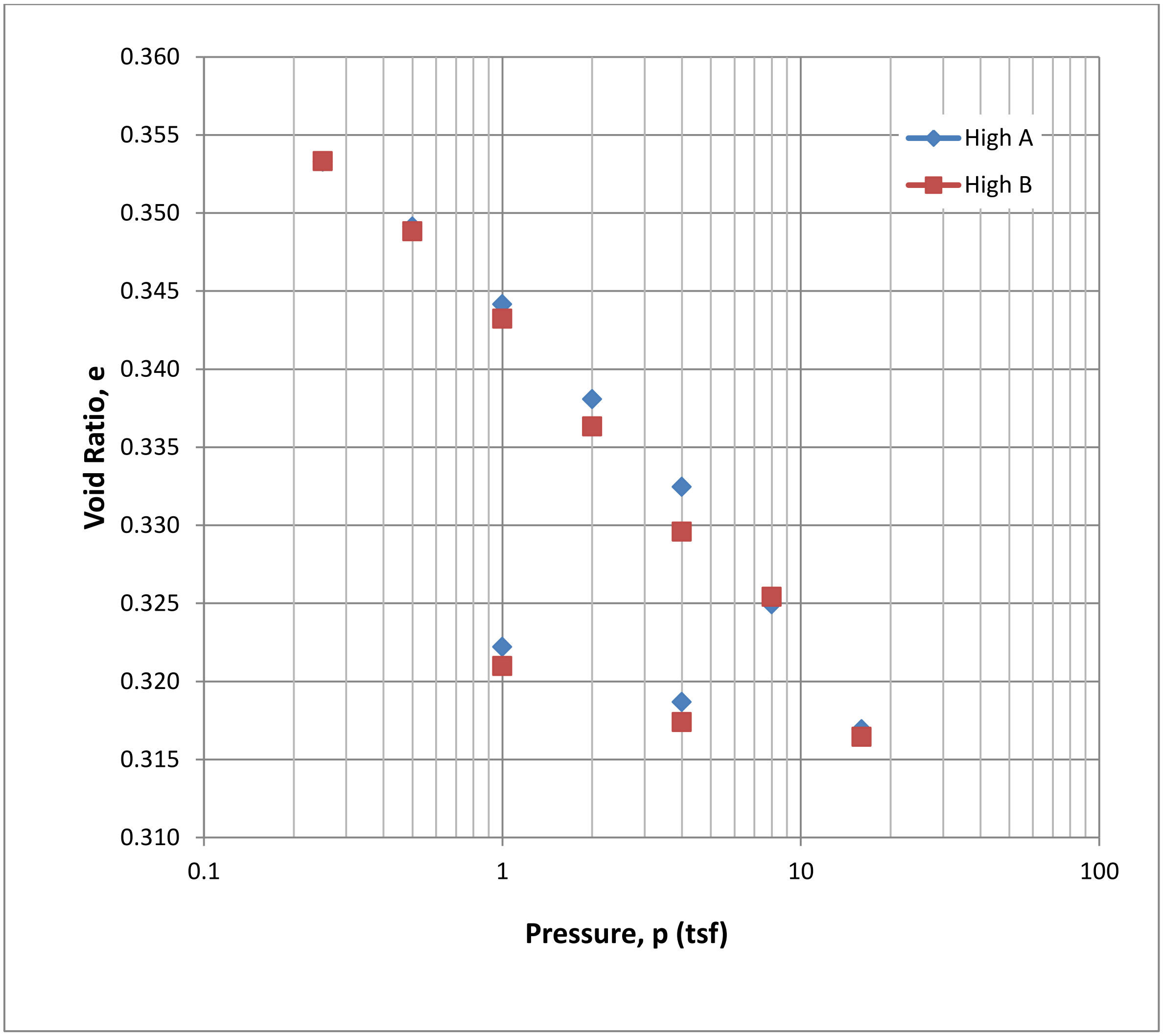

Figure E-20 – Void Ratio versus log-Pressure Curves for High LBR Soil and 16% #40 mesh GTR

E.3.4.2. #40 mesh GTR 32%

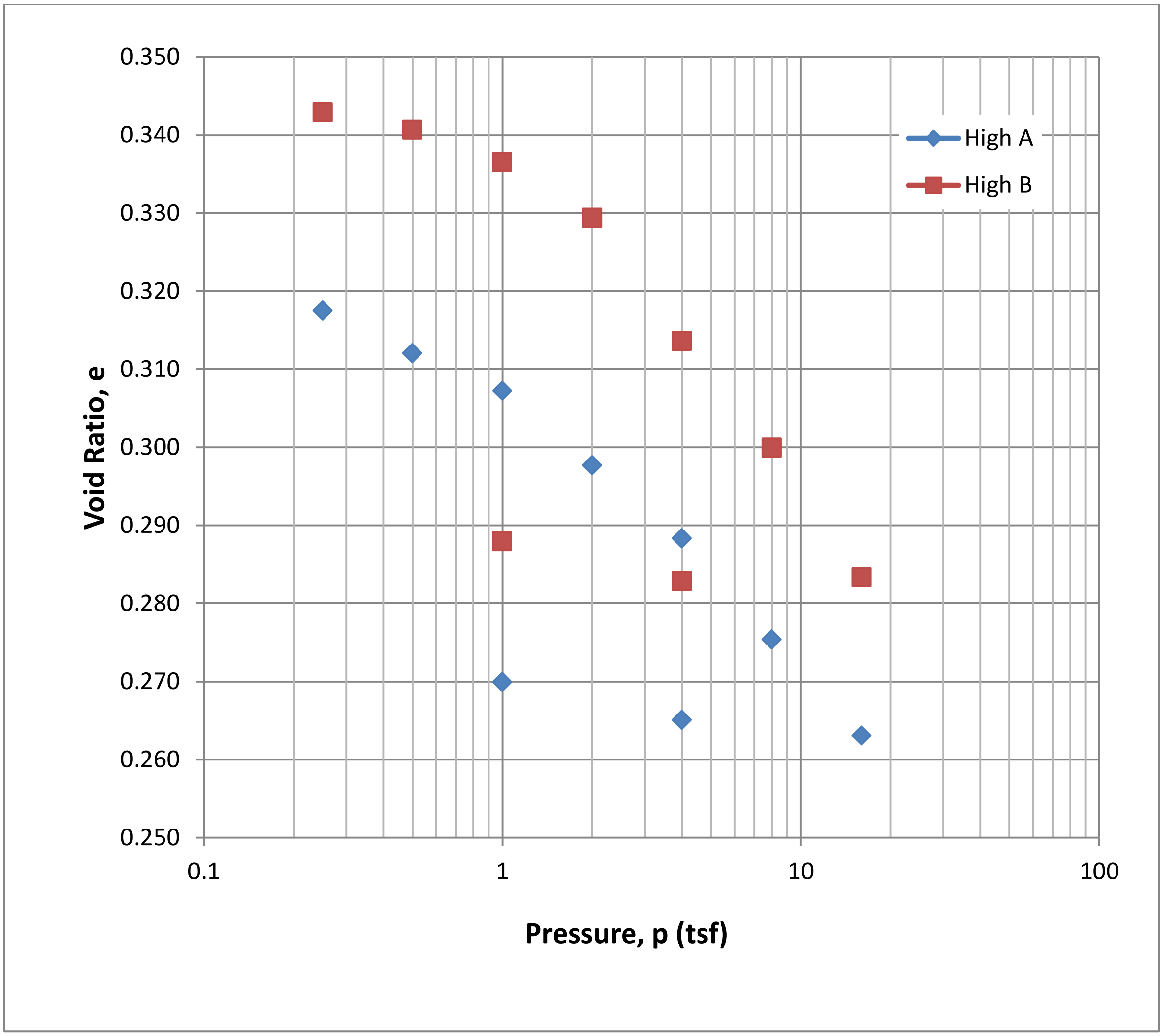

Figure E-21 – Void Ratio versus log-Pressure Curves for High LBR Soil and 32% #40 mesh GTR

Appendix F – Constant Head Permeability

F.1. Low LBR Soil

F.1.1. Virgin Material

Table F-1 – Permeability Data Sheet for Low LBR Soil

Soil	GTR	%	S	Trial	Q (cm^3)	t (sec)	h (in)	h (cm)	L (cm)	A (cm^2)	k (trial)	k (sample)	k (avg) [cm/sec]
Low	0	0%	A	1	110	600	16.0	40.64	11.64	182.90	2.9E-04	2.9E-04	3.7E-04
				2	115	600	16.0	40.64			3.0E-04		
				3	110	600	16.0	40.64			2.9E-04		
			B	1	150	600	16.0	40.64	11.64	182.90	3.9E-04	4.5E-04	
				2	135	300	23.5	59.69			4.8E-04		
				3	180	300	31.3	79.38			4.8E-04		

F.1.2. 1" GTR

Table F-2 – Permeability Data Sheet for Low LBR Soil and 1-inch GTR

Soil	GTR	%	S	Trial	Q (cm^3)	t (sec)	h (in)	h (cm)	L (cm)	A (cm^2)	k (trial)	k (sample)	k (avg) [cm/sec]
Low	1"	16%	A	1	170	600	16.0	40.64	11.64	182.90	4.4E-04	5.6E-04	4.2E-04
				2	385	600	31.3	79.50			5.1E-04		
				3	665	600	39.0	99.06			7.1E-04		
			B	1	50	300	16.0	40.64	11.64	182.90	2.6E-04	2.8E-04	
				2	70	300	23.5	59.69			2.5E-04		
				3	120	300	31.3	79.38			3.2E-04		
Low	1"	32%	A	1	75	1100	16.0	40.64	11.64	182.90	1.1E-04	3.0E-04	3.0E-04
				2	250	600	23.5	59.69			4.4E-04		
				3	270	600	31.3	79.38			3.6E-04		
			B	1	110	1100	16.0	40.64	11.64	182.90	1.6E-04	3.0E-04	
				2	190	600	23.5	59.69			3.4E-04		
				3	300	600	31.3	79.38			4.0E-04		

F.1.3. 3/8" GTR

Table F-3 – Permeability Data Sheet for Low LBR Soil and 3/8-inch GTR

Soil	GTR	%	S	Trial	Q (cm^3)	t (sec)	h (in)	h (cm)	L (cm)	A (cm^2)	k (trial)	k (sample)	k (avg) [cm/sec]
Low	3/8"	16%	A	1	135	600	16.0	40.64	11.64	182.90	3.5E-04	5.0E-04	4.5E-04
				2	465	720	31.3	79.50			5.2E-04		
				3	600	600	39.0	99.06			6.4E-04		
			B	1	100	600	16.0	40.64	11.64	182.90	2.6E-04	3.9E-04	
				2	430	720	31.3	79.50			4.8E-04		
				3	415	600	39.0	99.06			4.4E-04		
Low	3/8"	32%	A	1	80	360	23.5	59.69	11.64	182.90	2.4E-04	2.3E-04	2.3E-04
				2	240	900	31.3	79.50			2.1E-04		
				3	230	600	39.0	99.06			2.5E-04		
			B	1	70	360	23.5	59.69	11.64	182.90	2.1E-04	2.3E-04	
				2	250	900	31.3	79.50			2.2E-04		
				3	245	600	39.0	99.06			2.6E-04		

F.1.4. #40 mesh GTR

Table F-4 – Permeability Data Sheet for Low LBR Soil and #40 mesh GTR

Soil	GTR	%	S	Trial	Q (cm^3)	t (sec)	h (in)	h (cm)	L (cm)	A (cm^2)	k (trial)	k (sample)	k (avg) [cm/sec]
Low	#40	16%	A	1	465	1800	23.5	59.69	11.64	182.90	2.8E-04	3.0E-04	3.3E-04
				2	280	780	31.3	79.50			2.9E-04		
				3	630	1200	39.0	99.06			3.4E-04		
			B	1	510	1800	23.5	59.69	11.64	182.90	3.0E-04	3.7E-04	
				2	380	780	31.3	79.50			3.9E-04		
				3	780	1200	39.0	99.06			4.2E-04		
Low	#40	32%	A	1	295	600	16.0	40.64	11.64	182.90	7.7E-04	7.9E-04	5.5E-04
				2	570	720	23.5	59.69			8.4E-04		
				3	380	780	16.0	40.64			7.6E-04		
			B	1	105	600	16.0	40.64	11.64	182.90	2.7E-04	3.0E-04	
				2	250	720	23.5	59.69			3.7E-04		
				3	130	780	16.0	40.64			2.6E-04		

F.2. Medium LBR Soil

F.2.1. Virgin Material

Table F-5 – Permeability Data Sheet for Medium LBR Soil

Soil	GTR	%	S	Trial	Q (cm³)	t (sec)	h (in)	h (cm)	L (cm)	A (cm²)	k (trial)	k (sample)	k (avg) [cm/sec]
Med	0	0%	A	1	8	3600	23.5	59.69	11.64	182.90	2.4E-06	3.1E-06	2.8E-06
				2	15	3600	31.3	79.38			3.3E-06		
				3	10	1800	39.0	99.06			3.6E-06		
			B	1	10	4680	23.5	59.69	11.64	182.90	2.3E-06	2.5E-06	
				2	105	33900	31.3	79.38			2.5E-06		
				3	200	47100	39.0	99.06			2.7E-06		

F.2.2. 1" GTR

Table F-6 – Permeability Data Sheet for Medium LBR Soil and 1-inch GTR

Soil	GTR	%	S	Trial	Q (cm³)	t (sec)	h (in)	h (cm)	L (cm)	A (cm²)	k (trial)	k (sample)	k (avg) [cm/sec]
Med	1"	16%	A	1	180	93600	23.5	59.69	11.64	182.90	2.1E-06	2.4E-06	2.0E-06
				2	170	57600	31.3	79.50			2.4E-06		
				3	495	115200	39.0	99.06			2.8E-06		
			B	1	125	93600	23.5	59.69	11.64	182.90	1.4E-06	1.6E-06	
				2	100	57600	31.3	79.50			1.4E-06		
				3	365	115200	39.0	99.06			2.0E-06		
Med	1"	32%	A	1	195	93600	23.5	59.69	11.64	182.90	2.2E-06	2.6E-06	3.1E-06
				2	190	57600	31.3	79.50			2.6E-06		
				3	545	115200	39.0	99.06			3.0E-06		
			B	1	250	93600	23.5	59.69	11.64	182.90	2.8E-06	3.5E-06	
				2	235	57600	31.3	79.50			3.3E-06		
				3	785	115200	39.0	99.06			4.4E-06		

F.2.3. 3/8” GTR

Table F-7 – Permeability Data Sheet for Medium LBR Soil and 3/8-inch GTR

Soil	GTR	%	S	Trial	Q (cm^3)	t (sec)	h (in)	h (cm)	L (cm)	A (cm^2)	k (trial)	k (sample)	k (avg) [cm/sec]
Med	3/8"	16%	A	1	145	63000	23.5	59.69	11.64	182.90	2.5E-06	3.2E-06	2.8E-06
				2	570	158400	31.3	79.50			2.9E-06		
				3	60	9000	39.0	99.06			4.3E-06		
			B	1	120	63000	23.5	59.69	11.64	182.90	2.0E-06	2.3E-06	
				2	415	158400	31.3	79.50			2.1E-06		
				3	40	9000	39.0	99.06			2.9E-06		
Med	3/8"	32%	A	1	185	63000	23.5	59.69	11.64	182.90	3.1E-06	3.5E-06	3.2E-06
				2	655	158400	31.3	79.50			3.3E-06		
				3	55	9000	39.0	99.06			3.9E-06		
			B	1	165	63000	23.5	59.69	11.64	182.90	2.8E-06	2.9E-06	
				2	545	158400	31.3	79.50			2.8E-06		
				3	45	9000	39.0	99.06			3.2E-06		

F.2.4. #40 mesh GTR

Table F-8 – Permeability Data Sheet for Medium LBR Soil and #40 mesh GTR

Soil	GTR	%	S	Trial	Q (cm^3)	t (sec)	h (in)	h (cm)	L (cm)	A (cm^2)	k (trial)	k (sample)	k (avg) [cm/sec]
Med	#40	16%	A	1	115	82800	16.0	40.64	11.64	182.90	2.2E-06	2.1E-06	2.4E-06
				2	155	99000	23.5	59.69			1.7E-06		
				3	270	90000	31.3	79.50			2.4E-06		
			B	1	155	82800	16.0	40.64	11.64	182.90	2.9E-06	2.6E-06	
				2	230	99000	23.5	59.69			2.5E-06		
				3	285	90000	31.3	79.50			2.5E-06		
Med	#40	32%	A	1	140	72000	23.5	59.69	11.64	182.90	2.1E-06	3.2E-06	3.2E-06
				2	385	86400	31.3	79.50			3.6E-06		
				3	480	75600	39.0	99.06			4.1E-06		
			B	1	145	72000	23.5	59.69	11.64	182.90	2.1E-06	3.2E-06	
				2	400	86400	31.3	79.50			3.7E-06		
				3	425	75600	39.0	99.06			3.6E-06		

F.3. High LBR Soil

F.3.1. Virgin Material

Table F-9 – Permeability Data Sheet for High LBR Soil

Soil	GTR	%	S	Trial	Q (cm^3)	t (sec)	h (in)	h (cm)	L (cm)	A (cm^2)	k (trial)	k (sample)	k (avg) [cm/sec]
High	0	0%	A	1	955	79200	23.5	59.69	11.64	182.90	1.3E-05	1.1E-05	1.2E-05
				2	1015	93600	31.3	79.38			8.7E-06		
				3	1915	115200	39.0	99.06			1.1E-05		
			B	1	975	104400	23.5	59.69	11.64	182.90	1.0E-05	1.2E-05	
				2	105	7200	31.3	79.38			1.2E-05		
				3	115	4680	39.0	99.06			1.6E-05		

F.3.2. 1” GTR

Table F-10 – Permeability Data Sheet for High LBR Soil and 1-inch GTR

Soil	GTR	%	S	Trial	Q (cm^3)	t (sec)	h (in)	h (cm)	L (cm)	A (cm^2)	k (trial)	k (sample)	k (avg) [cm/sec]
High	1"	1%	A	1	35	3600	23.5	59.69	11.64	182.90	1.0E-05	1.4E-05	1.2E-05
				2	60	3600	31.3	79.50			1.3E-05		
				3	95	3600	39.0	99.06			1.7E-05		
			B	1	30	3600	23.5	59.69	11.64	182.90	8.9E-06	1.1E-05	
				2	50	3600	31.3	79.50			1.1E-05		
				3	80	3600	39.0	99.06			1.4E-05		
High	1"	16%	A	1	50	3600	23.5	59.69	11.64	182.90	1.5E-05	1.7E-05	1.8E-05
				2	85	3600	31.3	79.50			1.9E-05		
				3	90	3600	39.0	99.06			1.6E-05		
			B	1	45	3600	23.5	59.69	11.64	182.90	1.3E-05	1.9E-05	
				2	100	3600	31.3	79.50			2.2E-05		
				3	120	3600	39.0	99.06			2.1E-05		
High	1"	32%	A	1	165	3600	23.5	59.69	11.64	182.90	4.9E-05	4.2E-05	4.8E-05
				2	170	3600	31.3	79.50			3.8E-05		
				3	225	3600	39.0	99.06			4.0E-05		
			B	1	195	3600	23.5	59.69	11.64	182.90	5.8E-05	5.4E-05	
				2	230	3600	31.3	79.50			5.1E-05		
				3	290	3600	39.0	99.06			5.2E-05		

F.3.3. 3/8" GTR

Table F-11 – Permeability Data Sheet for High LBR Soil and 3/8-inch GTR

Soil	GTR	%	S	Trial	Q (cm^3)	t (sec)	h (in)	h (cm)	L (cm)	A (cm^2)	k (trial)	k (sample)	k (avg) [cm/sec]
High	3/8"	16%	A	1	1180	40500	23.5	59.69	11.64	182.90	3.1E-05	4.9E-05	4.3E-05
				2	1035	18000	31.3	79.50			4.6E-05		
				3	390	3600	39.0	99.06			7.0E-05		
			B	1	865	40500	23.5	59.69	11.64	182.90	2.3E-05	3.8E-05	
				2	775	18000	31.3	79.50			3.4E-05		
				3	315	3600	39.0	99.06			5.6E-05		
High	3/8"	32%	A	1	1940	40500	23.5	59.69	11.64	182.90	5.1E-05	6.7E-05	6.7E-05
				2	1525	18000	31.3	79.50			6.8E-05		
				3	455	3600	39.0	99.06			8.1E-05		
			B	1	2675	40500	23.5	59.69	11.64	182.90	7.0E-05	6.8E-05	
				2	1275	18000	31.3	79.50			5.7E-05		
				3	425	3600	39.0	99.06			7.6E-05		

F.3.4. #40 mesh GTR

Table F-12 – Permeability Data Sheet for High LBR Soil and #40 mesh GTR

Soil	GTR	%	S	Trial	Q (cm^3)	t (sec)	h (in)	h (cm)	L (cm)	A (cm^2)	k (trial)	k (sample)	k (avg) [cm/sec]
High	#40	16%	A	1	1410	82800	23.5	59.69	11.64	182.90	1.8E-05	3.1E-05	2.1E-05
				2	5215	151200	31.3	79.50			2.8E-05		
				3	395	5400	39.0	99.06			4.7E-05		
			B	1	1030	82800	23.5	59.69	11.64	182.90	1.3E-05	1.2E-05	
				2	2170	151200	31.3	79.50			1.1E-05		
				3	95	5400	39.0	99.06			1.1E-05		
High	#40	32%	A	1	2060	82800	23.5	59.69	11.64	182.90	2.7E-05	8.9E-05	5.7E-05
				2	14150	151200	31.3	79.50			7.5E-05		
				3	1400	5400	39.0	99.06			1.7E-04		
			B	1	1860	82800	23.5	59.69	11.64	182.90	2.4E-05	2.6E-05	
				2	4360	151200	31.3	79.50			2.3E-05		
				3	250	5400	39.0	99.06			3.0E-05		

Appendix G – Creep

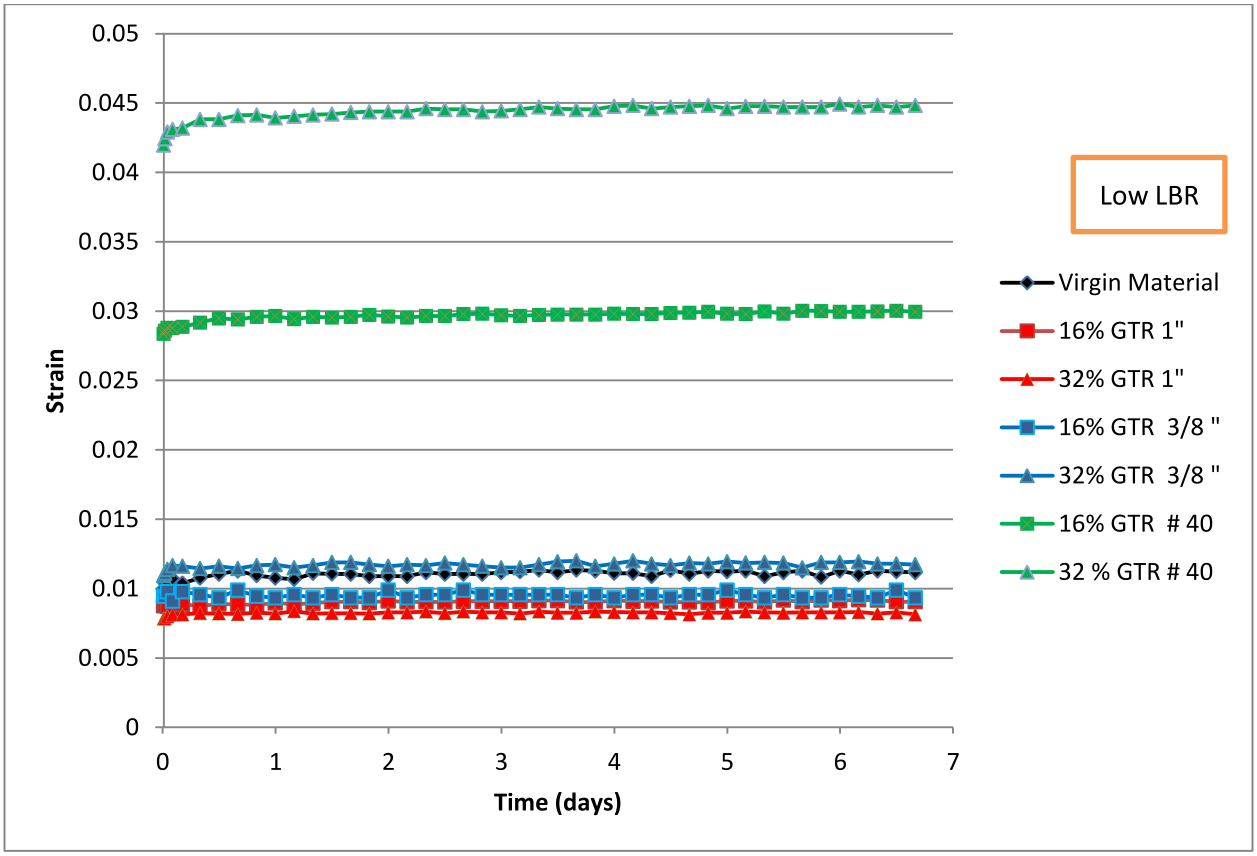

Figure G-1 Strain versus Time for Low LBR Subgrade GTR Blends

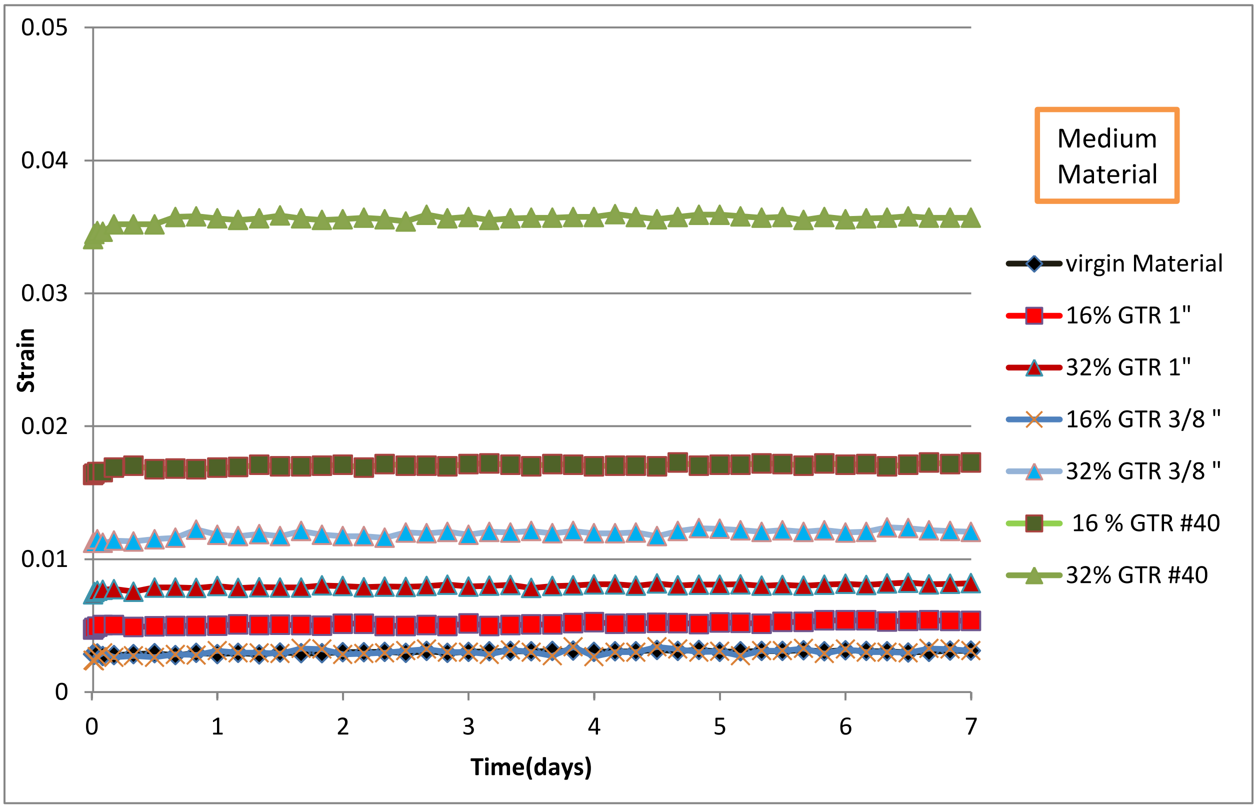

Figure G-2 Strain versus Time for Medium LBR Subgrade GTR Blends

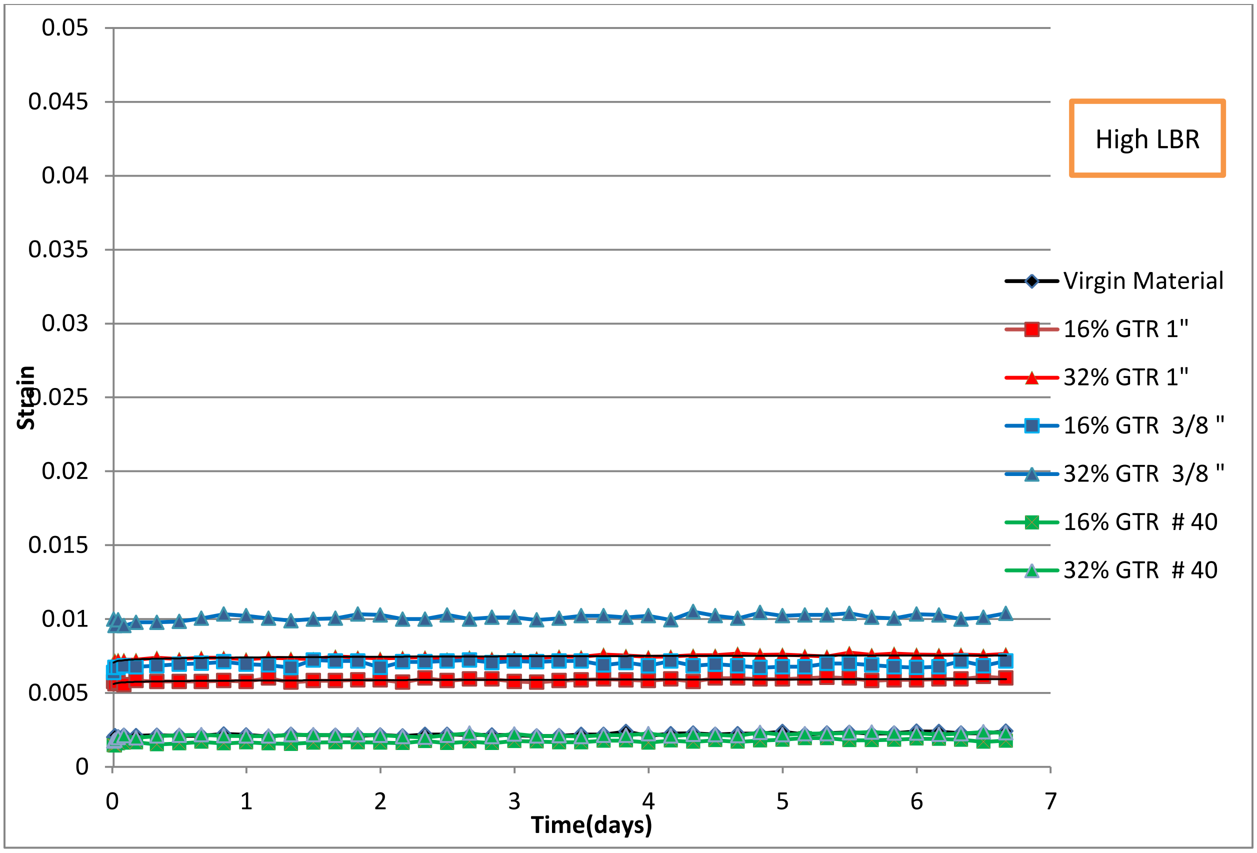

Figure G-3 Strain versus Time for High LBR Subgrade GTR Blends

Appendix H – Data Retrieval System

Part of this research project included the development of a data management system that assists in testing management and report generation. This system was developed as a web application that allows researchers to input data from any computer. This system also allows the project PIs to view key results and test status at a glance without being burdened with the details of the testing.

After logging into the system, the user is presented with the followig home screen (Figure H-1). The User Menu of the left side of the screen is customized listing the projects depending on the user logged in, showing only their assigned projects.

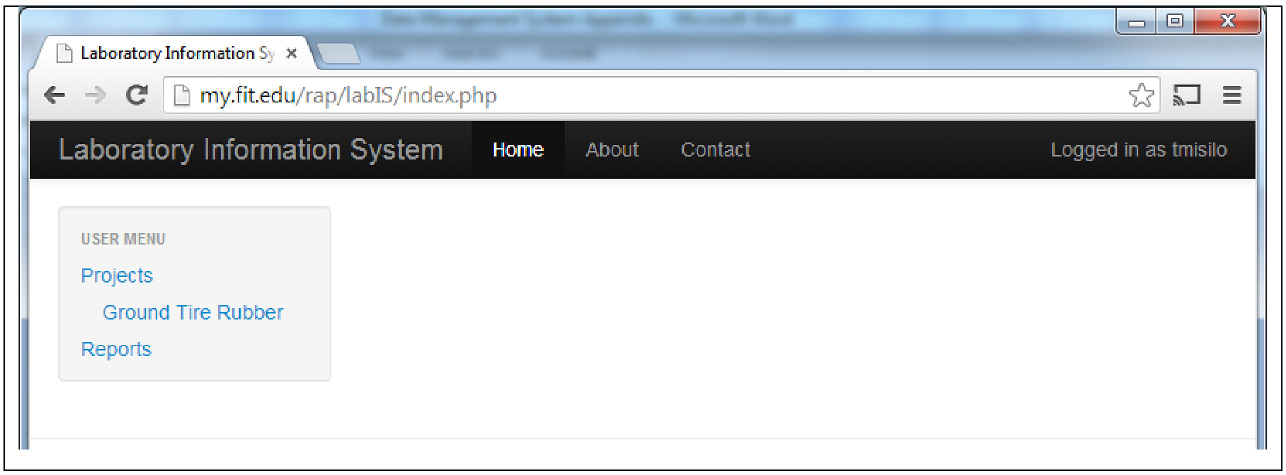

Figure H-1 Home Screen

If a user wants to create a new project they would click on the projects menu item which will show a list of all projects that the user is associated with as shown in Figure H-2. The user would then enter the Project name into the text entry box below the list of projects then click add project.

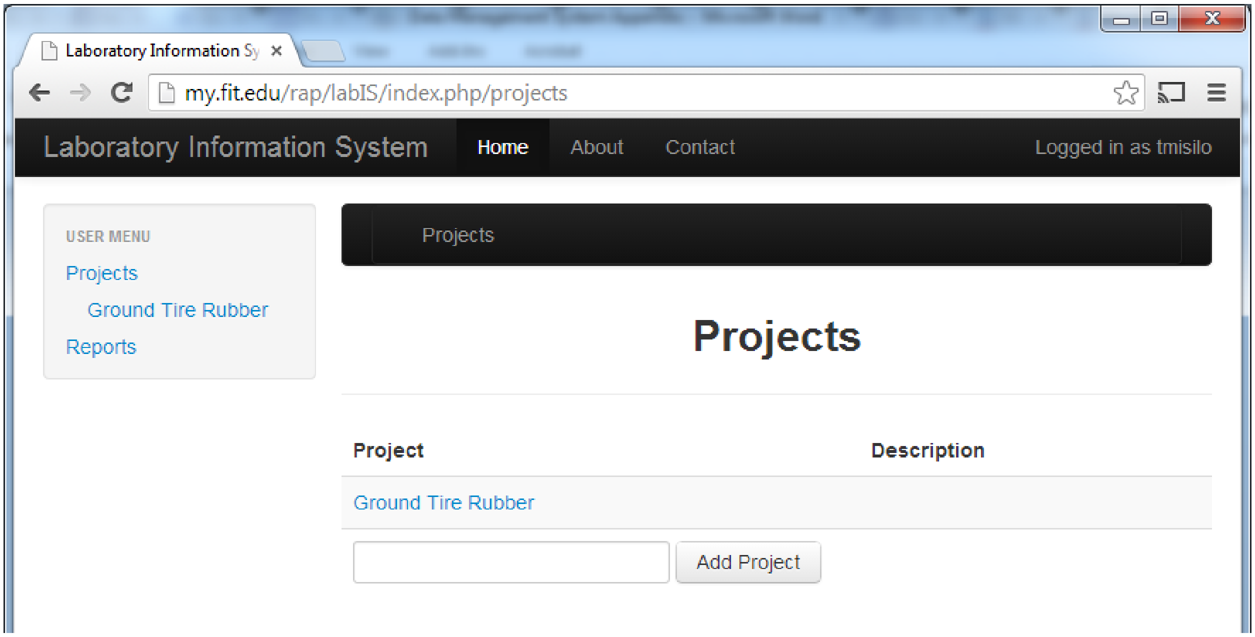

Figure H-2 Projects Screen

Clicking on the Name of a project from either the User Menu or the Projects Page will bring the user to a list of tests that have been created for a project, see Figure H-3. This page shows the key results of given test as well as the status of the test. This page is provided to give the researchers a overall picture of results and the status of testing for a project. Tests can be added at the beginning of a project to help manage the progression of a project, and give the users a visual representation of the testing needed to complete a project.

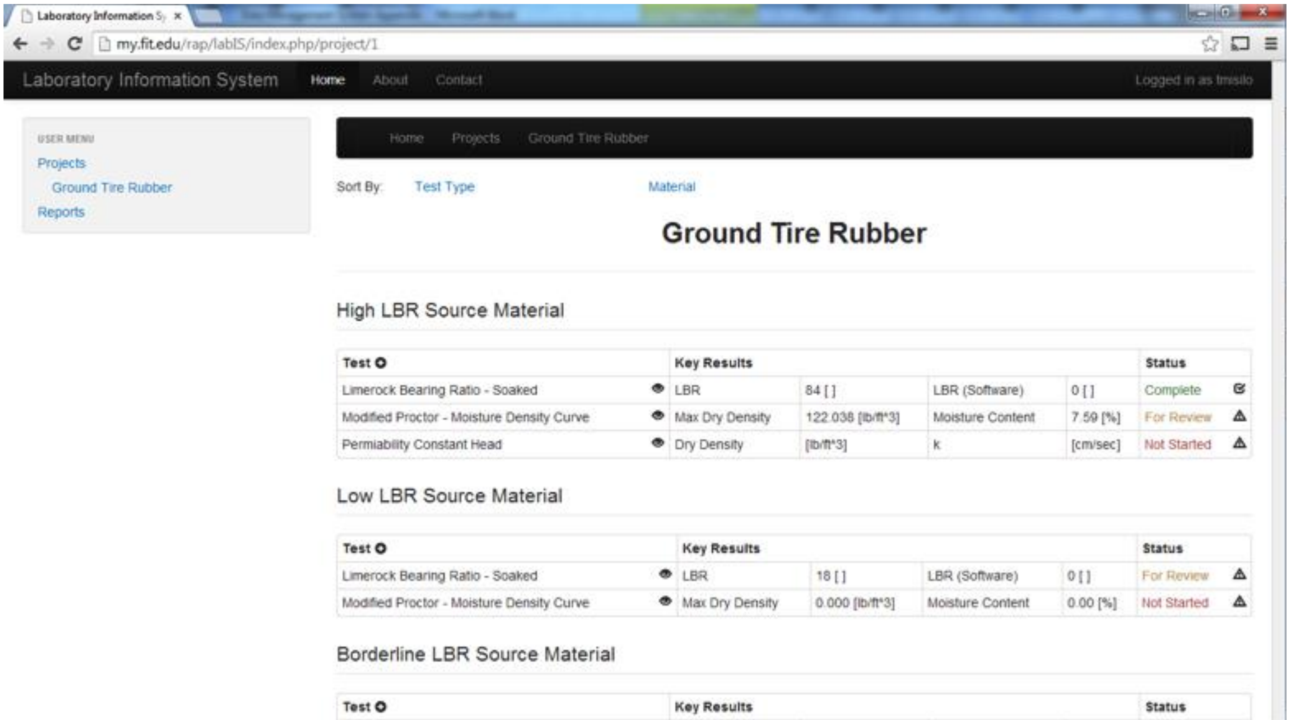

Figure H-3 Project Test Listing

Under each material is a + symbol next to the word test, by clicking this link a user is brought to a new page that will allow the addition of a test for a particular material type, see Figure H-4. This method auto selects the project and material to add the test to, and allows the user to select from a dropdown menu the type of test they would like to select. The expanded dropdown is shown in Figure H-5 after making a selection the user clicks the “Add Test” button.

When the user clicks on the eye to the left of a test name (Figure H-3) they are nvaigated to the details of the selected test. Figures Figure H-6 and Figure H-7show the test details page for the LBR and modified proctor tests respectively. When viewing test details clicking the Edit Link below the general test information will bring the user to a page where they can adjust the following test details:

- The project a test is assigned to.
- The material the test was performed on.
- The laboratory where the test was conducted.
- The test status.

The user can choose between five different test status values. They are Results Void / Discard, Not Started, In Progress, For Review, and Complete. The “Results Void / Discard, are for tests that have been started or completed, but the results should not be reported, usually because of some problem with testing protocol. The “Not Started” status indicates a test that has been created for a project but has yet to be started. The “In Progress” status indicated that a test has been started and results are not complete. The “For Review” status indicates that the test has been completed and should be reviewed and checked for user input errors. The “Complete” status indicated that the given test is complete and has been reviewed, no further changes to the test should be necessary.

Below the General test data in Figure H-6 is the Trial Information section, this section summarizes of the results of the different Trials for this test. The + symbol next to Trial Information when clicked will create a new Trial and prompt the user to insert detail of the trial. Clicking the edit link below each of the trials will present the user with a test specific form where the user will edit the information for a test trial. Calculations are handled internally, to prevent calculation errors; each calculation within this software has been verified to ensure accuracy.

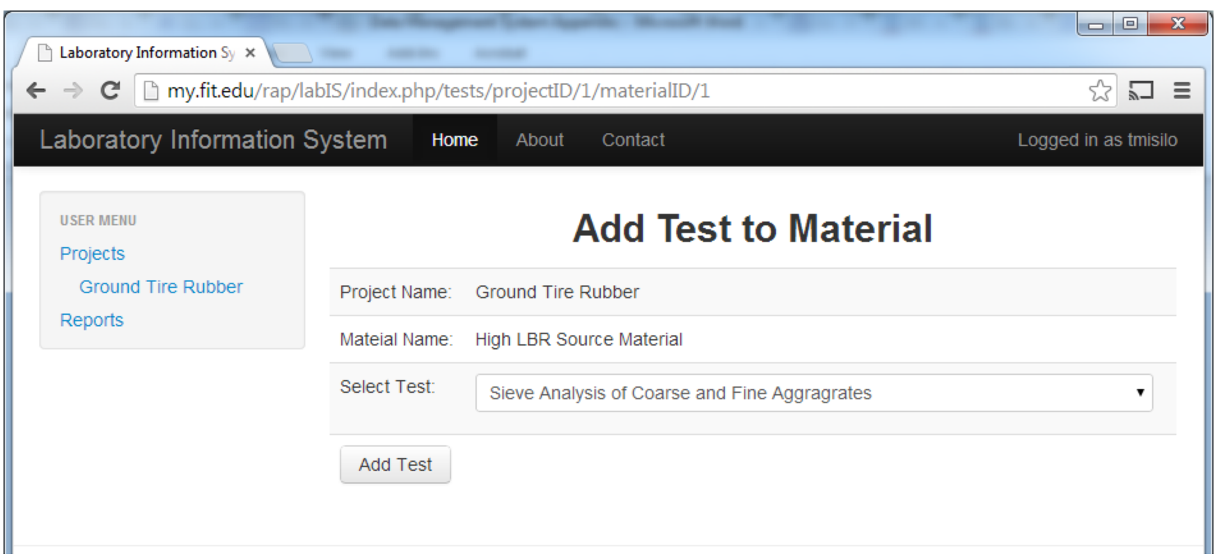

Figure H-4 Add Test to Material Screen

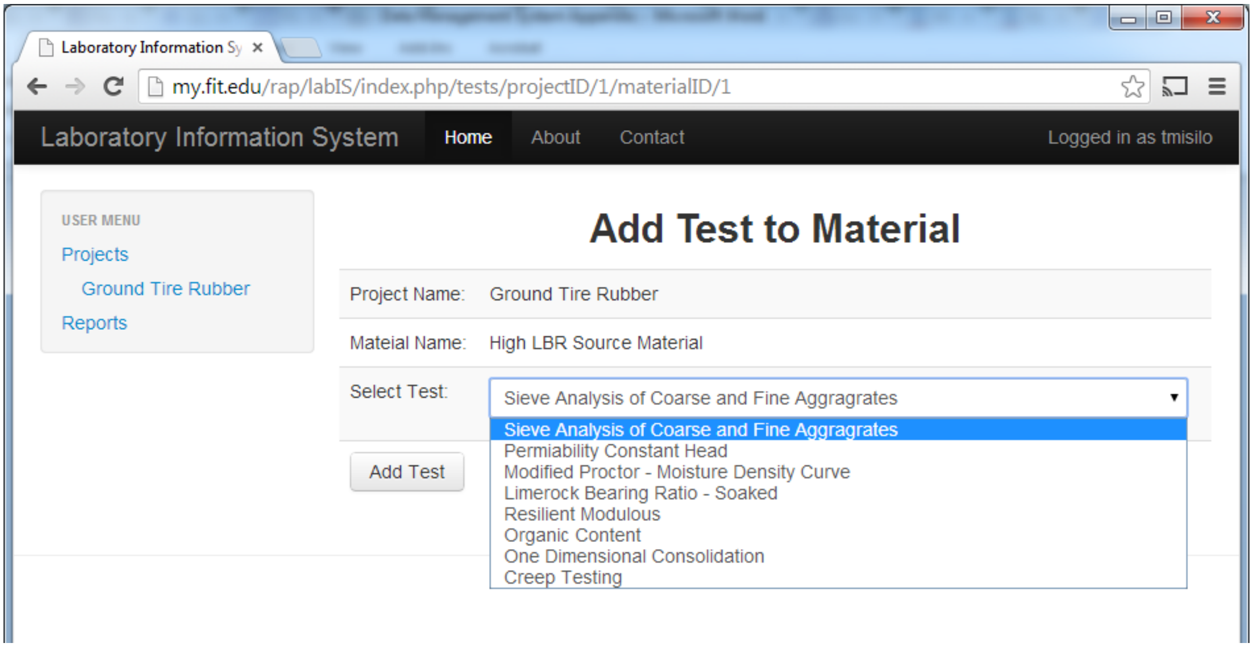

Figure H-5 Dropdown of Tests that can be added

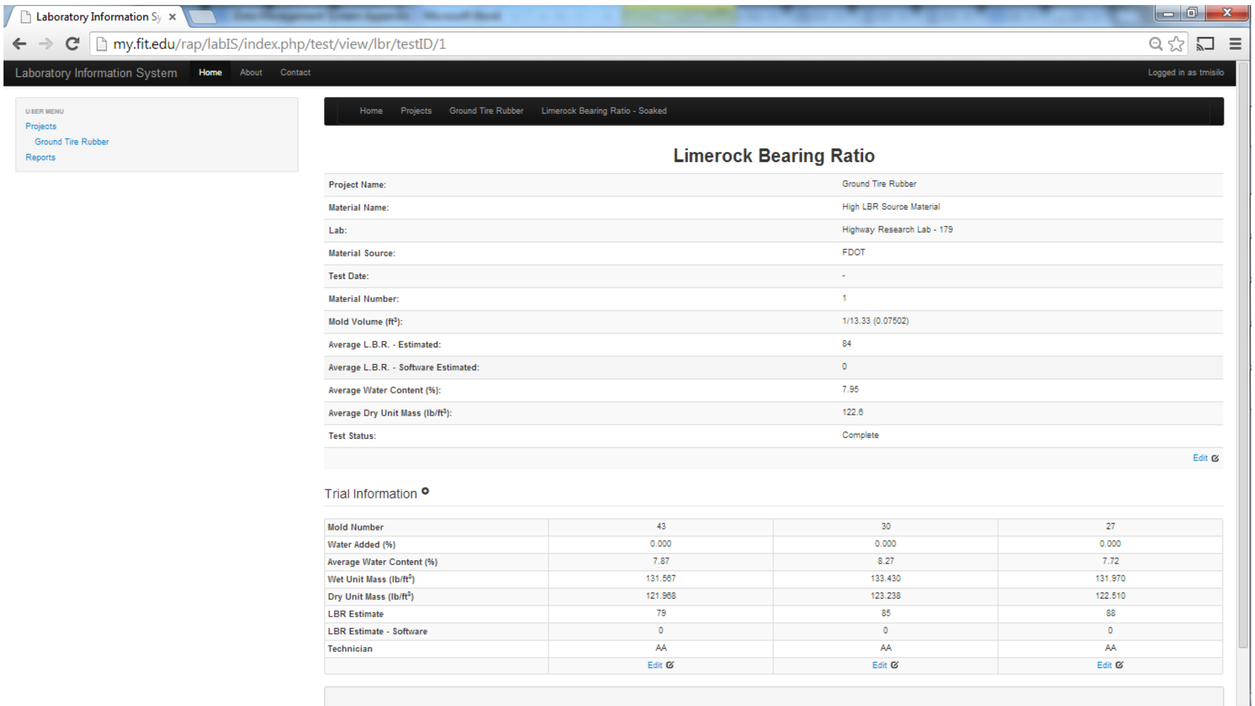

Figure H-6 Limerock Bearing Ratio Test Details

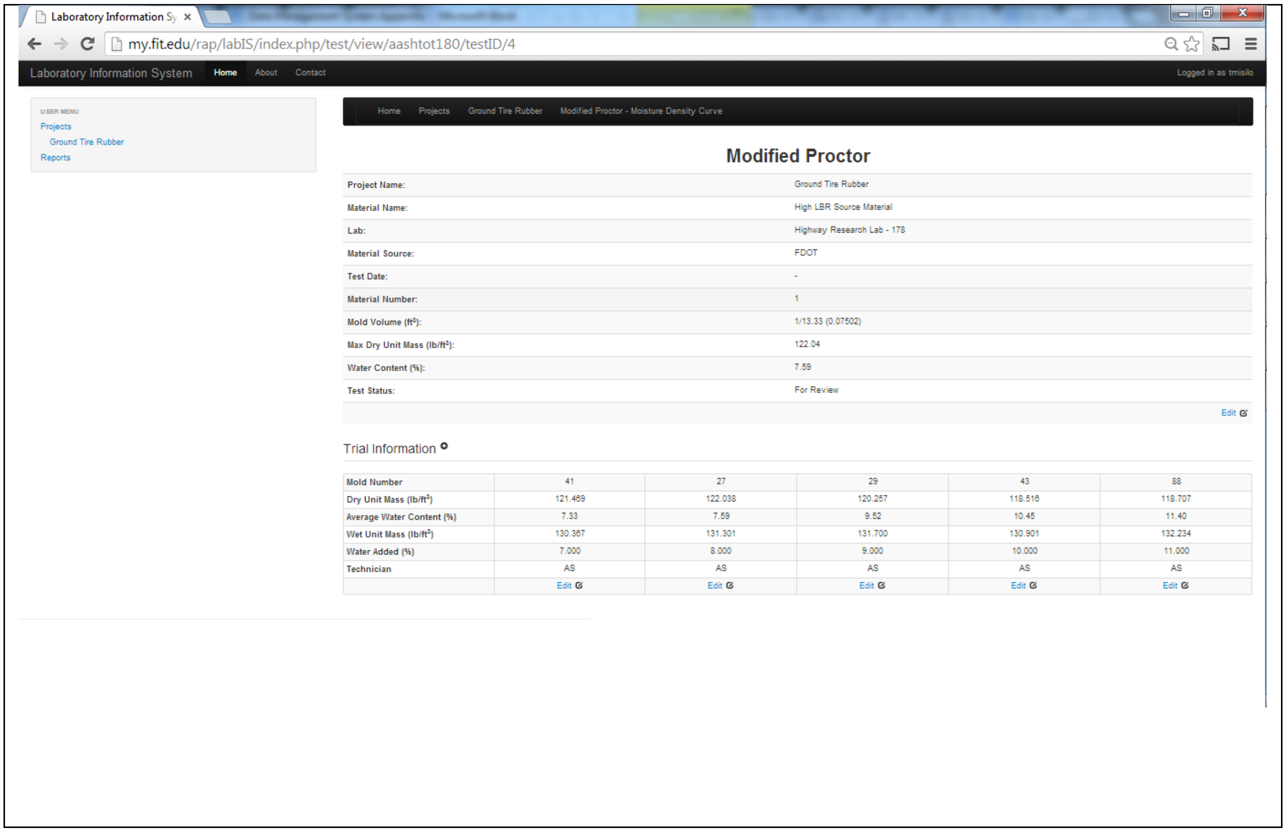

Figure H-7 Modified Proctor Test Details